OPTIMIZATION OF PRIMARY CHEMICAL FEED RATES AND APPLICATION POINTS AT AN EXISTING POTABLE WATER TREATMENT PLANT

By

Brently Keith Jordan

THESIS

Submitted in partial fulfillment of the requirements
for the degree of Master of Science in Civil (Environmental) Engineering at
The University of Texas at Arlington
May, 2023

Arlington, Texas

Supervising Committee:

Dr. Andrew Kruzic, Supervising Professor
Dr. Hyeok Choi
Dr. Victoria Chen

Optimization of Primary Chemical Feed Rates and Application Points at an Existing Potable Water Treatment Plant

Brently Keith Jordan
May, 2023

Supervising Committee:
Dr. Andrew Kruzic, Supervising Professor
Dr. Hyeok Choi
Dr. Victoria Chen

Acknowledgments

I would like to acknowledge several people for helping to make this thesis a reality:

I would like to thank my thesis advisor, Dr. Andrew Kruzic, who was very patient and understanding throughout the long process of doing the jar tests, performing the actual plant trials, and writing this thesis. I am very thankful for his insights, patience, and assistance.

I would like to thank my parents, Jake and Norma Jordan, who both passed away during this optimization effort, for teaching me how to learn and how to process information from a very young age.

I would like to thank Mr. Larry McDaniel, the General Manager of the Dallas County Park Cities Municipal Utility District, for his willingness to not only allow the use of the plant's equipment for the testing, but also for his willingness to allow the testing results to be applied to the actual treatment plant processes.

I would like to thank Mr. Mike Swint, the Maintenance Manager of the Dallas County Park Cities Municipal Utility District, as well as his entire maintenance staff, for assistance in changing the actual application points of the chemicals at the treatment plant, and for providing valuable information concerning the results of the changes made to the plant in terms of the changes in plant maintenance requirements due to the changes in the chemical feed systems.

I would also like to thank Mr. Jim Case, the (now retired) Operations Manager of the Dallas County Park Cities Municipal Utility District and his successor Mr. Travis Kruger, as well as their entire operations staff, for their valuable assistance in retrieving water samples, chemical samples, and running water quality tests.

Last of all, and most importantly, I would like to thank my wonderful wife Dianna Jordan for her patience and understanding while the effort to create this thesis took my time away from her. She was also very helpful with the final review of this document with regard to punctuation and capitalization.

Abstract

Due to a major upset in the treatment processes for the Dallas County Park Cities Municipal Utility District caused by a required change in treatment techniques, an optimization study was conducted to find the best treatment strategies for the primary coagulation, flocculation, and settled processes for the treatment plant. A methodology for determining how to optimize jar testing while injecting both ferric sulfate and calcium hydroxide in an almost simultaneous manner was developed, and a large number of jar tests were conducted to determine both the best dosages and the best application points of the two chemicals.

As a result of this study, it was determined that the primary contributor for optimal water quality in the primary treatment processes for the District's treatment plant was the application point of the chemicals used rather than the chemical dosages and/or velocity gradients used during primary treatment. At least for the District's treatment plant, feeding calcium hydroxide into the exit of the plant's rapid mixers, while feeding ferric sulfate into the plant's first stage flocculation basin provides the most optimal treatment of the water.

Two alternate chemicals (a poly ferric sulfate blend for coagulation, and sodium hydroxide rather than calcium hydroxide for pH and alkalinity control) was also investigated. The poly ferric sulfate blend showed inconclusive results (per the manufacturer), and the sodium hydroxide results showed that it is not an acceptable alternative chemical for calcium hydroxide for the District's treatment plant.

Jar testing for optimization is also not a one-time event. It must be periodically repeated due to changes in raw water quality parameters such as pH, temperature, alkalinity, organic content, and the type and magnitude of raw water turbidity

This study also resulted in a set of recommendations for the treatment plant's continuing optimization, including weekly and/or as-needed jar testing for optimal chemical dosages, additional research into even more precise optimization procedures, weekly calibration checks of the plant's coagulant feed pumps, the potential for utilization of magnetic flow metering to monitor actual coagulate feed rates, and adjustments to the plant's clarifier baffling systems.

Table of Contents

Acknowledgments I
Abstract II
Table of Contents III
List of Figures IV
List of Tables V
1. Background and Objectives 1
1.1. Plant History 3
2. Literature Review 6
2.1. Velocity Gradients 6
2.2. Critiques of Camp and Stein's 1943 Velocity Gradient Formula 9
2.3. Water Temperature Effects on Flocculation 10
2.4. Horizonal Radial Flow Clarification – Pros and Cons 11
2.5. Turbidity Effects of Lime Softening 11
2.6. Mass Transfer Rate of CO_2 11
2.7. Jar Tests versus Actual Plant Conditions 12
2.8. Clarifier Baffling 12
3. Materials and Methods 14
3.1. Materials used during the optimization process: 14
3.2. Methods, Part 1 14
3.3. Methods, Part 2 19
4. Results 20
4.1. Initial Optimization Attempts during the Compliance Crisis 20
4.2. Series 1 and Series 2 Optimization Tests after the Compliance Crisis 32
4.3. Analysis of the Actual Chemicals Used in Treatment 44
4.4. Series 3 and Series 4 Optimization Tests 46
4.5. Alternative Chemicals 59
4.6. Final Adjustments 62
5. Conclusions and Recommendations 63
6. Appendix 1: Treatment Plant Turbidity Data during the Plant Crisis 66
7. Appendix 2: Jar Tester Velocity Gradient & Speed Formula Derivations 68
7.1. Jar Test Apparatus Velocity Gradient Formula Derivation 68
7.2. Jar Test Apparatus Jar Speed Formula Derivation 72
8. Appendix 3: Rapid Mixer and Flocculator Velocity Gradient Derivations 75
8.1. Rapid Mixer Derivations 75
8.2. Flocculator Stage 1 Derivations 79
8.3. Flocculator Stage 2 Derivations 83
8.4. Flocculator Stage 3 Derivations 87
9. Appendix 4: Stock Solution Makeup Derivations 91
10. References 94

List of Figures

Figure 1.1: Elevation View of the Plant's Rapid Mixers 1
Figure 1.2: Typical Plant Flocculator (Stage 2) 2
Figure 1.3: Typical Plant Clarifier 2
Figure 1.4: Actual Plant Clarifier Effluent Turbidities During Plant Crisis 5
Figure 1.5: Actual Plant Effluent Turbidities During Plant Crisis 5
Figure 2.1: Clarifier Effluent Weir Section View 13
Figure 3.1: SCADA System Velocity Gradient Screen 17
Figure 4.1: Initial Test Results (Ferric Dosage Fixed at 25 mg/L as Fe^{3+}) 22
Figure 4.2: Initial Test Results (Lime Dosage Fixed at 60 mg/L as $Ca(OH)_2$) 23
Figure 4.3: Initial Test Results (Ferric Dosage Fixed at 23 mg/L as Fe^{3+}), Jar Set 1 24
Figure 4.4: Initial Test Results (Ferric Dosage Fixed at 23 mg/L as Fe^{3+}), Jar Set 2 25
Figure 4.5: Initial Test Results (All Chemicals to RM, Lime Dose Fixed at 60 mg/L as $Ca(OH)_2$) 26
Figure 4.6: Initial Test Results (All Chemicals to RM, Lime Dose Fixed at 70 mg/L as $Ca(OH)_2$) 27
Figure 4.7: Initial Test Results (All Chemicals to RM, Lime Dose Fixed at 80 mg/L as $Ca(OH)_2$) 28
Figure 4.8: Initial Test Results (All Chemicals to RM, Lime Dose Fixed at 80 mg/L as $Ca(OH)_2$) 29
Figure 4.9: Speciation of Carbon Dioxide in water relative to pH 32
Figure 4.10: Optimization Series 1/2 Jar Sets 17 and 18 Results 35
Figure 4.11: Optimization Series 1/2 Jar Sets 19 and 20 Results 36
Figure 4.12: Optimization Series 1/2 Jar Sets 33 and 34 Results 37
Figure 4.13: Optimization Series 1/2 Jar Sets 41 and 42 Results 38
Figure 4.14: Optimization Series 1/2 Jar Sets 57 and 58 Results 39
Figure 4.15: Series 2 Raw Water Temperature Versus Plant Settled Turbidity 42
Figure 4.16: Series 2 Jar Test Versus Plant pH and Turbidity 42
Figure 4.17: Series 2 Jar Test Versus Plant Alkalinity 43
Figure 4.18: Series 2 Expected Turbidity Removal versus Actual Turbidity Removal 43
Figure 4.19: Plant Bulk Calcium Hydroxide (Nominal 40% concentration) Tests 44
Figure 4.20: Plant Bulk Calcium Hydroxide (Nominal 30% concentration) Tests 46
Figure 4.21: Optimization Series 3/4 Jar Sets 73 and 74 Results 48
Figure 4.22: Optimization Series 3/4 Jar Sets 75 and 76 Results 49
Figure 4.23: Optimization Series 3/4 Jar Sets 83 and 84 Results 51
Figure 4.24: Optimization Series 3/4 Jar Sets 62 and 63 Results 52
Figure 4.25: Optimization Series 3/4 Jar Sets 71 and 72 Results 53
Figure 4.26: Series 4 Plant vs Jar Test pH and Turbidity 55
Figure 4.27: Series 4 Plant vs Jar Test Alkalinity 56
Figure 4.28: Series 4 Plant vs Jar Test Turbidity Regression 56
Figure 4.29: Series 4 Plant vs Jar Test Alkalinity Regression 57
Figure 4.30: Series 4 Raw Water Temperature vs Plant Turbidity 57
Figure 4.31: Series 4 Water Temperature vs Ferric Sulfate Dose Regression 58
Figure 4.32: Series 4 Expected vs Actual Turbidity Removal Percentages 58
Figure 5.1: Ferric Sulfate Pump Typical Calibration Curve 65
Figure 7.1: Phipps Bird Jar Test Apparatus Velocity Gradient Curves from Manufacturer 68
Figure 7.2: Phipps Bird Jar Test Apparatus Velocity Gradient Curves Magnified 69
Figure 7.3: Jar Test Apparatus Velocity Gradient Curves Regressed 70

Figure 7.4: Jar Test Apparatus Velocity Gradient Formula Coefficient A Regression 71
Figure 7.5: Jar Test Apparatus Velocity Gradient Formula Coefficient B Regression..... 71
Figure 7.6: Jar Test Apparatus Velocity Gradient Formula Coefficient C Regression..... 71
Figure 7.7: Jar Test Apparatus Velocity Gradient Formula Coefficient D Regression 72
Figure 7.8: Jar Test Apparatus Paddle Speed Curves Regressed 73
Figure 7.9: Jar Test Apparatus Speed (rpm) Formula Coefficient A Regression 73
Figure 7.10: Jar Test Apparatus Speed (rpm) Formula Coefficient B Regression..... 74
Figure 7.11: Jar Test Apparatus Speed (rpm) Formula Coefficient C Regression..... 74
Figure 7.12: Jar Test Apparatus Speed (rpm) Formula Coefficient D Regression 74
Figure 8.1: Rapid Mixer Velocity Gradient Chart..... 78
Figure 8.2: Flocculator Stage 1 Velocity Gradient Chart 82
Figure 8.3: Flocculator Stage 2 Velocity Gradient Chart 86
Figure 8.4: Flocculator Stage 3 Velocity Gradient Chart 90

List of Tables

Table 4.1: Initial Test Results (Ferric Dosage Fixed at 25 mg/L as Fe3+)..... 22
Table 4.2: Initial Test Results (Lime Dosage Fixed at 60 mg/L as $Ca(OH)_2$) 23
Table 4.3: Initial Test Results (Ferric Dosage Fixed at 23 mg/L as Fe3+), Jar Set 1 24
Table 4.4: Initial Test Results (Ferric Dosage Fixed at 23 mg/L as Fe3+), Jar Set 2 25
Table 4.5: Initial Test Results (All Chemicals to RM, Lime Dose Fixed at 60 mg/L as $Ca(OH)_2$) 26
Table 4.6: Initial Test Results (All Chemicals to RM, Lime Dose Fixed at 70 mg/L as $Ca(OH)_2$) 27
Table 4.7: Initial Test Results (All Chemicals to RM, Lime Dose Fixed at 80 mg/L as $Ca(OH)_2$) 28
Table 4.8: Initial Test Results (All Chemicals to RM, Lime Dose Fixed at 80 mg/L as $Ca(OH)_2$) 29
Table 4.9: Initial Test Results (J1 All Chemicals to RM, J2 Lime to RM & Ferric to Floc S1)..... 31
Table 4.10: Jar Test Versus Plant Data during Crisis Trials..... 33
Table 4.11: Jar Tests, Stirrers Running at Minimum Speed During Settling Versus Plant Data 34
Table 4.12: Optimization Series 1/2 Jar Sets 17 and 18..... 35
Table 4.13: Optimization Series 1/2 Jar Sets 19 and 20..... 36
Table 4.14: Optimization Series 1/2 Jar Sets 33 and 34..... 37
Table 4.15: Optimization Series 1/2 Jar Sets 41 and 42..... 38
Table 4.16: Optimization Series 1/2 Jar Sets 57 and 58..... 39
Table 4.17: Optimization Series 3/4 Jar Sets 73 and 74..... 48
Table 4.18: Optimization Series 3/4 Jar Sets 75 and 76..... 49
Table 4.19: Optimization Series 3/4 Jar Sets 83 and 84..... 51
Table 4.20: Optimization Series 3/4 Jar Sets 62 and 63..... 52
Table 4.21: Optimization Series 3/4 Jar Sets 71 and 72..... 53
Table 4.22: Jar Tests using Sodium Hydroxide for pH and Alkalinity Control..... 62
Table 6.1: Treatment Plant Turbidity Data During Plant Crisis..... 66
Table 9.1: Ferric Sulfate Dilution Method..... 91
Table 9.2: Calcium Hydroxide (40%) Dilution Method..... 92
Table 9.3: Calcium Hydroxide (30%) Dilution Method..... 93

1. Background and Objectives

The objective of this study is to optimize the flocculation, coagulation and, settling processes in the Dallas County Park Cities Municipal Utility District's potable water treatment plant. This treatment plant receives raw water from Grapevine Reservoir in North Central Texas. It is a lime-softening plant utilizing a nominal 30% solution calcium hydroxide delivered to the plant as a slurry (this was a nominal 40% solution at the beginning of this optimization study), with a primary coagulant of a nominal 60% solution liquid ferric sulfate. The plant is separated into two parallel treatment trains, each with a rapid mixer as shown in Figure 1.1 below, 4-basin (3 stage) flocculation tanks with horizontal "paddle-wheel" counter-rotating mixers as shown in Figure 1.2 below, and a radial-flow clarifier as shown in Figure 1.3 below. After settling, the water flows through granular activated carbon (GAC) filters, is disinfected with a combination of sodium hypochlorite and liquid ammonium sulfate (i.e., chloramine disinfection), and then undergoes a final filtering utilizing ultrafiltration (UF) membranes.

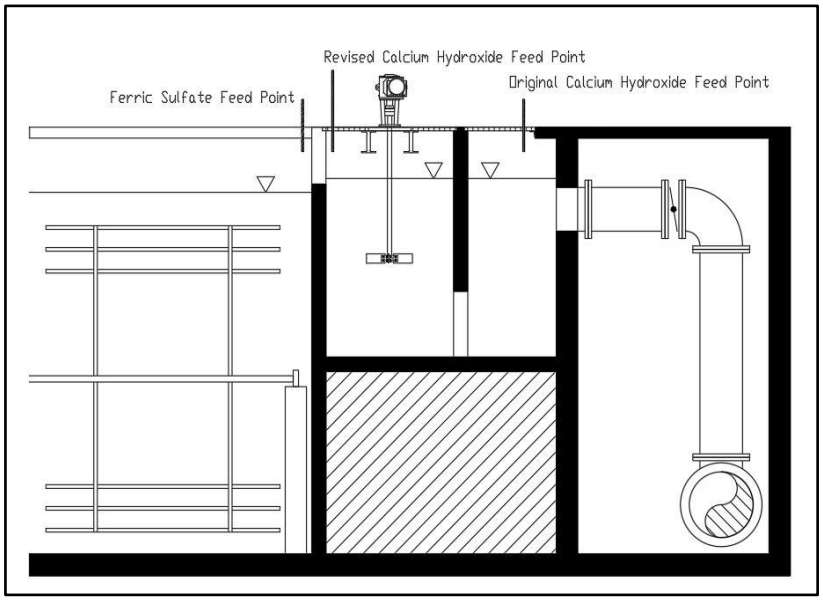

Figure 1.1: Elevation View of the Plant's Rapid Mixers

Figure 1.2: Typical Plant Flocculator (Stage 2)

Figure 1.3: Typical Plant Clarifier

During normal operations, the clarifier effluent turbidity should be reduced to about 3.0 to 8.0 ntu from a raw water turbidity between 10 and 100 ntu, and total alkalinity should be reduced to between 40 and 60 mg/L as $CaCO_3$ from a raw water alkalinity of between 80 and 120 mg/L as $CaCO_3$. The pH should be kept between 9.5 and 10.0 during this

process (filtration and disinfection processes after flocculation and settling will then reduce the pH to an 8.8 to 9.2 range).

The turbidity reduction needs to be accomplished to minimize loading on the plant's GAC filters (and therefore on the UF membrane filters used for final filtration). The alkalinity reduction needs to be accomplished to continue to meet the requirements for secondary TOC/Disinfection credit from the Texas Commission on Environmental Quality (TCEQ) regulation TAC 290.112.f.3.C.iii, which states that to be allowed alternative TOC/Disinfection credit, the total alkalinity of the water discharged from the treatment plant must be less than 60 mg/L as $CaCO_3$. The pH limitations are dictated by politics and by the desire of plant management to help reduce both distribution system nitrification and deposition of calcium carbonate in the distribution system piping.

1.1. Plant History

This optimization study was initiated when the treatment plant had a major upset that almost resulted in non-compliance with TCEQ regulations with regard to finished water turbidity. The treatment plant was originally placed in service in 1950, and for many years operated utilizing a high lime softening process which was in part mandated by politics (the customers supplied by the treatment plant desired a soft water) . Typical pH values at the end of flocculation were in the 10.0 to 11.5 range, and finished water pH was in the 9.5 to 10.0 range. During this period, chemical treatment was done using flocculation only, with no rapid mixing. Ferric sulfate was added to the raw water in the supply pipeline just prior to the entrance to the flocculators, and calcium hydroxide was added in the first flocculator. This treatment scheme worked well until the mid-1990's, when water quality rules changes mandated a maximum 9.49 pH in finished water quality.

At that time, rapid mixers were added to the treatment plant. The ferric sulfate application point did not change, but the calcium hydroxide feed was moved to the new rapid mixer. Within a month, rapid mixer failure occurred, due to a massive buildup of calcium carbonate on the mixer blades. At that time, calcium hydroxide was moved back to the first flocculator. Problems with adequate treatment continued, however. Increasingly massive dosages of ferric sulfate were added, with little effect on the final water quality. At the culmination of this treatment era, 80 mg/L as Fe^{3+} of ferric sulfate was being dosed. The clarifier effluent turbidities were at about 1.0 ntu, but the plant's dual media (sand and anthracite coal) filters struggled to reduce the finished water quality to 0.3 ntu.

At the plant, clarifier effluent water flows into a long, narrow channel (about 15' wide x 120' long x 12' deep) leading to the filters. There is no mechanical mixing in this channel. It was decided to add a small amount (2 to 5 mg/L as Fe^{3+}) of ferric sulfate to the head of this channel to create a certain amount of secondary coagulation. This treatment method was successful. The primary ferric sulfate dosage was lowered to about 20 mg/L as Fe^{3+} with a 3 to 5 mg/L as Fe^{3+}

"secondary" ferric dosage, and filter effluent turbidity dropped to about 0.1 to 0.2 ntu. Later, cationic polymer was added as a disinfection aid with dosages in the 1.0 to 3.0 mg/L range. Primary ferric sulfate dosage was then reduced to about 15 mg/L as Fe^{3+}, and secondary ferric dosage was reduced to about 2 mg/L as Fe^{3+}.

This treatment method remained in place until preparations began for conversion of the plant's filters from conventional dual-media to GAC filters with their primary function being taste and odor control, along with the installation of ultra-filtration (UF) membranes for use as the final filtration process. The plant's rapid mixers and flocculators were also replaced as a part of this project (still with horizontal paddle wheel mixing in the flocculators).

Due to the construction sequencing, the new rapid mixers, flocculators, and GAC filters were placed in service prior to the completion of the UF membrane system. Since the new UF membrane system manufacturer's requirements were that no polymer or undissolved iron could be fed into them due to the potential for severe fouling, both the polymer feed and the secondary ferric sulfate feed were discontinued. The treatment plant rapidly began struggling to produce finished water turbidity below 0.3 ntu. Clarifier effluent turbidities began ranging from 7.0 to 19.0 ntu (see Figures 1.4 and 1.5 below). The only way the plant was kept in TCEQ compliance was by activating an emergency interconnection with Dallas Water Utilities (DWU), in which potable water from the DWU system was fed into the plant's potable water clearwell to mix with the plant's water to bring the plant effluent turbidities below 0.3 ntu (see Figure 1.5 below). During this time, plant staff began varying chemical dosages from 0 to 158 mg/L as $Ca(OH)_2$ for calcium hydroxide and 21 to 50 mg/L as Fe^{3+} for ferric sulfate in an attempt to lower the turbidities. The plant's velocity gradients in both the rapid mixers and the flocculators were also varied by changing the speeds of the motors driving these devices. No jar testing was done during this period, and the attempts at turbidity reduction were not successful. It should be noted that velocity gradient changes showed little or no effect on the resultant water quality during this time (personal observation). This observation is reinforced from research (Clark, 1985), (Cleasby, 1984), (Han and Lawler, 1992). Appendix 1 shows the tabular turbidity data collected during this period.

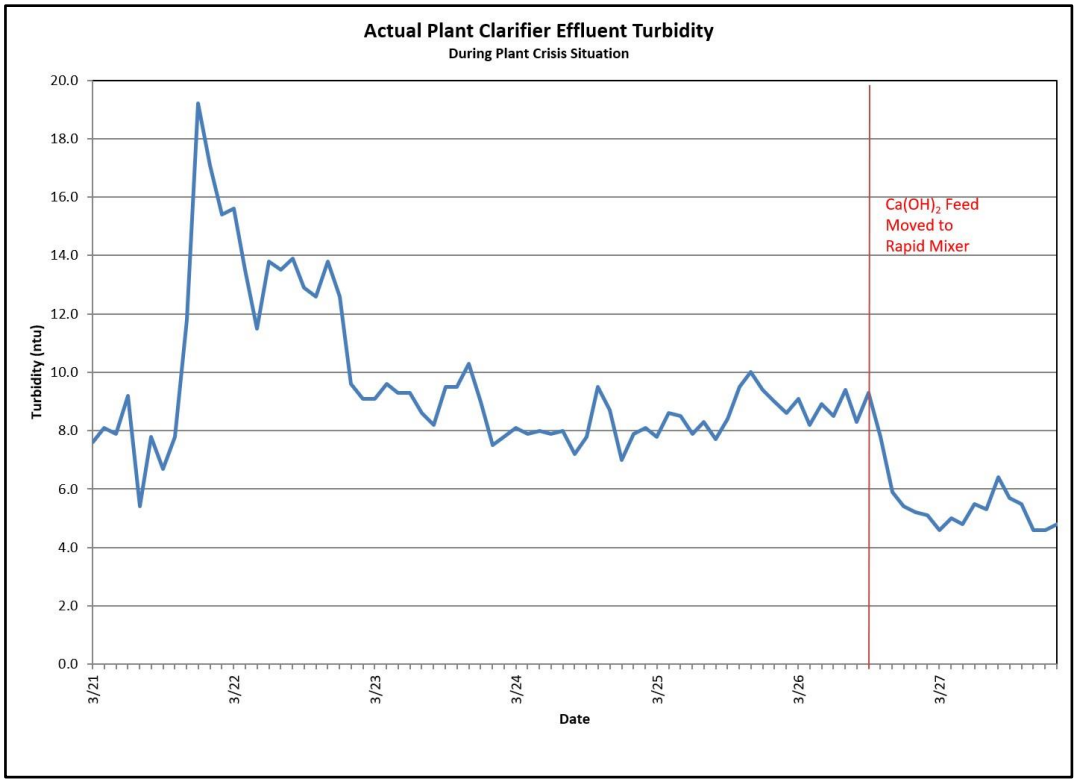

Figure 1.4: Actual Plant Clarifier Effluent Turbidities During Plant Crisis

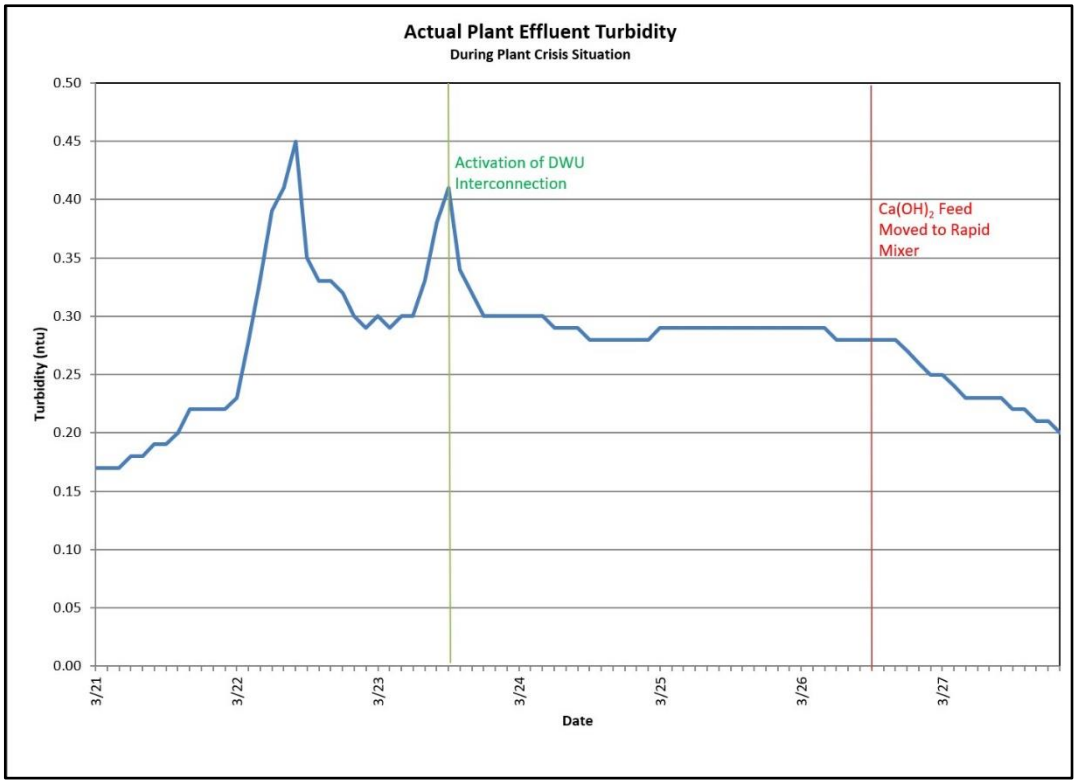

Figure 1.5: Actual Plant Effluent Turbidities During Plant Crisis

2. Literature Review

2.1. Velocity Gradients

In *Velocity Gradients and Internal Work in Fluid Motion* (1943), Camp and Stein developed the classic velocity gradient formula, which when used for rapid mixing and flocculation applications is typically stated as:

$$G = \left(\frac{P}{V\mu}\right)^3 \tag{2.1}$$

where G is the velocity gradient in sec-1, P is the power input in lb·ft/sec, V is the tank volume in ft^3, and μ is the dynamic viscosity of water in lb·sec/ft^2. This basic equation has been used in the design of rapid mixers and flocculation equipment ever since its development.

However, there is more to Camp and Stein's formula for G than meets the eye, primarily the P (power input) component. How do you derive the actual magnitude of this power input? Fortunately, since the plant's rapid mixers and flocculators were new, the magnitude of the power inputs were relatively easy to obtain. In a Microsoft Excel spreadsheet provided by CDM Smith, Inc, the engineering firm who designed the District's rapid mixers and flocculators, the following formula for power input was provided:

$$P = N_p\left(0.5\rho AC\left(0.76\left(\frac{2\pi rS}{60}\right)\right)^3\right) \tag{2.2}$$

Where P is the power input in lb·ft/sec, N_p is the number of blades on a mixer, ρ is the fluid density in slugs/ft^3, A is the area of one mixer blade in ft^2, C is the mixer blade drag coefficient, r is the mixer blade radius in ft, and S is the mixer blade speed in rpm. Values for Np, A, C, r, and S are also included in CDM Smith's spreadsheets:

A. The rapid mixers are vertical shaft units with 6 blades (i.e., N_p equals 6). A is given as 1.0 ft^2 per mixer blade, C is given as a unitless value of 1.8, and r is given as 1.375 ft. The value for S is mixer speed dependent (the mixer motor is driven by a variable speed drive). The motor has a name-plate rpm of 1760 rpm at 60 Hz, and the total gear reduction ratio is 17.42:1, so the mixer speed S in rpm can be defined as

$$S = \frac{\frac{1760h}{60}}{17.42} \tag{2.3}$$

where h is the variable frequency drive output in Hz.

B. The stage 1 flocculators are horizontal shaft "paddle-wheel" mixers with 3 sets of paddles with a single variable speed drive controlled motor. Each set of paddles has 3 paddle arms mounted 120° apart, and each paddle

arm has 3 beams with centerlines mounted at 3.354 ft, 4.771 ft, and 6.188 ft from the shaft centerline. For paddle 1, the beam length is 11.167 ft, and for paddles 2 and 3, the beam length is 10.667 ft. Each beam has a width of 0.625 ft. Since each of the paddles is turning at the same speed, the calculation for Power input can therefore be simplified by adding the length of each set of beams (11.167 + 10.667 + 10.667 ≈ 32.5 feet) and then multiplying the total length of each beam set by the beam width of 0.625 ft to get an area for each beam set of 20.313 ft^2. The individual power inputs for each beam set are then summed to obtain a combined power input. Therefore, N_p can be interpreted as 3 beams. A is calculated as 20.313 ft^2 per mixer beam, C is given as a unitless value of 1.8, and the three r values (one for each beam) are given as 3.354 ft, 4.771 ft, and 6.188 ft. The value for S is mixer speed dependent (the mixer motor is driven by a variable speed drive). The motor has a name-plate rpm of 1800 rpm at 60 Hz, and the total gear reduction ratio is 388.66:1, so the mixer speed S in rpm can be defined as

$$S = \frac{\frac{1800h}{60}}{388.66} \tag{2.4}$$

where h is the variable frequency drive output in Hz.

C. The stage 2 flocculators are horizontal shaft "paddle-wheel" mixers with 2 sets of paddles with a single variable speed drive controlled motor. Each set of paddles has 2 paddle arms mounted 180° apart, and each paddle arm has 3 beams mounted at 3.771 ft, 5.021 ft, and 6.271 ft from the shaft centerline. Each beam length is 10.5 ft, and each beam has a width of 0.458 ft, for an area of each beam of 4.813 ft^2. The individual power inputs for each beam set are then summed to obtain a combined power input., and then summing the individual power inputs for each beam set (each beam has a width of 0.625 ft) to obtain a combined power input. Therefore, N_p is given as 4 beams, A is given as 4.813 ft^2 per mixer beam, C is given as a unitless value of 1.8, and the three r values (one for each beam) are given as 3.771 ft, 5.021 ft, and 6.271 ft. The value for S is mixer speed dependent (the mixer motor is driven by a variable speed drive). The motor has a name-plate rpm of 1800 rpm at 60 Hz, and the total gear reduction ratio is 422.40:1, so the mixer speed S in rpm can be defined as

$$S = \frac{\frac{1800h}{60}}{422.4} \tag{2.5}$$

where h is the variable frequency drive output in Hz.

D. The stage 3 flocculators are horizontal shaft "paddle-wheel" mixers with 2 sets of paddles with a single variable speed drive controlled motor. Each set of paddles has 2 paddle arms mounted 180° apart, and each paddle arm has 3 beams mounted at 3.771 ft, 5.021 ft, and 6.271 ft from the shaft

centerline. Each beam length is 10.5 ft, and each beam has a width of 0.458 ft, for an area of each beam of 4.813 ft^2. The individual power inputs for each beam set are then summed to obtain a combined power input., and then summing the individual power inputs for each beam set (each beam has a width of 0.625 ft) to obtain a combined power input. Therefore, N_p is given as 4 beams, A is given as 4.813 ft^2 per mixer beam, C is given as a unitless value of 1.8, and the three r values (one for each beam) are given as 3.771 ft, 5.021 ft, and 6.271 ft. The value for S is mixer speed dependent (the mixer motor is driven by a variable speed drive). The motor has a name-plate rpm of 1800 rpm at 60 Hz, and the total gear reduction ratio is 471.07:1, so the mixer speed S in rpm can be defined as

$$S = \frac{\frac{1800h}{60}}{471.07} \tag{2.6}$$

where h is the variable frequency drive output in Hz.

In the same spreadsheet obtained from CMD Smith, Inc, the volumes of each rapid mix and flocculation basin were provided. The spreadsheet states that each rapid mixer has a volume of 551.0 ft^3, that each Stage 1 flocculation basin has a volume of 10,242 ft^3, and that each Stage 2 and Stage 3 flocculation basin has a volume of 6,482 ft^3.

As seen in formula 2.2 above, the power input also has a fluid density term ρ in units of slugs/ft^3. This fluid density, even for flocculation basins with large floc particles, is typically defined as the density of water at any given temperature since the volume of the water is so large when compared to the volume of particles. The density of water at a given temperature is typically obtained from a table. However, as discussed in the Materials and Methods section below, this method does not work well with Programmable Logic Controller (PLC) programming. Adding "tables" to a PLC and then interpolating between the table values is very memory intensive and requires extensive calculations in the PLC programming (personal knowledge). So, a single function was needed that provides a fluid density output based on an input of water temperature. Metgen's *Metrology Article N°18: Calculation of the Density of Water* provided a basic formula for use, with a temperature input in °C and a density output in kg/m^3. This formula was revised to produce an output in slugs/ft^3 by simply using the conversion factors of 1 slug = 14.5939 kg and 1 m^3 = 35.315 ft^3. The resulting formula (after combining constants) is:

$$\rho = \frac{(999.972)\left\{1-\left[\frac{\left(((t-3.983)^2)(t+301.797)\right)}{(522528.9(t+69.349))}\right]\right\}}{515.387} \tag{2.7}$$

where ρ is the density of water in slugs/ft^3 and t is the water temperature in °C.

In the spreadsheet provided by CDM Smith,Inc., the volumes (V in equation 2.1) of the rapid mixer basins and the volumes of each flocculation basin are provided. The spreadsheet states that each rapid mixer has a volume of 551.0 ft^3, that each Stage 1 flocculation basin has a volume of 10,242 ft^3, and that each Stage 2 and Stage 3 flocculation basin has a volume of 6,482 ft^3.

Using equations 2.2 through 2.7 above, the only variable not defined by an equation is the dynamic viscosity of water, μ. As with water density, this value is typically obtained from a table, but as discussed above, this method does not work well with PLC programming. The National Institute of Standards and Technology's *Dynamic Viscosity of Water*, and as corroborated in *Viscosity of Liquid Water in the Range -8°C to 150°C* (Kestin, Sokolov, and Wakeham, 2009) provided a basic formula for use, with a temperature input in °C and a viscosity output in Pa·sec, assuming a viscosity at 20 °C of 0.001002 Pa·sec. This formula was revised to produce an output in lb·sec/ft^2 by simply using the conversion factor of 1 Pa·sec = 0.020886 lb·sec/ft^2. The resulting formula (after combining constants) is:

$$\mu = (2.0928x10^{-5})\left\{10^{\left[\left(\frac{(20-t)\left\{1.2378-\left((1.303x10^{-3})(20-t)\right)+\left((3.06x10^{-6})((20-t)^2)\right)+\left(\left((2.55x10^{-8})((20-t)^3)\right)\right)\right\}}{t+96}\right)\right]}\right\} \quad (2.8)$$

where μ is the dynamic viscosity of water in lb·sec/ft2 and t is the water temperature in °C.

The velocity gradient curves for the Phipps & Bird jar testing apparatus were obtained from the Phipps & Bird website. These curves are simple charts, which were then methodically reproduced into a Microsoft Excel workbook so that a set of equations could be produced for use in matching the treatment plant's rapid mix and flocculation velocity gradients to the jar testing apparatus' jars (refer to the Materials and Methods Section below).

Formulas 2.1 through 2.8 above, along with the velocity gradient curves for the Phipps & Bird jar testing apparatus, are used in the development of the final velocity gradient formulas discussed in the Materials and Methods Section and in Appendixes 2 and 3 below.

2.2. Critiques of Camp and Stein's 1943 Velocity Gradient Formula

Modern research has increasingly critiqued Camp and Stein's Velocity Gradient Formula as being incorrect.

In Mark M. Clark`'s 1985 research paper *Critique of Camp and Stein's RMS Velocity Gradient*, the primary conclusions are that Camp and Stein's velocity gradient determinations are incorrect as they require that three-dimensional flow

characteristics be modeled by two-dimensional flows, and that although there may be a Mean Velocity Gradient for a particular flow, no real evidence exists on how to actually compute it.

In John L Cleasby's 1984 research paper *Is Velocity Gradient a Valid Turbulent Flocculation Parameter?*, he concludes that G is only valid for flocculation when the floc particles are smaller than the typical particle size observed in typical flocculation practices.

In Mooyoung Han and Desmond Lawler's 1992 research paper *The (Relative) Insignificance of G in Flocculation*, the conclusion is that the importance of the velocity gradient has typically been over-emphasized, and that it has much less significance than simply keeping the particles in suspension to allow collisions by Brownian motion and differential settling.

In Francisco Pedocchi and Ismael Peidra-Cueva's 2005 research paper *Camp and Stein's Velocity Gradient Formalization*, they conclude that Camp and Stein's root mean square velocity gradient is inaccurate as a parameter for complex nonuniform flows.

2.3. Water Temperature Effects on Flocculation

The temperature of the water has been shown in multiple research papers to have a major effect on the efficiency of flocculation.

In Hanson and Cleasby's 1990 research paper *The Effects of Temperature on Turbulent Flocculation*, the authors indicate that the water industry has a good working knowledge of the coagulation-flocculation process at water temperatures around 20 °C, but that much less is understood about the process temperatures less than 10 °C. Their research further indicated that a decreasing water temperature had adverse effects on turbidity removal due to changes in the characteristics of the floc as water temperature decreased.

In Morris and Knocke's 1984 research paper *Temperature Effect on the Use of Metal-Ion Coagulants for Water Treatment*, their primary conclusion was that water temperature has a large effect on turbidity removal when using metal-ion coagulants such that very low water temperature conditions reduce the efficiency of turbidity removal.

In Goula, Kostoglou, Larapantsios, and Zouboulis's 2008 research paper *The Effect of Influent Temperature Variations in a Sedimentation Tank for Potable Water Treatment – A Computational Fluid Dynamics Study*, the authors studied the effects on influent water temperature changes on turbidity in a circular radial flow sedimentation tank much like the sedimentation tanks used at the District's treatment plant. Using Computational Fluid Dynamics (CFD) techniques, they conclude that a rising influent temperature (as compared to the temperature of

the overall tank) can result in short-circuiting in the tank because the surface flow rate is greater than the effluent flow rate which then lowers the settling efficiency of the tank by as much as 23%. Their CFD study also indicates that as the warmer water continues to inflow (i.e. as the overall tank water temperature warms towards the influent water temperature), this effect gradually subsides. Their research further indicates that if the influent water temperature is colder than the overall tank temperature, there seems to be little to no effect on the turbidity removal efficiency.

2.4. Horizonal Radial Flow Clarification – Pros and Cons

In James K Edzwald's 2011 edition of *Water Quality and Treatment – A Handbook on Drinking Water* (9.28), it is postulated that horizontal radial flow clarification is attractive in theory, as the flow velocity decreases continuously as the fluid flows outward from the centrally located inlet, and that since the collection of settled water at the clarifier is typically a weir around the outer edge, there is a substantially large weir length which reduces weir loading rates.

However, it is also stated that the difference between the theory and the reality of radial flow clarification introduces some issues, as even very minor elevation differences in weir height around the edge of the tank can lead to differential flows (i.e., short-circuiting). Achieving a good flow distribution from a central inlet into a large open area can be extremely difficult in actual practice (9.28).

In Goula, Kostoglou, Larapantsios, and Zouboulis's 2008 research paper *The Effect of Influent Temperature Variations in a Sedimentation Tank for Potable Water Treatment – A Computational Fluid Dynamics Study*, as discussed above, influent water temperature can also influence short-circuiting. Their research also indicates that even wind speed can produce a short-circuiting effect.

2.5. Turbidity Effects of Lime Softening

In James K Edzwald's 2011 edition of *Water Quality and Treatment – A Handbook on Drinking Water* (13.61),the author indicates that the turbidity of the settled water is typically higher when using lime softening as compared to the turbidity of the settled water in coagulation-only plants, in that typical settled water turbidities when lime softening ranges from 2 to 5 ntu, and in some cases can exceed 10 ntu.

2.6. Mass Transfer Rate of CO_2

In James K Edzwald's 2011 edition of *Water Quality and Treatment – A Handbook on Drinking Water* (8.35 and 8.65), the author indicates that the rate of mass transfer of CO_2 at the air/water interface is typically very different when comparing full-scale treatment plant basins to laboratory batch reaction basins. The CO_2 transfer rate in the laboratory batch reaction basins is typically much

higher than in actual treatment plant basins due primarily to the much higher surface area to volume ratio in the laboratory basins (8.35 and 8.65).

2.7. Jar Tests versus Actual Plant Conditions

It can be difficult, if not impossible, to fully simulate the actual conditions in a full scale water treatment plant by using jar tests.

In Stanley and Smith's 1995 research paper *Measurement of Turbulent Flow in Standard Jar Test Apparatus*, the authors indicate that simulation of plant hydraulic conditions has been criticized and questioned many times, and that most research attempts to account for discrepancies by reasoning that the velocity gradient in a laboratory jar can be related to actual plant conditions by including some multiple of the root mean square velocity gradient. They further state that this multiple is typically obtained from chemical engineering studies for tanks that are very different in design from typical flocculation basins.

In Reed and Robinson's 1984 research paper *Similitude Interpretation of Jar Test Data*, the authors indicate that although jar testing is traditionally used by both designers and operations to evaluate water treatment parameters, the jar test can be inherently flawed by the lack of correlation between the jar test results and the actual plant conditions.

2.8. Clarifier Baffling

In Metcalf and Eddy's 2003 edition of *Wastewater Engineering – Treatment and Reuse*, the authors state that with a circular clarifier that has an overflow weir at the outer tank perimeter, baffling such as Stamford baffles should be used such that density currents, which can cause "wall climb" are re-directed back towards the tank center.

Although this type of baffling is more common in secondary clarifiers for wastewater treatment than in clarifiers at potable water treatment plants, the design of the District's clarifiers is very much like a secondary clarifier commonly found in wastewater plants. At many locations around the outer perimeter of the District's clarifiers, the overflow weir is effectively suspended just inside the outer wall, and overflow into this weir occurs from both sides (see Figure 2.1 below, which shows a weir support, with the weir itself shown cross-hatched in the center). The inner side of the weir is effectively baffled by the flat bottom of the weir, but the outer side is not baffled at all, which means that "wall climb" can result in floc particles entering the weir. A Stamford baffle could help to mitigate this effect.

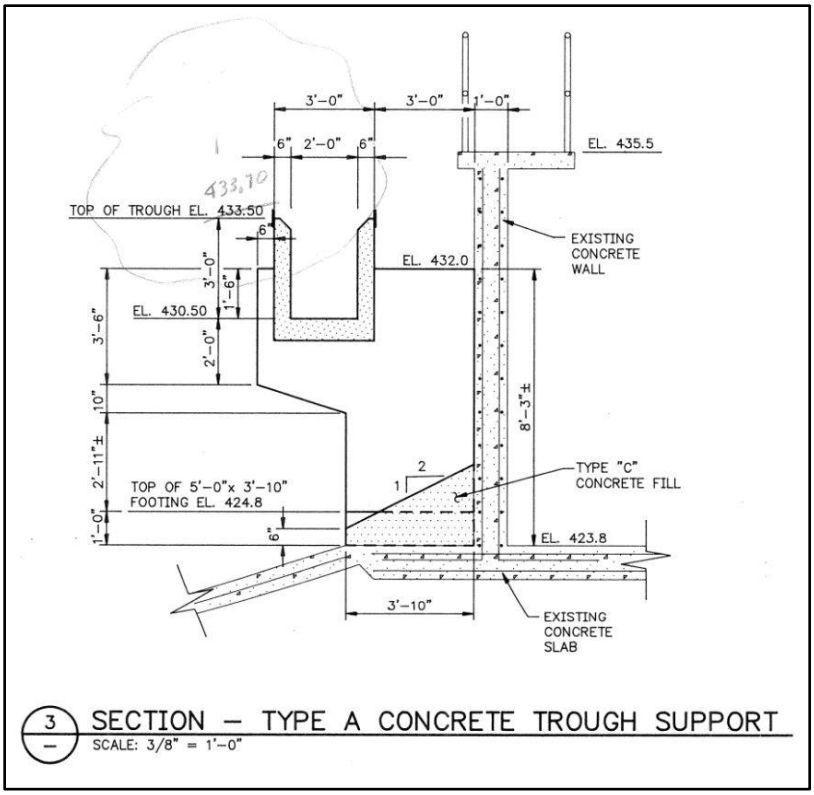

Figure 2.1: Clarifier Effluent Weir Section View

3. Materials and Methods

Because the treatment plant had historically not run jar tests, the first step in the optimization process was research. Somewhat surprisingly, we could find no cases of research where jar-test optimization of chemical feed was performed while using two different chemicals simultaneously. Therefore, we had to produce our own test procedures from scratch.

3.1. Materials used during the optimization process:

A. Phipps & Bird PB-900 Jar Testing Apparatus;

B. Hach 2100N Laboratory Turbidity Analyzer;

C. Hach HQ Series Laboratory pH Analyzer;

D. Primary actual treatment chemicals obtained from the District's storage tanks (ferric sulfate and calcium hydroxide);

E. Alternate treatment chemical obtained from the District's storage tanks (sodium hydroxide); and

F. Alternate treatment chemical provided and used by Global Specialty Chemicals (a proprietary poly ferric sulfate blend).

3.2. Methods, Part 1

The following test procedures were originally developed and used in the initial testing:

A. Establish a repeatable, easy-to-use method to match jar velocity gradients and mixing times to the actual plant conditions. This is important in actual plant operations to prevent operational mistakes when relying on complex formulas for dosage and/or dilution calculations.

Fortunately, since the flocculation systems were new, velocity gradient design data and basin volumetric data was available from the design engineer and from the rapid mixer and flocculation mixer manufacturers. This data, along with the formulas obtained for the power input (CDM Smith, 2012), the dynamic viscosity of water (NIST, 2012) and the density of water (Metgen, 2012) as described in the Literature Review Section above (formulas 2.2 through 2.8) was used to create a set of formulas originating with the basic velocity gradient equation formula 2.1 (Camp and Stein, 1943) to determine the current velocity gradients in each plant basin where the only independent variables are the plant's mixer speeds (each mixer is operated via a variable frequency drive) and the temperature of the water. The derivations of these formulas are included

in Appendix 3. **NOTE:** For the rapid mixers only, the data provided by CDM Smith used a Drag Coefficient of 1.8, which was the same coefficient used in their flocculator calculations. However, when the formulas were derived, it was found that the results did not properly match the velocity gradient tables provided by the rapid mixer manufacturer (since these tables are considered proprietary information by the manufacturer, they are not included here). As a result, the drag coefficient for the rapid mixers was altered from a value of 1.8 to a value of 0.9605. The resulting formula results matched the rapid mixer manufacturer's tables almost precisely with a maximin difference of 0.1 sec^{-1}. CDM Smith verbally acknowledged their error.

Then a second set of formulas was derived based on charts from Phipps-Bird (the manufacturer of the plant's jar test mechanism) that generates the jar mixer speed required to match the velocity gradient of the basin in question. The derivation of these formulas are included in Appendix 2. **NOTE:** Since the only information available from Phipps-Bird was a chart, the data on the chart was manually imported into a Microsoft Excel spreadsheet and then regressed using Excel's Trendline functionality to obtain a family of formulas for velocity gradient versus paddle speed. It was experimentally determined that the best Trendline curve fit was a fourth-order polynomial function ($Ax^4 + Bx^3 + Cx^2 + Dx$). Each curve in the family is based on a different water temperature (5°C, 10°C, 15°C, 20°C, 25°C, and 30°C curves were provided on the Phipps-Bird Chart). The A, B, C, and D coefficients for these six curves were then individually regressed to obtain individual formulas for A, B, C, and D. The results were then combined into final formulas for Velocity Gradients and Jar Speeds.

One last set of formulas was derived to calculate the detention time for each basin, based on design data (CDM Smith, 2012). Since the detention time formulas are simply the volume of the basin in gallons divided by the flow rate in gpm, derivations for these equations are not shown. The resulting formulas for each basin are:

Definitions:

G = velocity gradient in sec^{-1}
t = water temperature in °C
h = mixer/flocculator motor speed in hertz
S = jar tester paddle speed in rpm
T = detention time in either seconds (for rapid mixers) or minutes (for flocculators)
Q = water flow rate in gpm

For the plant's rapid mixers:

$$G = (1.7418)\left\{\frac{\left[1-\left(\frac{\left(((t-3.983)^2)(t+301.797)\right)}{(522528.9(t+69.3488))}\right)\right](h^3)}{\left[\frac{(20-t)\left(1.2378-\left((1.303e^{-3})(20-t)\right)+\left((3.06e^{-6})((20-t)^2)\right)+\left(\left((2.55e^{-8})((20-t)^3)\right)\right)\right)}{(t+96)}\right]_{10}}\right\}^{0.5} \quad (3.1)$$

$$\boldsymbol{T = \frac{247288.8}{Q}} \quad (3.2)$$

For the plant's stage 1 flocculators:

$$G = (2.1260)\left\{\frac{\left[1-\left(\frac{\left(((t-3.983)^2)(t+301.797)\right)}{(522528.9(t+69.3488))}\right)\right](h^3)}{\left[\frac{(20-t)\left(1.2378-\left((1.303e^{-3})(20-t)\right)+\left((3.06e^{-6})((20-t)^2)\right)+\left(\left((2.55e^{-8})((20-t)^3)\right)\right)\right)}{(t+96)}\right]_{10}}\right\}^{0.5} \quad (3.3)$$

$$\boldsymbol{T = \frac{74759.61}{Q}} \quad (3.4)$$

For the plant's stage 2 flocculators:

$$G = (1.3811)\left\{\frac{\left[1-\left(\frac{\left(((t-3.983)^2)(t+301.797)\right)}{(522528.9(t+69.3488))}\right)\right](h^3)}{\left[\frac{(20-t)\left(1.2378-\left((1.303e^{-3})(20-t)\right)+\left((3.06e^{-6})((20-t)^2)\right)+\left(\left((2.55e^{-8})((20-t)^3)\right)\right)\right)}{(t+96)}\right]_{10}}\right\}^{0.5} \quad (3.5)$$

$$\boldsymbol{T = \frac{48545.2}{Q}} \quad (3.6)$$

For the plant's stage 3 flocculators:

$$G = (1.1727)\left\{\frac{\left[1-\left(\frac{\left(((t-3.983)^2)(t+301.797)\right)}{(522528.9(t+69.3488))}\right)\right](h^3)}{\left[\frac{(20-t)\left(1.2378-\left((1.303e^{-3})(20-t)\right)+\left((3.06e^{-6})((20-t)^2)\right)+\left(\left((2.55e^{-8})((20-t)^3)\right)\right)\right)}{(t+96)}\right]_{10}}\right\}^{0.5} \quad (3.7)$$

$$\boldsymbol{T = \frac{48545.2}{Q}} \quad (3.8)$$

For the Phipps Bird jar testing apparatus:

$$\boldsymbol{G = \left(\left((1.380e^{-10})(t) + 3.545e^{-9}\right)(S^4)\right) + \left(\left((-5.860e^{-8})(t) - 5.366e^{-6}\right)(S^3)\right) + \left(\left((1.364e^{-5})(t) + 3.215e^{-3}\right)(S^2)\right) + \left(\left((6.500e^{-3})(t) + 3.115e^{-1}\right)(S)\right)} \quad (3.9)$$

$$S = \left(\left(\left((-4.410e^{-11})(t^2)\right) + (3.297e^{-9})(t) - 8.271e^{-8}\right)(G^4)\right) +$$
$$\left(\left(\left((2.271e^{-8})(t^2)\right) - (1.871e^{-6})(t) + 5.562e^{-5}\right)(G^3)\right) +$$
$$\left(\left(\left((-3.695e^{-6})(t^2)\right) + (3.516e^{-4})(t) - 1.359e^{-2}\right)(G^2)\right) +$$
$$\left(\left(\left((2.401e^{-4})(t^2)\right) - (3.091e^{-2})(t) + 2.365\right)(G)\right)$$

(3.10)

Formulas 3.1 through 3.10 above were then incorporated into the plant's Supervisory, Control, and Data Acquisition (SCADA) system such that a computer screen automatically displays the velocity gradient, mixing time, and matching jar speed for each basin, as shown in Figure 3.1 below (When this screen shot from the plant's SCADA system was obtained, Train B was not in operation, so no detention times are shown for the train). The exact derivations for each of the basins' formulas are shown in Appendix 3 below, and the formula derivations for the jar test apparatus are shown in Appendix 2 below.

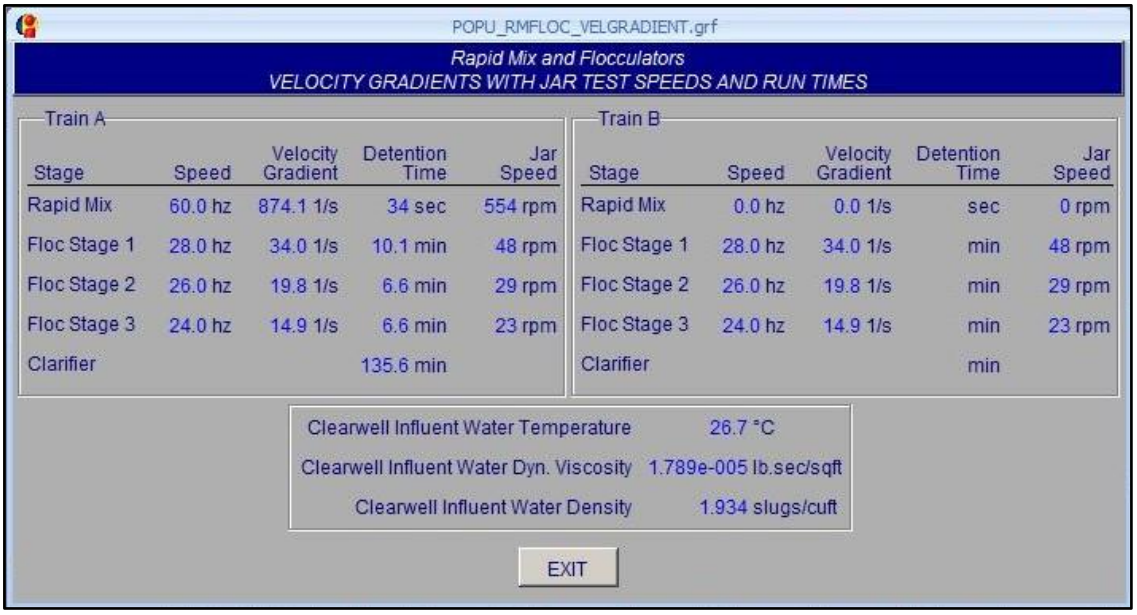

Figure 3.1: SCADA System Velocity Gradient Screen

Plant operators can therefore use the SCADA computer screen shown in Figure 3.1 above to easily determine the jar test speeds and times to theoretically match the jar tester's velocity gradients and detention times to the actual treatment plant's velocity gradients and detention times.

B. Utilize the actual plant chemicals in jar tests by establishing a repeatable, easy-to-use dilution method for both the ferric sulfate and the calcium

hydroxide (the treatment plant feeds these chemicals into the water stream 'neat', i.e., with no dilution water). Utilization of the actual bulk chemicals used in the treatment process should eliminate uncertainties that could be introduced into the tests by using reagent-grade chemicals from a lab, as impurities and solution strengths are typically much better controlled in reagent-grade chemicals versus mass-produced chemicals for use in actual water treatment.

Based on the chemical supplier's SDS information for the plant's bulk calcium hydroxide and ferric sulfate, the following dilution methods for the plant's bulk chemicals for making stock solutions for use in jar tests were developed (see Appendix 4 for derivations and details):

For Ferric Sulfate (60% Solution):

Put 10.77 mL of bulk plant ferric sulfate into a 1000 mL beaker and fill with distilled water to the 500 mL line and cover. As this is a true solution, no stirring after makeup is required. This results in 1 mL of stock solution equaling a dosage of 10 mg/L as Fe^{3+} when added to a 2 liter jar.

For Calcium Hydroxide (40% solution):

Put 20.08 mL of bulk plant calcium hydroxide into a 1000 mL beaker and fill with distilled water to the 500 mL line. As this is technically a suspension rather than a solution, cover the stock "solution" and stir continuously with a magnetic stirring mechanism. This results in 1 mL of stock solution equaling a dosage of 10 mg/L as $Ca(OH)_2$ when added to a 2 liter jar.

For Calcium Hydroxide (25.9% solution):

Put 32.76 mL of bulk plant calcium hydroxide into a 1000 mL beaker and fill with distilled water to the 500 mL line. As this is technically a suspension rather than a solution, cover the stock "solution" and stir continuously with a magnetic stirring mechanism. This results in 1 mL of stock solution equaling a dosage of 10 mg/L as $Ca(OH)_2$ when added to a 2 liter jar.

C. Run a jar test series, adding only ferric sulfate, to determine the best turbidity results (at a reasonable chemical cost).

D. Using the best turbidity versus chemical cost from the jar test using only ferric sulfate, run a jar test series with the ferric sulfate fixed at this dosage in each jar while varying the calcium hydroxide dosage to determine the dosage that produces the best combination of pH, turbidity, and alkalinity, while also considering the following:

1. Chemical costs (if a large chemical dosage increase results in only a small increase in water quality, then that increase may or may not be feasible).

2. Maintenance requirements (if a chemical dosage change or a change in the type of chemical(s) used results in an increase in required maintenance, or in a decrease in reliability, then even if the change produces desirable results, the change may or may not be feasible).

3. Safety: The safety of both plant personnel and the public must be considered (a chemical or chemical dosage change that results in higher risk to employees and/or the public may or may not be feasible).

3.3. Methods, Part 2

The original test procedures were modified slightly after converting from a nominal 40% calcium hydroxide solution to a nominal 30% calcium hydroxide solution as described in the Results Sections below:

A. Parts A through C of the original test procedures described above were retained.

B. Rather than attempting to vary the calcium hydroxide dosage to obtain a "best" simultaneous result of turbidity, pH and alkalinity, the test should attempt to determine the proper dosage of calcium hydroxide for obtaining a pH in the range of 9.5 to 10.0 and an alkalinity in the range of 40 to 60 mg/L as $CaCO_3$ as measured at the effluent of the flocculators. The pH range was chosen because historic plant operational data shows that these values will consistently produce a plant discharge pH of between 8.9 and 9.2, with an alkalinity below 60 mg/L as $CaCO_3$. As stated in the Background and Objectives Section above, the plant discharge alkalinity must be kept at 60 mg/L as $CaCO_3$ or below to satisfy TCEQ regulation TAC 290.112.f.3.C.iii, and the pH range is required to minimize system nitrification and scaling.

4. Results

As previously stated, the treatment plant utilizes a radial flow clarification process. In theory, radial flow clarification should be very effective, primarily due to the constant decrease in velocity as the fluid flows outward into an increasing cross-sectional volume (Edzwald, 2011). However, achieving a consistent flow distribution from a central point into a large area can be problematic, and even minor elevation variances in the effluent weir across a large diameter tank can introduce differential flow or short-circuiting in and/or around a tank (Edzwald, 2011). "Wall-climb" of suspended particles at the effluent weir can also be problematic (personal observation). In addition, the turbidity of the settled water in a lime-softening plant is typically higher than those found in coagulation plants that do not lime soften, with a typical settled water turbidity in the range of 2 to 5 ntu, and in some cases over 10 ntu (Edzwald, 2011). Historic plant data confirms that the range of settled water turbidities falls within these ranges. Therefore, the target value for clarifier effluent turbidity was set to a range of 3.0 to 8.0 ntu. Due to the plant being almost out of compliance as a result of high plant effluent turbidities, alkalinity values were not considered as important during the early optimization attempts described in Section 4.1 below, but were still desired to be in the 40 to 65 mg/L as $CaCO_3$ range. **NOTE:** Due to the size of the raw data for the jar and plant testing presented in the sections below, much of the raw tabular data used to create the charts presented is not included in this report. This data is available upon request.

4.1. Initial Optimization Attempts during the Compliance Crisis

NOTE: It should be understood that during this portion of the optimization process, the methods described in the Materials and Methods Section above were not yet developed. This portion of the optimization process was performed in 'Crisis mode' in a hurried attempt to bring the treatment plant back into compliance with TCEQ turbidity regulations.

After the unsuccessful plant trials discussed in the Plant History Section above, intensive jar testing was begun in an attempt to bring the plant back into some form of operational control. At this point, time was critical, so matching of velocity gradients and detention times between the jars and the actual plant conditions was only very roughly estimated. During these initial tests, ferric sulfate was being fed into the plant's rapid mixer basins (at the basin inlet), and calcium hydroxide was being fed into the plant's stage 1 flocculation basin (at the basin inlet). The results showed an unacceptable water quality. In the jars, ferric sulfate dosages ranging from 15 to 35 mg/L as Fe^{3+} were rapid mixed, and then calcium hydroxide was added at 40 to 140 mg/L as $Ca(OH)_2$ at the beginning of flocculation stage 1. Only a single jar (out of 18) gave turbidity results less than 10 ntu. The average of the turbidities was 34.6 ntu. Most of the total alkalinity readings in the jars were above 60 mg/L as $CaCO_3$, with an average of 66 mg/L as $CaCO_3$. The pH ranged from 8.91 to 10.96, with an average of 9.52. These initial tests are summarized in

Tables 4.1 through 4.4 and Figures 4.1 through 4.4 below. Note that the water temperature for all of these tests was 21.0°C.

In the first jar set (Table 4.1 and Figure 4.1), the ferric sulfate dosage was fixed at 25 mg/L as Fe^{3+}, and the calcium hydroxide was varied from 40 to 120 mg/L as $Ca(OH)_2$. Interestingly, as the calcium hydroxide dose was increased, the turbidity also increased, as did the pH and the Total Alkalinity.

In the second jar set (Table 4.2 and Figure 4.2), the calcium hydroxide dosage was fixed at 60 mg/L as $Ca(OH)_2$, and the ferric sulfate dosage was varied from 15 to 35 mg/L as Fe^{3+}. In this set of jars, as the ferric sulfate dosage was increased, the turbidity, alkalinity, and pH tended to decrease. The turbidities were still far too high, but the alkalinity values were acceptable for ferric sulfate dosages of 25, 30, and 35 mg/L as Fe^{3+}. From the chart in Figure 4.2, it appeared that the alkalinity would drop to 60 mg/L as $CaCO_3$ at about a 23 mg/L as Fe^{3+} dosage of ferric sulfate.

So, for the third jar set (Table 4.3 and Figure 4.3), the ferric sulfate dosage was fixed at 23 mg/L as Fe^{3+}, and the calcium hydroxide dosage was varied from 60 to 140 mg/L as $Ca(OH)_2$. In this set of jars, the alkalinity values were in the acceptable range for calcium hydroxide dosages of 120 and 140 mg/L as $Ca(OH)_2$, but the turbidity values climbed rapidly as the calcium hydroxide dosage was increased. Somewhat surprisingly, the pH stayed relatively constant, with values ranging only from a low of 8.91 to a high of 9.12.

A fourth jar set (Table 4.4 and Figure 4.4) was then run using the same parameters as jar set 3 to see if there would be any repeatability. However, two things occurred: first, the paddles in jars 4 and 5 stopped turning (it was determined after the fact that the set screws holding the shafts had loosened), and second, due to a mistake, the first jar was accidentally dosed with both ferric sulfate and calcium hydroxide in the rapid mix. However, this “mistake” proved to be very advantageous. As shown in the results, this jar had a turbidity of only 8.2 ntu, whereas jars 2 and 3 still had turbidities well above 10 ntu. Jars 2 and 3 also indicated a lack of repeatability between jar set 3 and jar set 4 as seen by the pH and Alkalinity values. However, this lack of repeatability was not investigated at the time as the focus was on the result of jar 1, since the turbidity of this jar was so low.

Jar #	Lime Dosage (mg/L as $Ca(OH)_2$)	Ferric Dosage (mg/L as Fe^{3+})	pH	Turbidity (ntu)	Total Alkalinity (mg/L as $CaCo_3$)	Water Temperature (°C)
1	40	25	9.50	36.5	56	21
2	60	25	9.94	49.9	56	21
3	80	25	10.44	55.4	65	21
4	100	25	10.77	62.0	77	21
5	120	25	10.96	62.0	89	21

Table 4.1: Initial Test Results (Ferric Dosage Fixed at 25 mg/L as Fe3+)

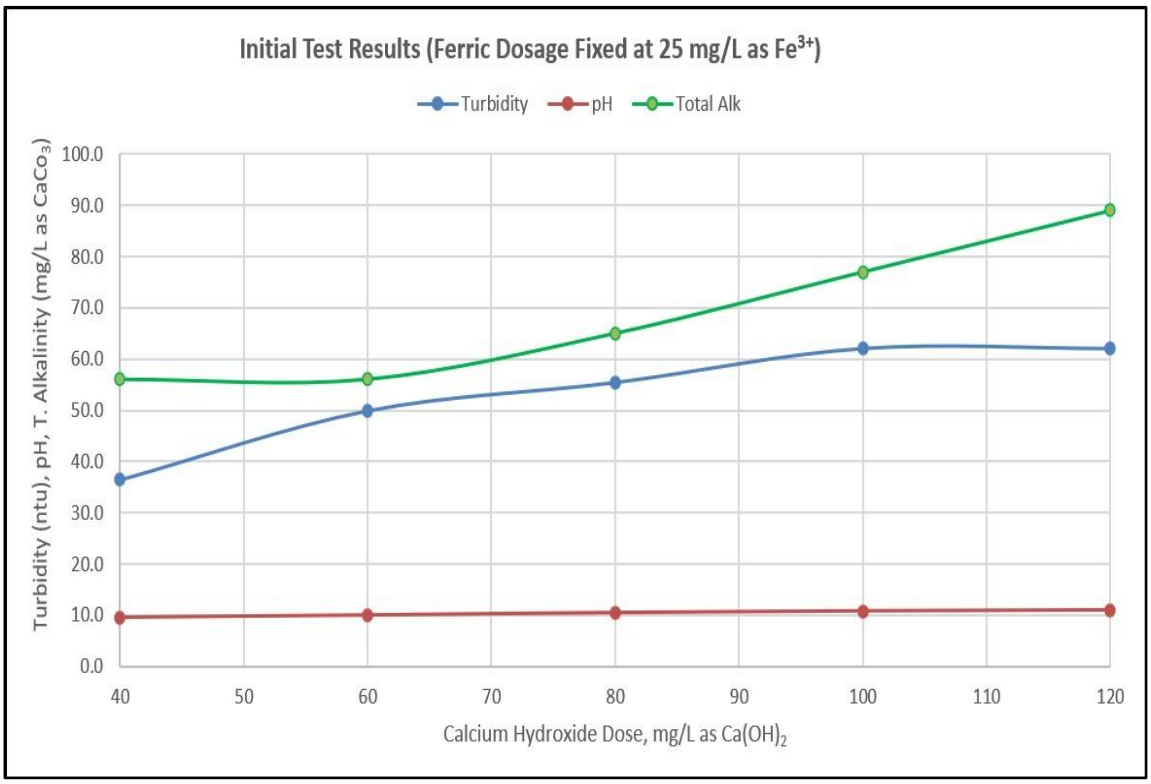

Figure 4.1: Initial Test Results (Ferric Dosage Fixed at 25 mg/L as Fe^{3+})

Jar #	Lime Dosage (mg/L as $Ca(OH)_2$)	Ferric Dosage (mg/L as Fe^{3+})	pH	Turbidity (ntu)	Total Alkalinity (mg/L as $CaCo_3$)	Water Temperature (°C)
1	60	15	9.70	45.1	74	21
2	60	20	9.29	34.0	64	21
3	60	25	9.21	29.8	57	21
4	60	30	9.12	30.5	56	21
5	60	35	9.03	26.0	58	21

Table 4.2: Initial Test Results (Lime Dosage Fixed at 60 mg/L as $Ca(OH)_2$)

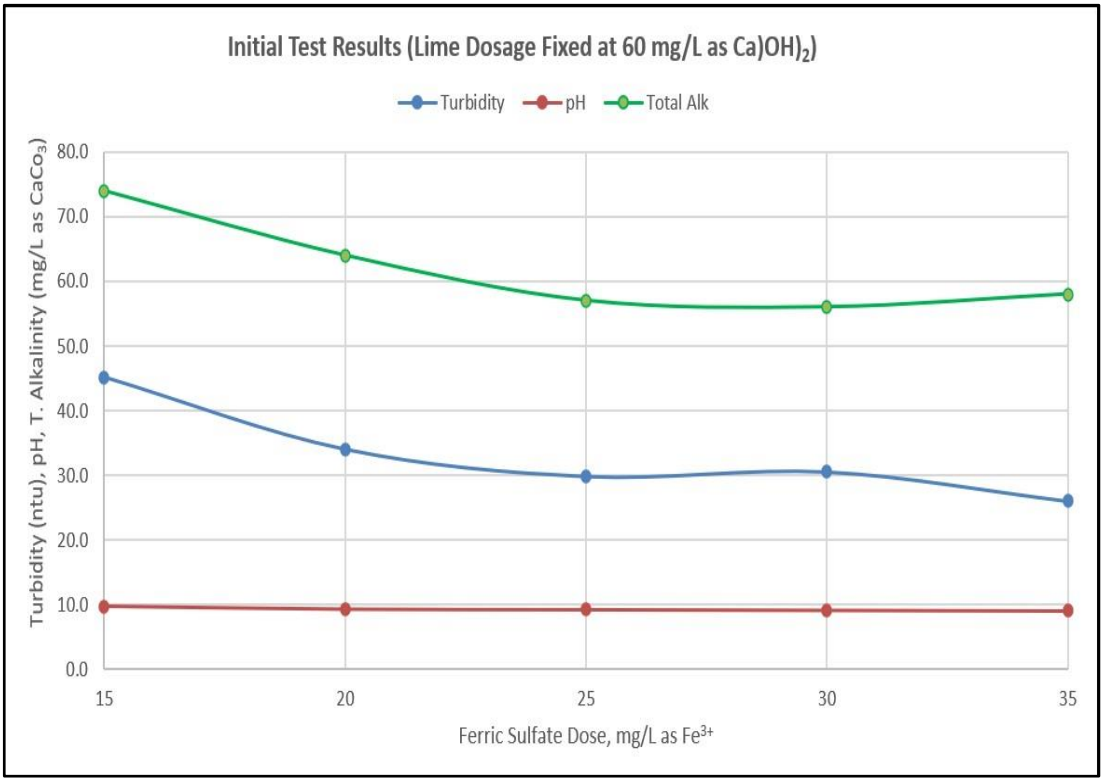

Figure 4.2: Initial Test Results (Lime Dosage Fixed at 60 mg/L as $Ca(OH)_2$)

Jar #	Lime Dosage (mg/L as $Ca(OH)_2$)	Ferric Dosage (mg/L as Fe^{3+})	pH	Turbidity (ntu)	Total Alkalinity (mg/L as $CaCo_3$)	Water Temperature (°C)
1	60	23	9.03	14.0	91	21
2	80	23	8.91	21.3	78	21
3	100	23	8.93	28.5	62	21
4	120	23	9.05	34.2	59	21
5	140	23	9.12	52.0	40	21

Table 4.3: Initial Test Results (Ferric Dosage Fixed at 23 mg/L as Fe3+), Jar Set 1

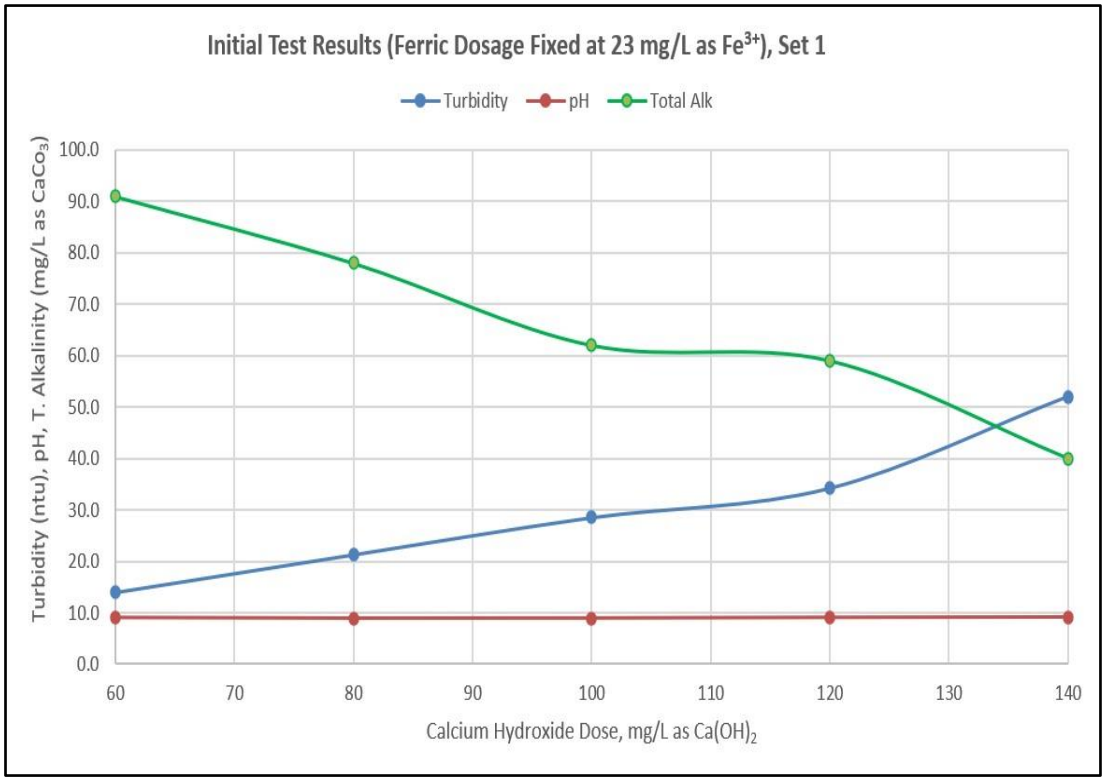

Figure 4.3: Initial Test Results (Ferric Dosage Fixed at 23 mg/L as Fe^{3+}), Jar Set 1

Jar #	Lime Dosage (mg/L as $Ca(OH)_2$)	Ferric Dosage (mg/L as Fe^{3+})	pH	Turbidity (ntu)	Total Alkalinity (mg/L as $CaCo_3$)	Water Temperature (°C)
1	60	23	9.30	8.2	90	21
2	80	23	9.30	14.1	67	21
3	100	23	9.81	18.9	50	21

Table 4.4: Initial Test Results (Ferric Dosage Fixed at 23 mg/L as Fe3+), Jar Set 2

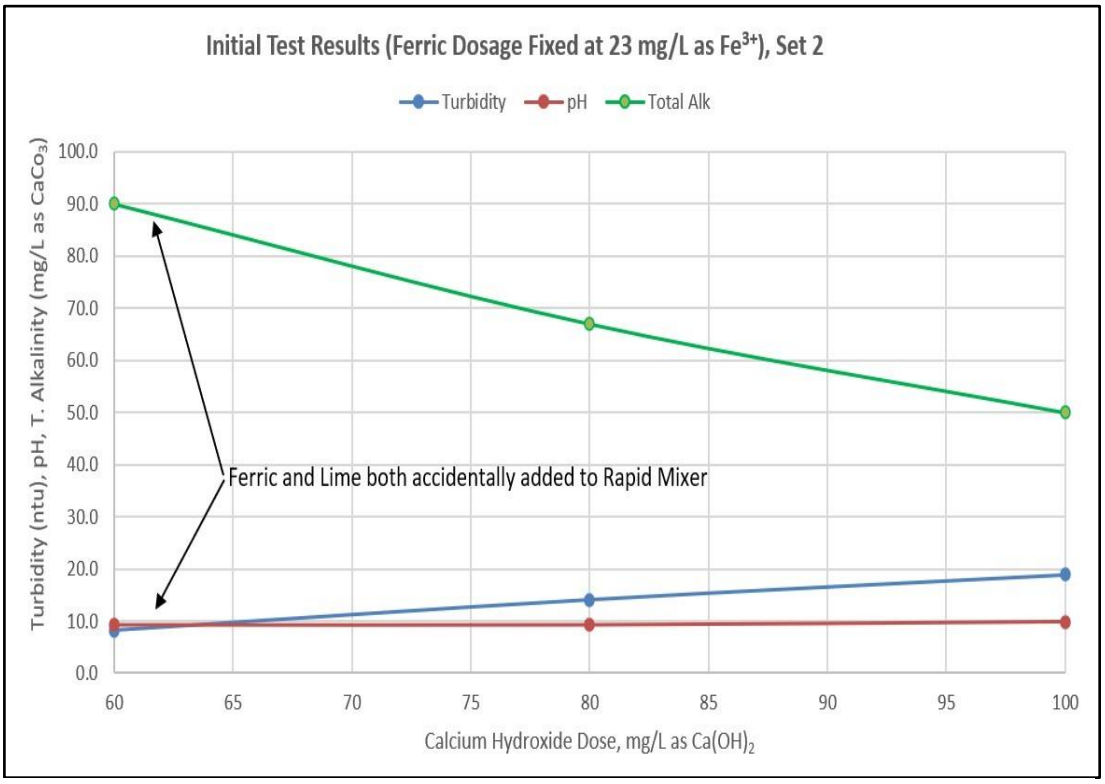

Figure 4.4: Initial Test Results (Ferric Dosage Fixed at 23 mg/L as Fe^{3+}), Jar Set 2

Based on the results from the one "mistake" jar, additional jar tests were performed. In these tests, both the ferric sulfate and the calcium hydroxide were intentionally added to the rapid mix portion (20 to 60 mg/L as Fe^{3+} of ferric sulfate and 40 to 80 mg/L as $Ca(OH)_2$ of calcium hydroxide). The results of this series of tests are shown in Tables 4.5 through 4.8 and Figures 4.5 through 4.8 below. As shown in the figures, the average turbidity dropped from 34.6 ntu in the initial series of tests to 7.0 ntu in this series of tests, and the average pH dropped from 9.52 to 9.44. Interestingly (almost assuredly as a result of coincidence), the average total alkalinity remained at 66 mg/L as $CaCO_3$. The water temperatures for this set of jar tests were all between 21 and 23°C.

Jar #	Lime Dosage (mg/L as $Ca(OH)_2$)	Ferric Dosage (mg/L as Fe^{3+})	pH	Turbidity (ntu)	Total Alkalinity (mg/L as $CaCo_3$)	Water Temperature (°C)
1	60	20	9.66	4.6	54	21
2	60	25	9.58	5.8	50	21
3	60	30	9.34	2.5	58	21
4	60	35	9.36	3.9	57	21
5	60	40	9.35	6.6	52	21

Table 4.5: Initial Test Results (All Chemicals to RM, Lime Dose Fixed at 60 mg/L as $Ca(OH)_2$)

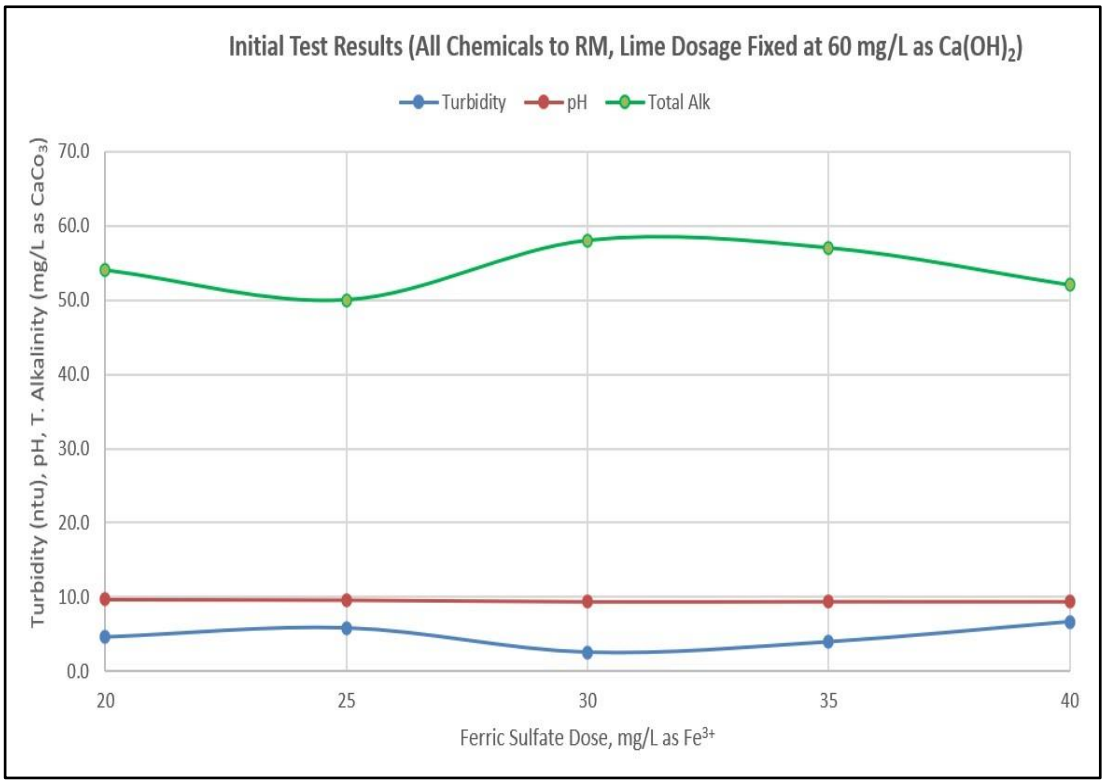

Figure 4.5: Initial Test Results (All Chemicals to RM, Lime Dose Fixed at 60 mg/L as $Ca(OH)_2$)

Jar #	Lime Dosage (mg/L as $Ca(OH)_2$)	Ferric Dosage (mg/L as Fe^{3+})	pH	Turbidity (ntu)	Total Alkalinity (mg/L as $CaCo_3$)	Water Temperature (°C)
1	70	20	9.41	14.1	67	22
2	70	25	9.33	11.0	70	22
3	70	30	9.30	10.0	67	22
4	70	35	9.18	10.6	66	22
5	70	40	9.44	10.7	48	22

Table 4.6: Initial Test Results (All Chemicals to RM, Lime Dose Fixed at 70 mg/L as $Ca(OH)_2$)

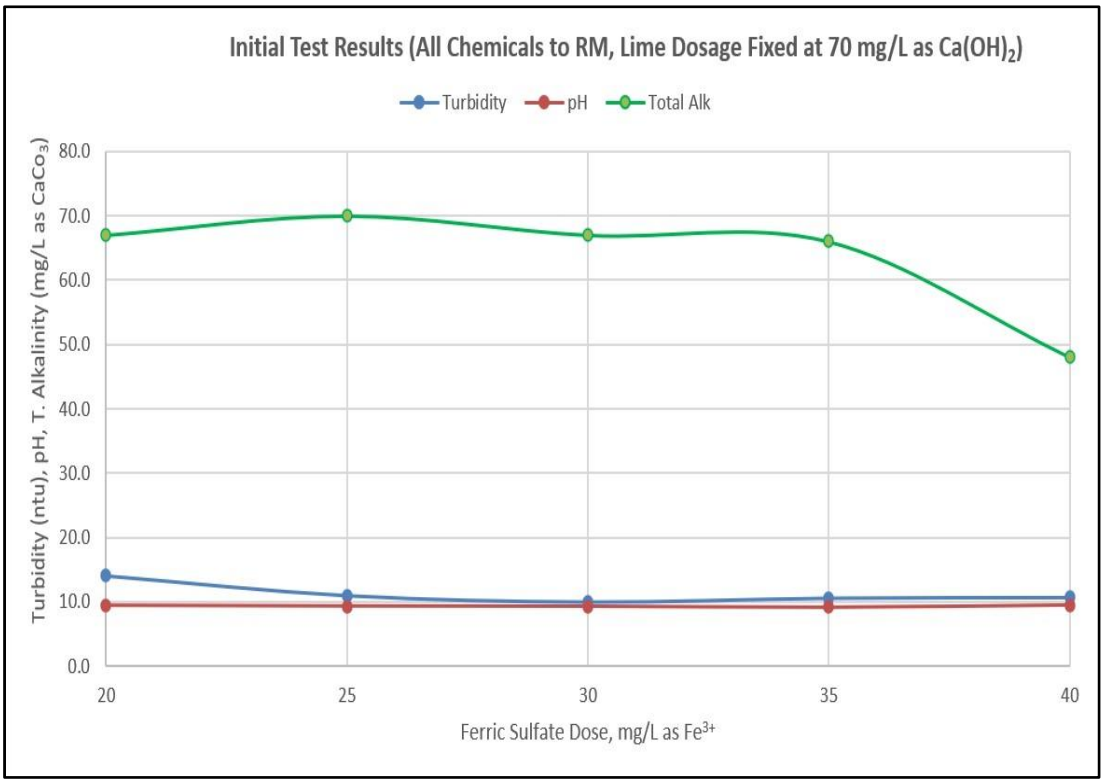

Figure 4.6: Initial Test Results (All Chemicals to RM, Lime Dose Fixed at 70 mg/L as $Ca(OH)_2$)

Jar #	Lime Dosage (mg/L as $Ca(OH)_2$)	Ferric Dosage (mg/L as Fe^{3+})	pH	Turbidity (ntu)	Total Alkalinity (mg/L as $CaCo_3$)	Water Temperature (°C)
1	80	20	9.45	13.1	77	22
2	80	30	9.34	11.4	80	22
3	80	40	9.29	9.8	79	22
4	80	50	9.18	10.0	79	22
5	80	60	9.16	4.9	86	22

Table 4.7: Initial Test Results (All Chemicals to RM, Lime Dose Fixed at 80 mg/L as $Ca(OH)_2$)

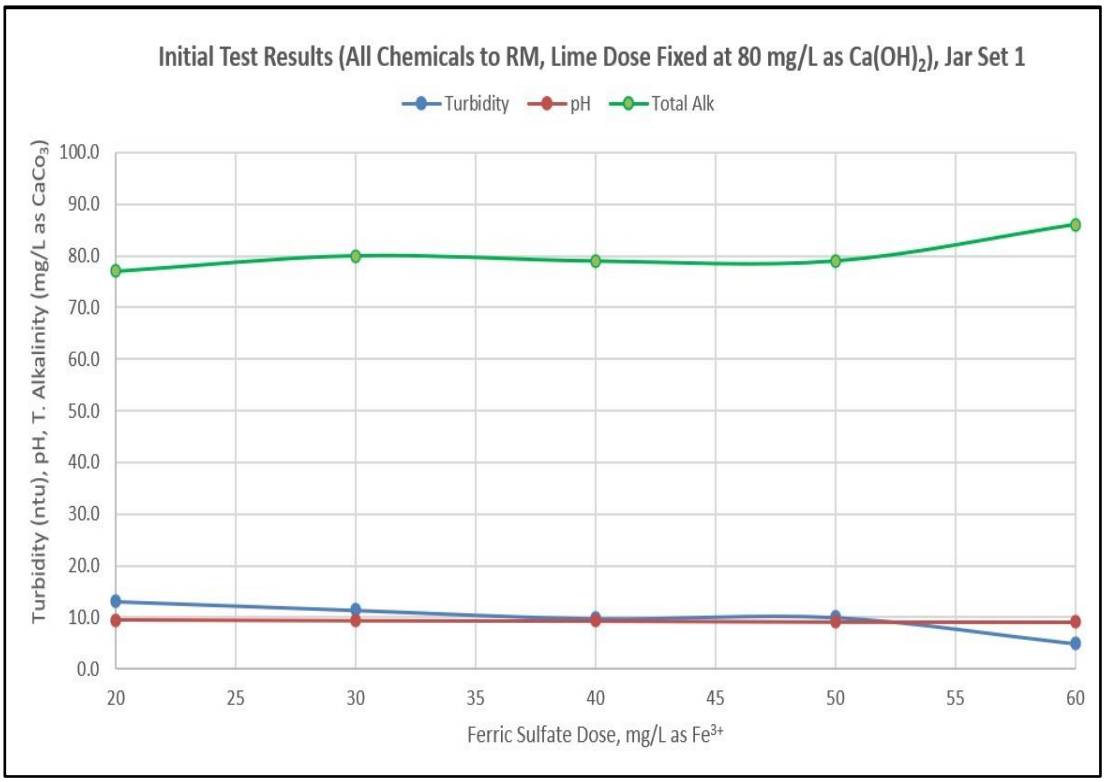

Figure 4.7: Initial Test Results (All Chemicals to RM, Lime Dose Fixed at 80 mg/L as $Ca(OH)_2$)

Jar #	Lime Dosage (mg/L as $Ca(OH)_2$)	Ferric Dosage (mg/L as Fe^{3+})	pH	Turbidity (ntu)	Total Alkalinity (mg/L as $CaCo_3$)	Water Temperature (°C)
1	80	20	9.87	2.0	60	22
2	80	22	9.80	3.8	57	23
3	80	24	9.78	3.0	57	23
4	40	26	9.26	1.1	88	23
5	80	28	9.66	1.3	58	23

Table 4.8: Initial Test Results (All Chemicals to RM, Lime Dose Fixed at 80 mg/L as $Ca(OH)_2$)

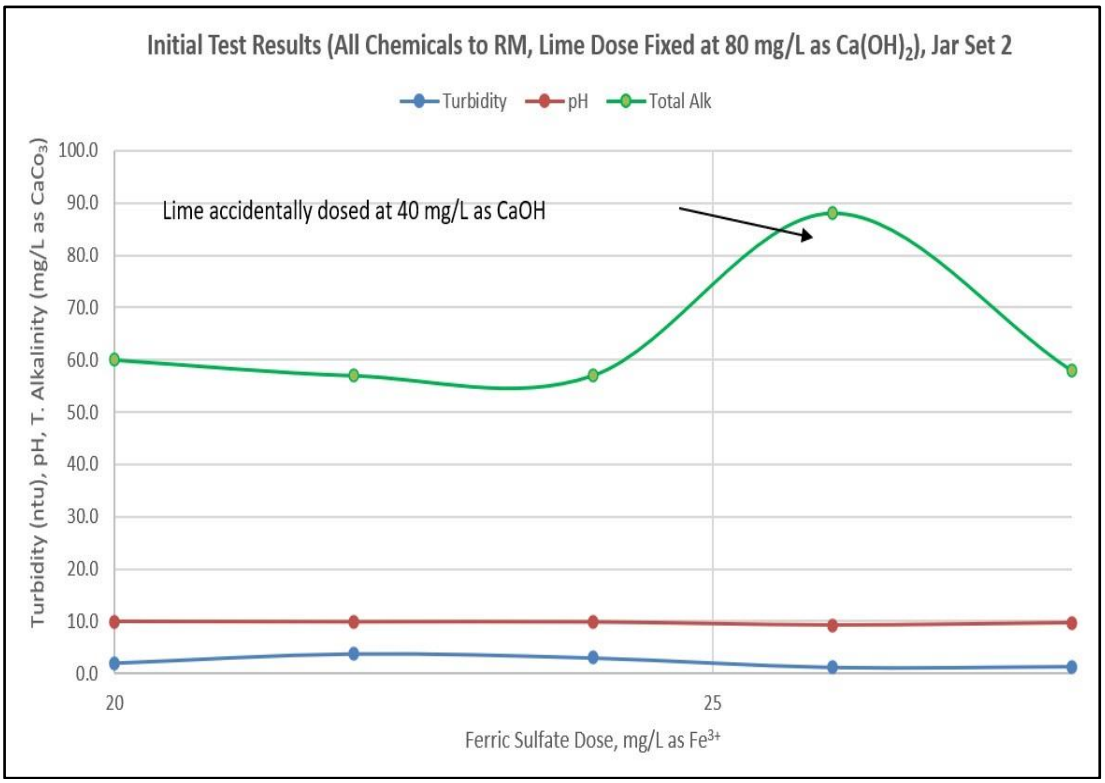

Figure 4.8: Initial Test Results (All Chemicals to RM, Lime Dose Fixed at 80 mg/L as $Ca(OH)_2$)

In the first set of jars in this series of tests (Table 4.5 and Figure 4.5 above), the calcium hydroxide dosage was fixed at 60 mg/L as $Ca(OH)_2$, and the ferric sulfate dosage was varied from 20 to 40 mg/L as Fe^{3+}. The resulting alkalinity values ranged between 50 and 58 mg/L as $CaCO_3$, the pH values ranged from a high of 9.66 (at the lowest ferric sulfate dosage) to a low of 9.35 (at the highest ferric sulfate dosage), and most importantly, the turbidity values were all less than 8.0, with the lowest turbidity (2.5 ntu) occurring at a ferric sulfate dosage of 30 mg/L as Fe^{3+}. Interestingly, the turbidity values actually increased as the ferric sulfate dosage was increased above 30 mg/L as Fe^{3+}.

In the second set of jars in this series of tests (Table 4.6 and Figure 4.6 above), the calcium hydroxide dosage was fixed at 70 mg/L as $Ca(OH)_2$, and the ferric sulfate dosage was varied from 20 to 40 mg/L as Fe^{3+}. The resulting alkalinity values ranged between 48 and 70 mg/L as $CaCO_3$, the pH values ranged from a high of 9.44 (at the highest ferric sulfate dosage) to a low of 9.18 (at the second-highest ferric sulfate dosage), and the turbidity values, although they were all at 10 ntu or greater, were still much lower than when the ferric sulfate was being fed to the rapid mixer and the lime was being fed to the first flocculation stage.

In the third set of jars in this series of tests (Table 4.7 and Figure 4.7 above), the calcium hydroxide dosage was fixed at 80 mg/L as $Ca(OH)_2$, and the ferric sulfate dosage was varied from 20 to 60 mg/L as Fe^{3+}. The resulting alkalinity values were higher than the alkalinity values from the first two sets of jars in this series, ranging 77 and 86 mg/L as $CaCO_3$. The pH values ranged from a high of 9.45 (at the lowest ferric sulfate dosage) to a low of 9.16 (at the highest ferric sulfate dosage), and the turbidity values varied between 13.1 and 4.9 ntu, in an overall downward slope as ferric sulfate dosages increased.

In the fourth set of jars in this series of tests (Table 4.8 and Figure 4.8 above), the calcium hydroxide dosage remained fixed at 80 mg/L as $Ca(OH)_2$, and the ferric sulfate dosage was varied in a much tighter range, from 20 to 28 mg/L as Fe^{3+}. Note, however, that jar 4 was accidentally dosed at 40 mg/L as $Ca(OH)_2$ rather than 80 mg/L as $Ca(OH)_2$. This time, the resulting alkalinity values were very consistent in the 57 to 60 mg/L as $CaCO_3$, except for the jar accidentally dosed at 40 mg/L rather than 80 mg/L as $Ca(OH)_2$, which resulted in a much higher alkalinity value of 88 mg/L as $CaCO_3$. The pH values ranged from a high of 9.87 (at the lowest ferric sulfate dosage) to a low of 9.66 (at the highest ferric sulfate dosage) if the pH value for the mistakenly dosed jar is ignored, and the turbidity values surprisingly were much lower than in the third sets of jars in this series, varying between 1.1 and 3.8 ntu.

It became apparent from this series of jar tests that something was not quite right due to the non-repeatability of results, but as was stated earlier, no optimization method had been established at this point. We were simply attempting to get the plant under control, so no real investigation into the reasons for the non-repeatability was conducted at that time.

As a result of this series of tests, the plant's calcium hydroxide feed point was moved into the influent of the rapid mixer (although calcium carbonate still builds up on the mixer blades, the new rapid mixers were designed to operate successfully with this build-up). As shown in Figures 1.4 and 1.5 in the Plant History Section above, the effect was dramatic. Plant chemical dosages were set at about 75 to 80 mg/L as $Ca(OH)_2$ of calcium hydroxide and 25 mg/L as Fe^{3+} of ferric sulfate. Clarifier effluent turbidity was reduced by almost 50%, and the plant effluent turbidity was reduced from about 0.3 ntu to about 0.2 ntu (the lag in plant

effluent turbidity decrease versus clarifier effluent turbidity decrease was due to the extremely large size (10 MG) of the plant's potable water clearwell) and the potable water being supplied into the clearwell from DWU was shut off.

One other jar test was then run using two jars. In Jar 1, 75 mg/L as $Ca(OH)_2$ of lime and 25 mg/L as Fe^{3+} of ferric was dosed simultaneously into the rapid mix part of the jar, and in Jar 2, the same dosages were added but the lime was dosed into the rapid mix while the ferric was dosed into floc stage 1. As shown in Table 4.9 below, the turbidity went from 1.27 ntu in Jar 1 to 0.82 ntu in Jar 2, and the alkalinity went from 76 mg/L as $CaCO_3$ in Jar 1 to 57 mg/L as $CaCO_3$ in Jar 2. Based on this quick test, the plant's ferric sulfate feed was moved into the first flocculation stage while the plant's lime continued to feed into the rapid mixer. Actual plant conditions improved and stabilized, with all parameters within TCEQ compliance as shown in Figures 1.4 and 1.5 in the Plant History Section above.

Jar #	Lime Dosage (mg/L as $Ca(OH)_2$)	Ferric Dosage (mg/L as Fe^{3+})	pH	Turbidity (ntu)	Total Alkalinity (mg/L as $CaCo_3$)	Water Temperature (°C)
1	75	25	9.11	1.3	76	22
2	75	25	9.02	0.8	57	22

Table 4.9: Initial Test Results (J1 All Chemicals to RM, J2 Lime to RM & Ferric to Floc S1)

In retrospect, this result could have been predicted. Primary treatment of the plant's raw water depends greatly on the formation of calcium carbonate and ferric hydroxide for floc stability and size, as well as for alkalinity removal and softening (the plant's incoming raw water turbidity is in the 7.0 to 8.0 pH range with an average pH of about 7.9, an alkalinity in the 74 to 120 mg/L as $CaCO_3$ range with an average alkalinity of 96 mg/L as $CaCO_3$, and a hardness in the 70 to 160 mg/L as $CaCO_3$ range with an average hardness of 100 mg/L as $CaCO_3$, nearly all of which is calcium hardness. Feeding ferric sulfate prior to feeding calcium hydroxide reduces the pH, driving it down from the average pH into the 7.5 range. As seen in Figure 4.9 below, at this pH range, the carbon dioxide in the water is almost all either H_2CO_3 or HCO_3^-. Little to no CO_3^{2+} is present, and therefore no calcium carbonate will form. By feeding calcium hydroxide before feeding ferric sulfate, the pH of the water is raised to the 9.5 to 10.0 range, resulting in a much greater CO_3^{2+} concentration, which then allows the formation of calcium carbonate.

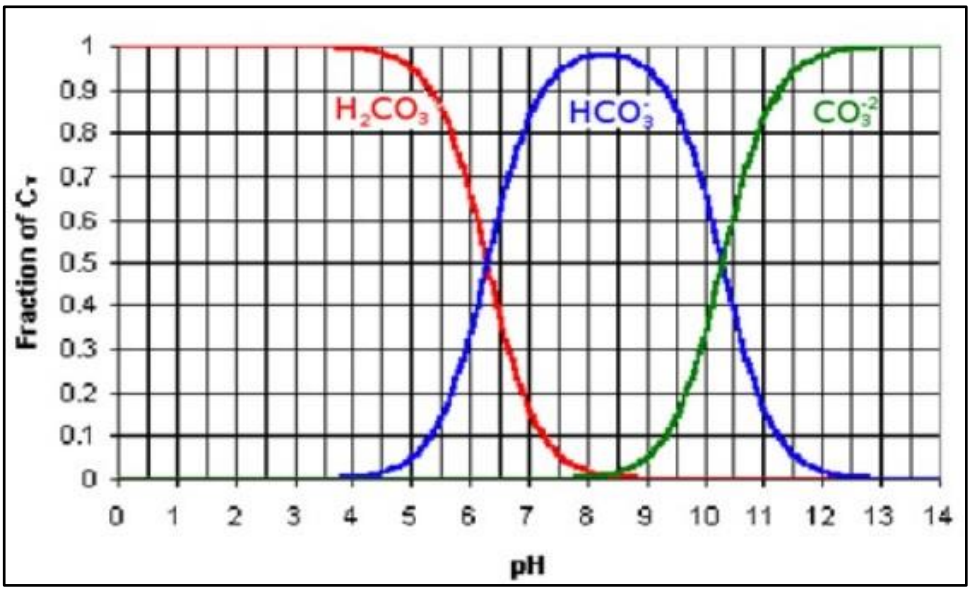

Figure 4.9: Speciation of Carbon Dioxide in water relative to pH

Since the potential crisis was now mitigated, actual optimization of the primary chemical feed systems could begin.

4.2. Series 1 and Series 2 Optimization Tests after the Compliance Crisis

During the initial optimization attempts during the compliance crisis, it became apparent from the results of both the jar tests and the actual plant operational data as described above that the primary driving force behind proper treatment of the plant's raw water was not necessarily a function of the dosages of the chemicals, but rather the application points of the chemicals. However, it was noted that although plant performance somewhat mirrored the jar test results in terms of trends, the numerical values for pH, turbidity and alkalinity from the plant's operational data were typically very different from the values obtained from the jar tests while using identical dosages and application points, as shown in Table 4.10 below (Tests 1-8, 10, 11, and 13 are not shown since these tests were run at completely different dosages than the plant was running. Also, for Test 9, the plant's ferric sulfate feed dosage was at 25 mg/L as Fe^{3+} which is why results for this test are shown for jar dosages of both 20 mg/L as Fe^{3+} and 30 mg/L as Fe^{3+}).

Test Number	Lime Dosage (mg/L as $Ca(OH)_2$)	Ferric Dosage (mg/L as Fe^{3+})	Jar pH	Plant pH	Jar Turbidity (ntu)	Plant Turbidity (ntu)	Jar Alkalinity (mg/L as $CaCO_3$)	Plant Alkalinity (mg/L as $CaCO_3$)
9	80.0	20.0	9.45	9.30	13.10	9.40	77	59
9	80.0	30.0	9.34		11.40		80	
12	80.0	24.0	9.78	9.27	3.01	5.30	57	60
14	75.0	25.0	9.11	9.40	1.27	6.00	76	53
15	75.0	25.0	9.02	9.49	0.82	5.50	57	53

Table 4.10: Jar Test Versus Plant Data during Crisis Trials

Based on this observation, it was clear that the jar test procedures used during the crisis needed to be adjusted. The initial assumptions made to explain the variations between jar test and actual plant data were:

A. That mismatching of velocity gradients in the jars versus the plant could be causing the variations;

B. That the pH in the jars may be higher due to CO_2 differences, as there can be a higher CO_2 mass transfer in the jars due to a higher surface area to volume ratio in the jars versus the plant basins (Edzwald, 2011); and/or

C. That since during jar testing, settling is effectively fully quiescent, whereas in the plant the water is still in some form of motion (especially with regard to turbidities), the difference in water velocities could be causing the variations.

Assumption A was addressed with the procedures for jar testing that were developed (see the Materials and Methods section above).

Assumption B has no known correction methodology due to the mechanical design of the jar testing mechanism.

As for Assumption C, an attempt was made to test this assumption by keeping the jar mixers spinning at the minimum possible rotation speed available to the jar testing mechanism during the "settling" time (This was done after the velocity gradients in the jars were matched to the velocity gradients in the plant based on Assumption A above). The results of this test are shown in Table 4.11 below (Test 35A is the jar test compared to the Plant's Treatment Train A data, and Test 35B is the jar test compared to the Plant's Treatment Train B data).

Test Number	Lime Dosage (mg/L as $Ca(OH)_2$)	Ferric Dosage (mg/L as Fe^{3+})	Jar pH	Plant pH	Jar Turbidity (ntu)	Plant Turbidity (ntu)	Jar Alkalinity (mg/L as $CaCO_3$)	Plant Alkalinity (mg/L as $CaCO_3$)
35A	69.0	20.0	9.38	9.35	6.31	3.30	59	47
35B	69.0	20.0	9.38	9.13	6.31	2.90	59	52

Table 4.11: Jar Tests, Stirrers Running at Minimum Speed During Settling Versus Plant Data

As shown in Table 4.11 above, attempting to simulate water motion in the actual plant settling basins with the jar testing equipment still resulted in major differences between the jar test turbidity results and the actual plant turbidities. This could be due to the minimum jar speed of the jar testing equipment (5 rpm) being too high as compared to the actual motion of the water in the plant's settling basins.

Following the development of the theoretical optimization steps as described in the Materials and Methods Section above, jar tests and plant trials for optimization began. A large number of jar tests were performed following procedures described in the Materials and Methods Section above:

A "Series 1" jar test, utilizing ferric sulfate only, would be run to determine the best ferric sulfate dosage based on both turbidity values and chemical costs. Immediately thereafter, a "Series 2" jar test with the ferric sulfate dosage fixed at the dosage determined from the "Series 1" test and then the calcium hydroxide dosage varied would be run to determine the best calcium hydroxide dosage in terms of turbidity, alkalinity, pH, and chemical costs.

Test Examples:

A. Depicted below are three representative sets of results from these "Series 1" and "Series 2" jar tests at high water temperatures, e.g. above 20°C (Tables 4.12 through 4.14 and Figures 4.10 through 4.12), and two representative sets of results from these "Series 1" and "Series 2" jar tests at low water temperatures, e.g. below 20°C (Tables 4.15 through 4.16 and Figures 4.13 through 4.14). Many factors contribute to the optimum dosages, including the type and quantity of raw water turbidity, the raw water pH, the raw water temperature, and the actual raw water flow rates. Note also that additional factors not shown (such as the current state of nitrification in the distribution system) can influence the selection of the "best" results from the tests.

Jar #	Lime Dosage (mg/L as $Ca(OH)_2$)	Ferric Dosage (mg/L as Fe^{3+})	pH	Turbidity (ntu)	Total Alkalinity (mg/L as $CaCo_3$)	Total Alkalinity (cg/L as $CaCo_3$)	Water Temperature (°C)
1		20		4.3			23
2		25		1.0			23
3		30		1.5			23
4		35		1.0			23
5		40		1.8			23
6		45		1.6			23
1	60	25	9.08	1.5	66	6.6	23
2	70	25	9.19	1.2	56	5.6	23
3	80	25	9.35	0.9	51	5.1	22
4	90	25	9.50	1.4	48	4.8	22
5	100	25	9.60	1.5	39	3.9	22

Table 4.12: Optimization Series 1/2 Jar Sets 17 and 18

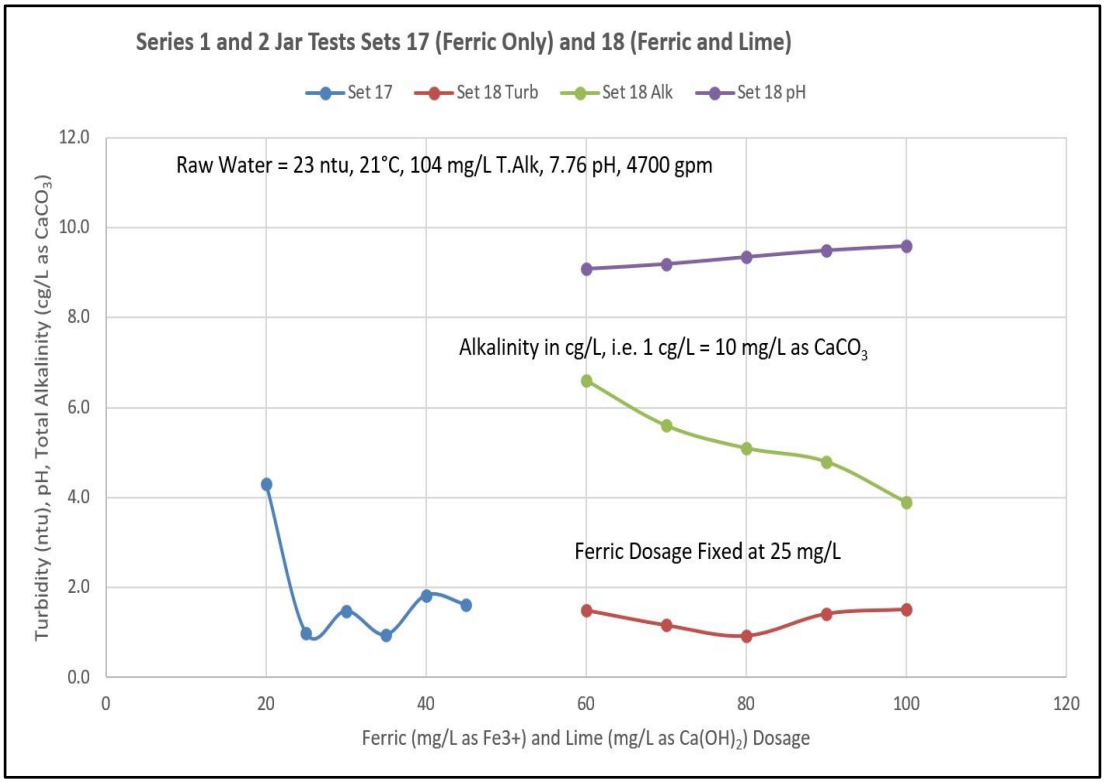

Figure 4.10: Optimization Series 1/2 Jar Sets 17 and 18 Results

Jar #	Lime Dosage (mg/L as $Ca(OH)_2$)	Ferric Dosage (mg/L as Fe^{3+})	pH	Turbidity (ntu)	Total Alkalinity (mg/L as $CaCo_3$)	Total Alkalinity (cg/L as $CaCo_3$)	Water Temperature (°C)
1		22		0.9			21
2		23		0.8			21
3		24		0.6			21
4		25		0.7			21
5		26		0.8			21
6		27		0.8			21
1	70	24	8.63	2.6	58	5.8	21
2	75	24	8.76	1.4	55	5.5	21
3	80	24	8.78	1.6	52	5.2	21
4	85	24	8.91	1.7	48	4.8	21
5	90	24	9.20	1.6	35	3.5	21
6	95	24	9.29	1.4	32	3.2	21

Table 4.13: Optimization Series 1/2 Jar Sets 19 and 20

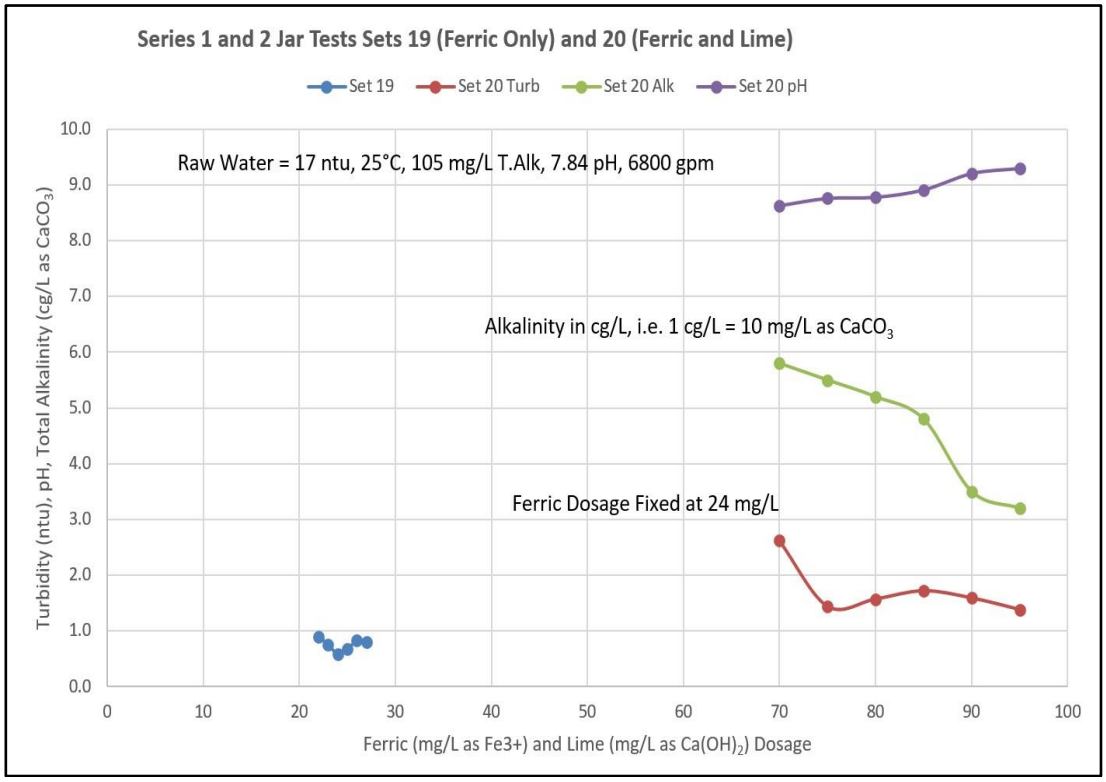

Figure 4.11: Optimization Series 1/2 Jar Sets 19 and 20 Results

Jar #	Lime Dosage (mg/L as $Ca(OH)_2$)	Ferric Dosage (mg/L as Fe^{3+})	pH	Turbidity (ntu)	Total Alkalinity (mg/L as $CaCo_3$)	Total Alkalinity (cg/L as $CaCo_3$)	Water Temperature (°C)
1		14		1.3			30
2		16		1.2			30
3		18		1.0			30
4		20		1.3			30
5		22		1.4			30
6		24		1.7			30
1	60	18	9.51	1.4	41	4.1	30
2	63	18	9.55	1.6	40	4	30
3	66	18	9.63	1.6	40	4	30
4	69	18	9.70	1.7	37	3.7	30
5	72	18	9.81	1.8	35	3.5	30
6	75	18	10.17	2.9	33	3.3	30

Table 4.14: Optimization Series 1/2 Jar Sets 33 and 34

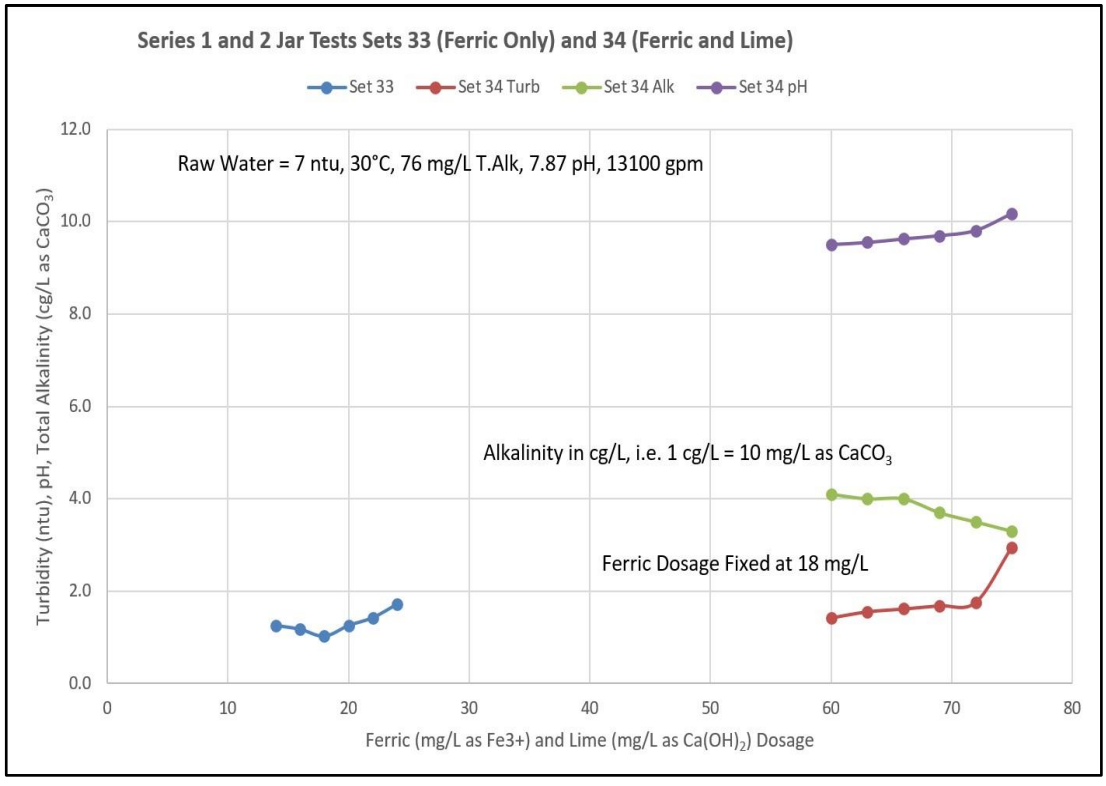

Figure 4.12: Optimization Series 1/2 Jar Sets 33 and 34 Results

Jar #	Lime Dosage (mg/L as $Ca(OH)_2$)	Ferric Dosage (mg/L as Fe^{3+})	pH	Turbidity (ntu)	Total Alkalinity (mg/L as $CaCo_3$)	Total Alkalinity (cg/L as $CaCo_3$)	Water Temperature (°C)
1		14		5.0			17
2		16		7.1			17
3		18		6.7			17
4		20		6.7			17
5		22		5.2			17
6		24		4.9			17
1	80	22	9.48	1.8	68	6.8	17
2	82	22	9.57	3.2	67	6.7	17
3	84	22	9.65	3.3	65	6.5	17
4	86	22	9.73	7.7	61	6.1	17
5	88	22	9.86	8.1	59	5.9	17
6	90	22	9.88	7.8	56	5.6	17

Table 4.15: Optimization Series 1/2 Jar Sets 41 and 42

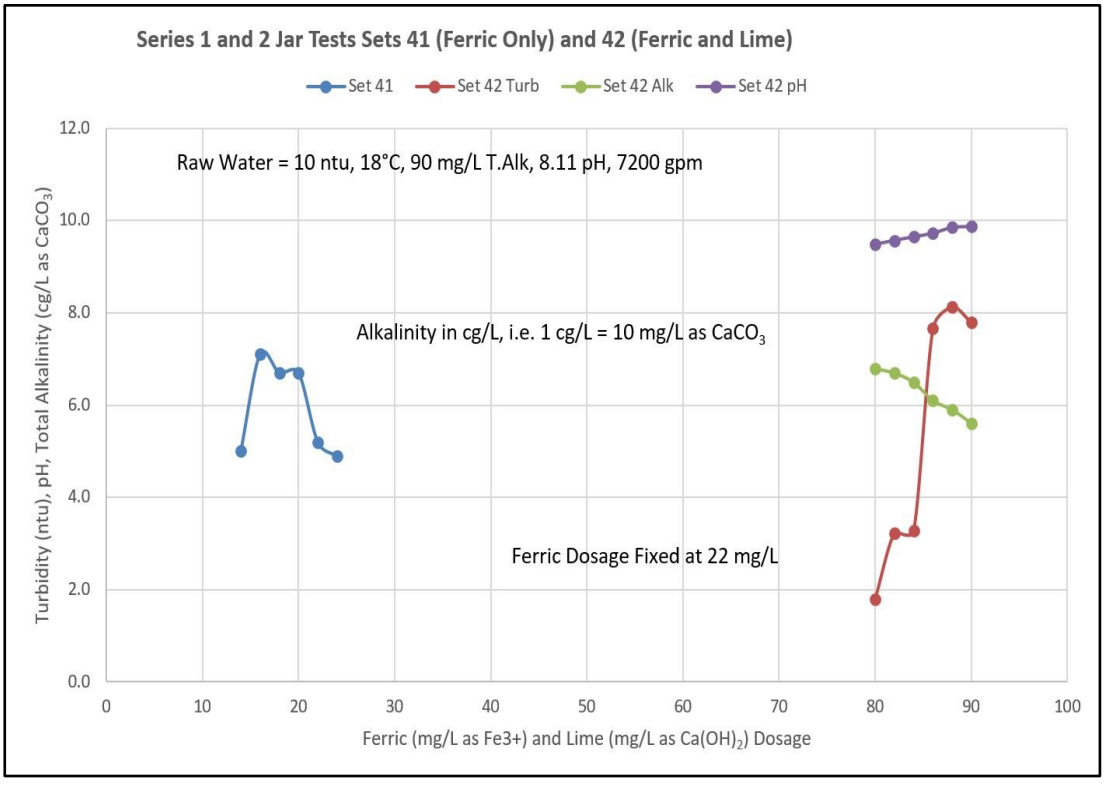

Figure 4.13: Optimization Series 1/2 Jar Sets 41 and 42 Results

Jar #	Lime Dosage (mg/L as $Ca(OH)_2$)	Ferric Dosage (mg/L as Fe^{3+})	pH	Turbidity (ntu)	Total Alkalinity (mg/L as $CaCo_3$)	Total Alkalinity (cg/L as $CaCo_3$)	Water Temperature (°C)
1		17		18.7			14
2		19		15.4			14
3		21		12.7			14
4		23		10.0			14
5		25		2.5			13
6		27		2.0			13
1	78	25	9.76	1.0	73	7.3	14
2	80	25	9.66	0.7	74	7.4	14
3	82	25	9.69	0.7	76	7.6	13
4	84	25	9.86	1.2	79	7.9	13
5	86	25	9.89	2.4	78	7.8	13
6	88	25	9.80	13.1	59	5.9	13

Table 4.16: Optimization Series 1/2 Jar Sets 57 and 58

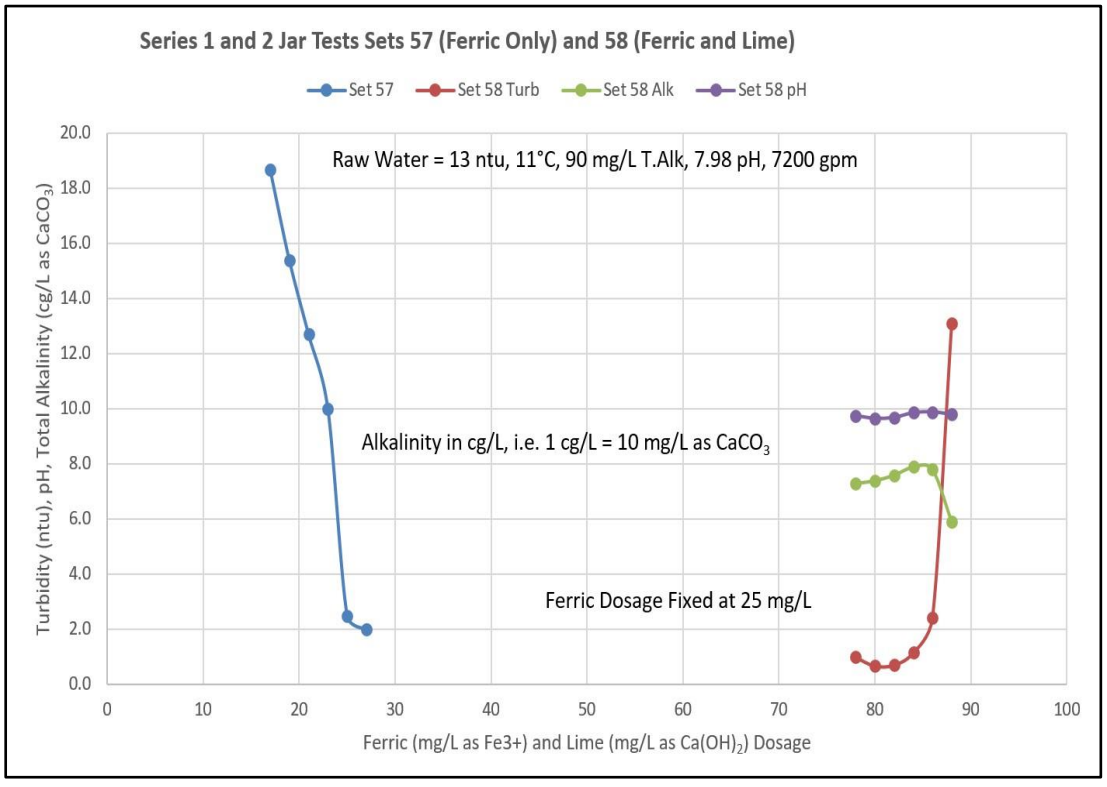

Figure 4.14: Optimization Series 1/2 Jar Sets 57 and 58 Results

A. Table 4.12 and Figure 4.10 above show that for test set 17 with only the ferric sulfate, the best turbidity results were obtained at ferric sulfate dosages of 25 and 35 mg/L as Fe^{3+}. Therefore, the 25 mg/L dosage was selected for the corresponding test set 18. Test set 18, with the ferric sulfate dosage fixed while varying the calcium hydroxide dosage, showed that the best calcium hydroxide dosage was 80 mg/L as $Ca(OH)_2$ based on a combination of turbidity, pH, and total alkalinity. The selected 'optimum' values are shown in red in Table 4.12 above.

B. Table 4.13 and Figure 4.11 above show that for test set 19 with only the ferric sulfate, the best turbidity results were obtained at a ferric sulfate dosage of 24 mg/L as Fe^{3+}. Therefore, the 24 mg/L dosage was selected for the corresponding test set 20. Test set 20, with the ferric sulfate dosage fixed while varying the calcium hydroxide dosage, showed that the best calcium hydroxide dosage was 85 mg/L as $Ca(OH)_2$ based on a combination of turbidity, pH, and total alkalinity. Note that the pH range is below optimum, but the small increase in pH for higher dosages does not justify the additional cost of the chemical. The selected 'optimum' values are shown in red in Table 4.13 above.

C. Table 4.14 and Figure 4.12 above show that for test set 33 with only the ferric sulfate, the best turbidity results were obtained at a ferric sulfate dosage of 18 mg/L as Fe^{3+}. Therefore, the 18 mg/L dosage was selected for the corresponding test set 34. Test set 34, with the ferric sulfate dosage fixed while varying the calcium hydroxide dosage, showed that the best calcium hydroxide dosage was 60 mg/L as $Ca(OH)_2$ based on a combination of turbidity, pH, and total alkalinity. The selected 'optimum' values are shown in red in Table 4.14 above.

D. Table 4.15 and Figure 4.13 above show that for test set 41 with only the ferric sulfate, the best turbidity results were obtained at a ferric sulfate dosage of 24 mg/L as Fe^{3+}. However, the difference in turbidity between 22 mg/L as Fe^{3+} and 24 mg/L as Fe^{3+} was small enough that the additional 2 mg/L dosage was not cost effective. Therefore, the 22 mg/L dosage was selected for the corresponding test set 42. Test set 42, with the ferric sulfate dosage fixed while varying the calcium hydroxide dosage, showed that the best calcium hydroxide dosage was 88 mg/L as $Ca(OH)_2$ based on a combination of turbidity, pH, and total alkalinity. The selected 'optimum' values are shown in red in Table 4.15 above.

E. Table 4.16 and Figure 4.14 above show that for test set 57 with only the ferric sulfate, the best turbidity results were obtained at a ferric sulfate dosage of 27 mg/L as Fe^{3+}. However, the difference in turbidity between 25 mg/L as Fe^{3+} and 27 mg/L as Fe^{3+} was small enough that the additional 2 mg/L dosage was not cost effective. Therefore, the 25 mg/L dosage was

selected for the corresponding test set 58. Test set 58, with the ferric sulfate dosage fixed while varying the calcium hydroxide dosage, showed that the best calcium hydroxide dosage was 86 mg/L as $Ca(OH)_2$ based on a combination of turbidity, pH, and total alkalinity. In this case, even though the preferred alkalinity range was not met, an increase from 86 mg/L to 88 mg/L in calcium hydroxide dosage resulted in a turbidity that was excessively out of range. The selected 'optimum' values are shown in red in Table 4.16 above.

Overall, the results of the combined "Series 1" and "Series 2" jar tests showed a relatively wide range of ferric sulfate dosages that resulted in jar turbidities below 8.0 ntu, with the majority of these dosages in the 20.0 to 30.0 mg/L as Fe^{3+} range. Alkalinity values were shown to typically decrease, and pH values were shown to typically increase as the calcium hydroxide dose was increased (refer to Figures 4.10 to 4.14 above). These alkalinity and pH value changes are in line with what a lime softening plant is supposed to produce, which indicated that the change in application point of the chemicals was working properly.

Somewhat unexpectedly, although there was some evidence of a water temperature effect on turbidity, it was not as large as expected (Hanson and Cleasby, 1990) (Morris and Knocke, 1984). There was some indication that at water temperatures below about 20 °C, turbidities would begin to rise, but perhaps due to the limited number of samples at low temperatures, this was indeterminate (refer to Figure 4.15 below).

Typically (but not always due to differences of opinion among plant staff about jar testing procedures), after running a "Series 1-2" test set, the resulting 'best' dosages were then applied to the actual treatment plant. However, when comparing the jar test results to the actual plant data, once again there were typically large differences between the test data and the operational data. Even with the jar test velocity gradients set to match plant conditions, there did not seem to be any discernable pattern detectable from the results (see Figures 4.16 and 4.17 below). In addition, the expected turbidity removal percentages (based on jar test results) showed no discernable correlation between the jar results and the actual plant results (see Figure 4.18 below).

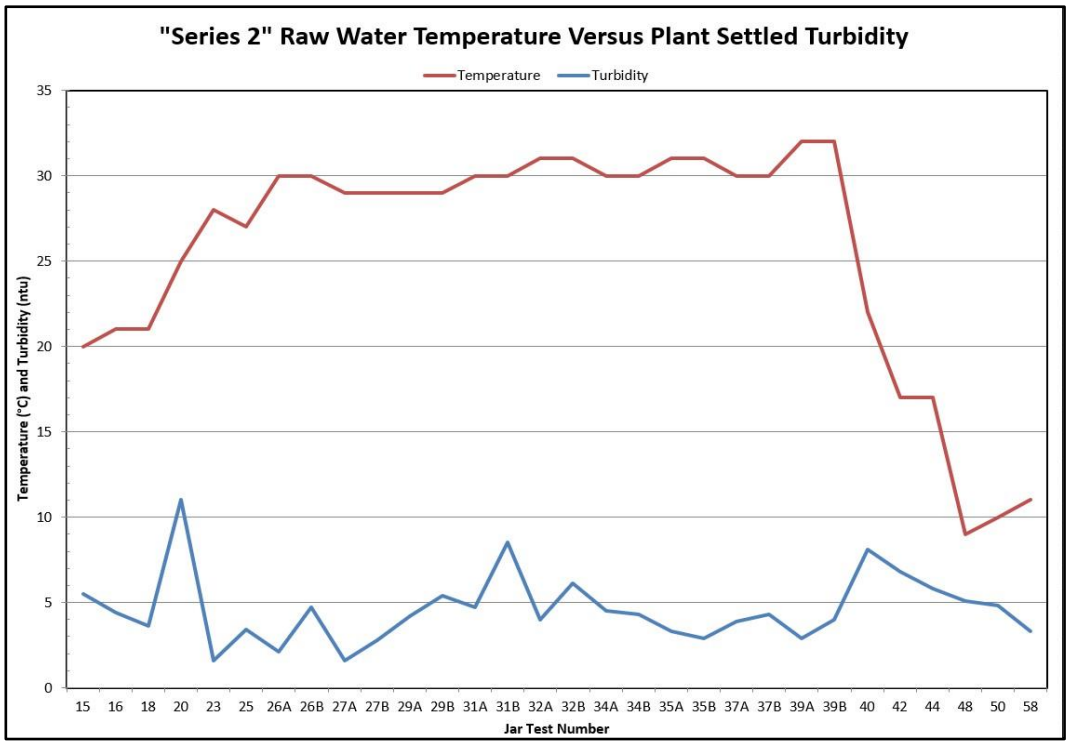

Figure 4.15: Series 2 Raw Water Temperature Versus Plant Settled Turbidity

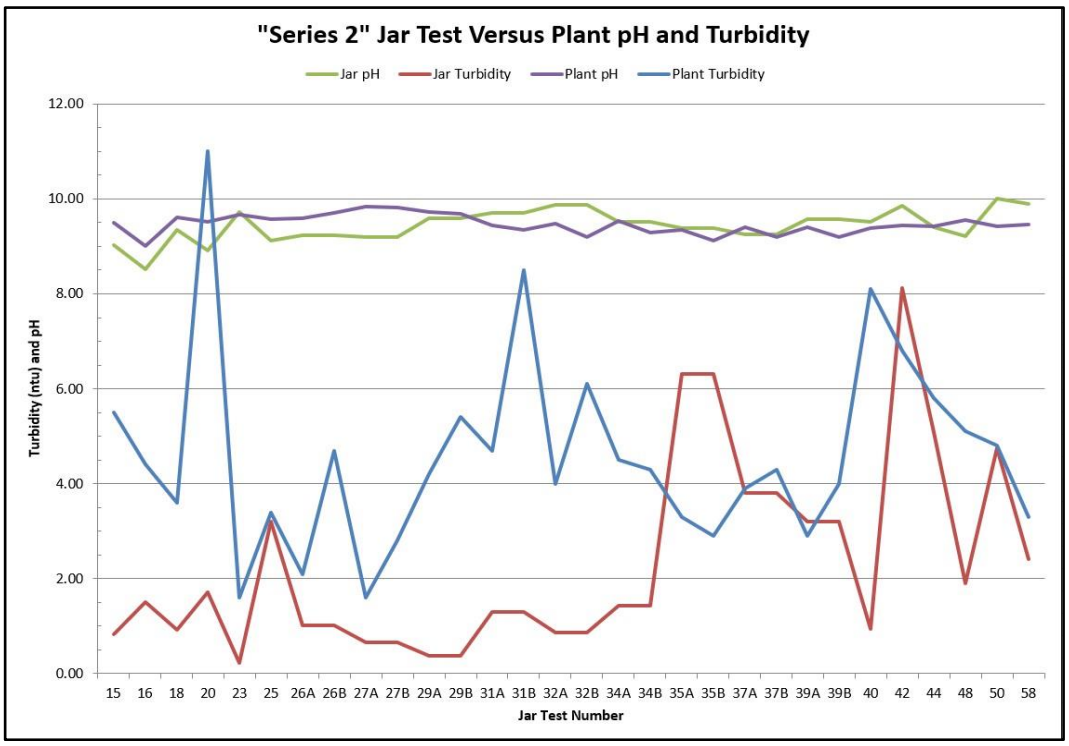

Figure 4.16: Series 2 Jar Test Versus Plant pH and Turbidity

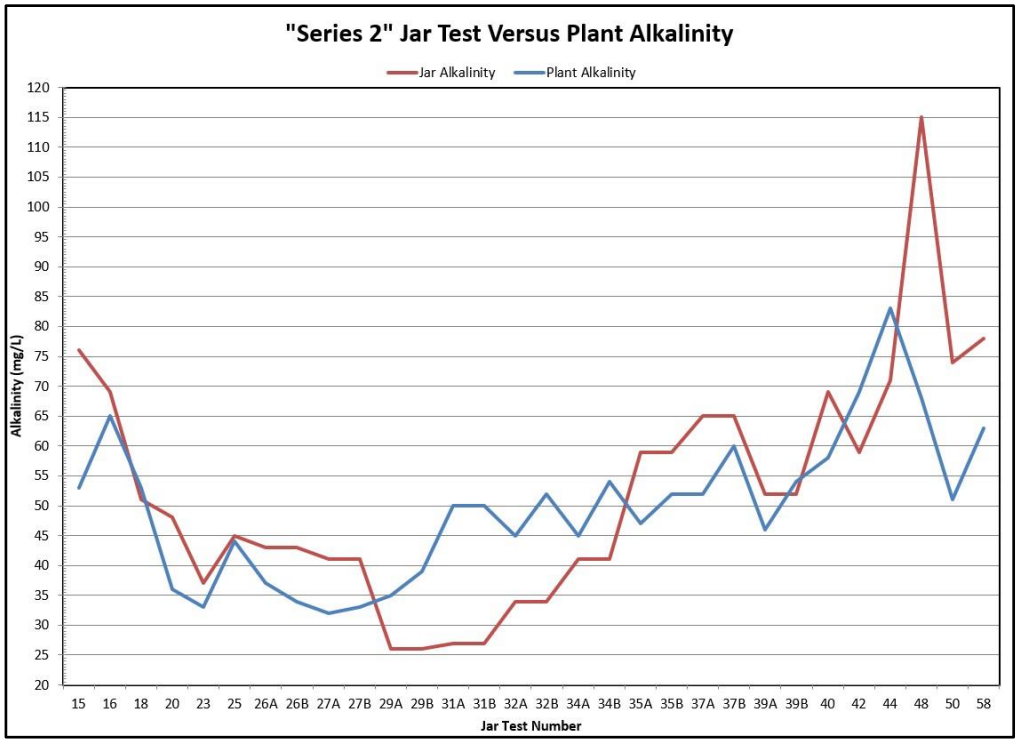

Figure 4.17: Series 2 Jar Test Versus Plant Alkalinity

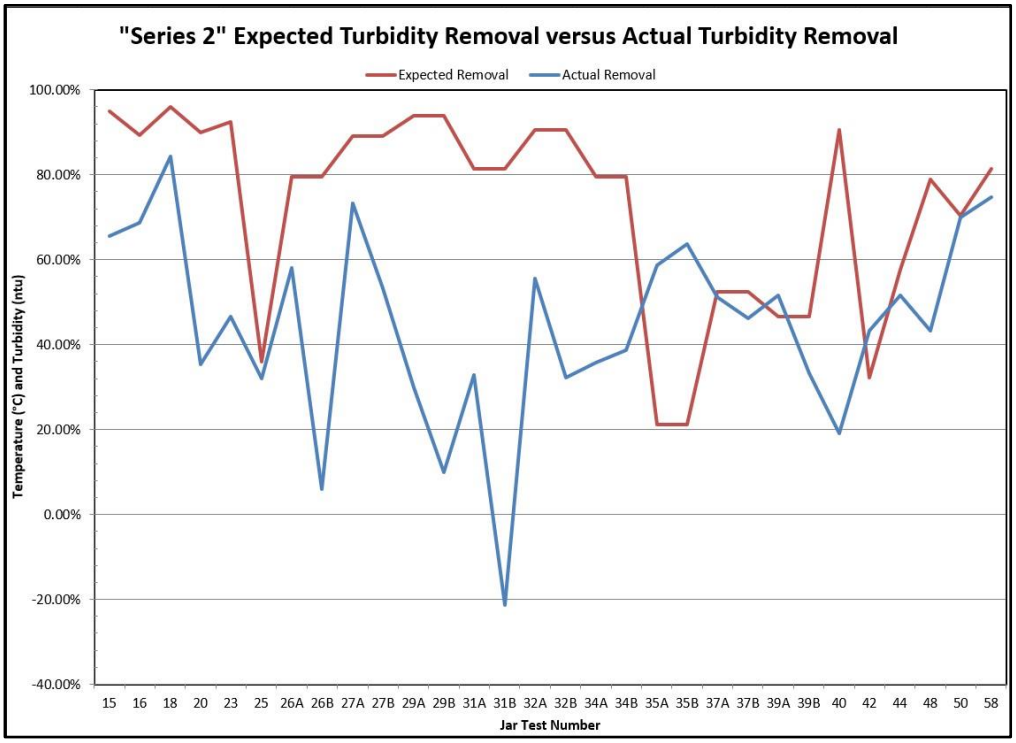

Figure 4.18: Series 2 Expected Turbidity Removal versus Actual Turbidity Removal

4.3. Analysis of the Actual Chemicals Used in Treatment

Following the "Series 2" tests described above, since it was apparent that no real discernable correlation between the jar tests and the actual plant conditions could be observed, it was decided to undertake an analysis of the actual chemicals being used in the treatment process. The plant's bulk ferric sulfate (nominally a 60% solution) from historical plant data showed that it is a very consistent solution, varying from tanker load to tanker load by less than 1%. This is to be expected, since the ferric sulfate is a true solution with highly stable properties. However, the plant's bulk calcium hydroxide was a different matter. This was a nominal 40% "solution" chemical, but it was not truly a solution, but rather a suspension. It must be continuously mixed while stored in the bulk tanks at the plant. In addition, for unknown reasons, this chemical was historically not tested for quality after delivery. Therefore, a series of tests was run in which a total of six 1-liter jars of bulk calcium hydroxide were drawn from the tank, one after another, and tested per the manufacturer's guidelines for concentration. The results are shown in Figure 4.19 below.

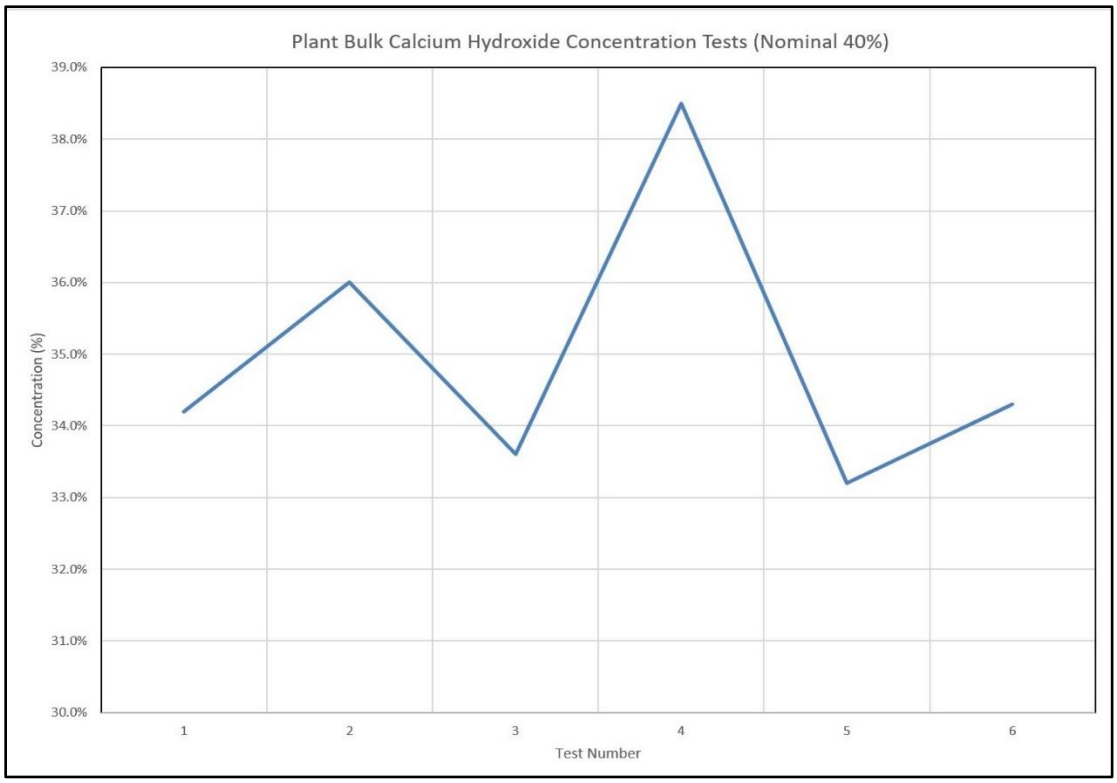

Figure 4.19: Plant Bulk Calcium Hydroxide (Nominal 40% concentration) Tests

As shown in Figure 4.19, the results of this concentration test showed a large (and unpredictable) variance in concentration from one test to the next. The

concentrations varied from a low of 33.2% to a high of 38.5% (variance of 5.3%). During plant operations, this variance tends to balance itself due to the large volumes of water and chemical involved. However, for use in jar testing, only a small amount of chemical is drawn off, and is then diluted to make the stock solutions used in the jar tests. This can result in a large variability in jar test accuracy.

In addition, the 40% calcium hydroxide used at the time was typically delivered freshly slaked from the manufacturer, and could have temperatures as high as 180 °F. Careful handling of the chemical was required for burn prevention. This chemical also had a rather high non-soluble grit content that historically resulted in frequent blockages to the plant's chemical feed lines.

A discussion was held with the manufacturer, and it was found that they had another form of calcium hydroxide which was not only processed thru a finer set of screens to eliminate much more of the non-soluble grit, but was also retained at the manufacturing facility long enough before delivery such that it was cooled to approximately 75 °F at delivery time, which effectively indicated that most if not all of the chemical reaction converting CaO to $Ca(OH)_2$ had been completed. According to the manufacturer, it would result in far fewer feed line blockages. This particular calcium hydroxide, however was only a nominal 30% concentration rather than a 40% concentration. From a price standpoint however, it was only about 2% more expensive than the 40% concentration calcium hydroxide.

It was decided that the slightly higher cost of the chemical was worth the price for the reduced maintenance costs, higher reliability, and safer handling due to lower temperatures. The plant's bulk storage tanks were emptied and cleaned (one at a time), and then re-filled with the new calcium hydroxide solution. After filling, and thereafter periodically, quality tests were run on the new chemical. A sampling of these test results are shown in Figure 4.20 below. As seen in the Figure, the new chemical has a much lower variability in concentration, with a high of 26.2% and a low of 25.8%, for a total variance of only 0.4%, with an average of 25.9%.

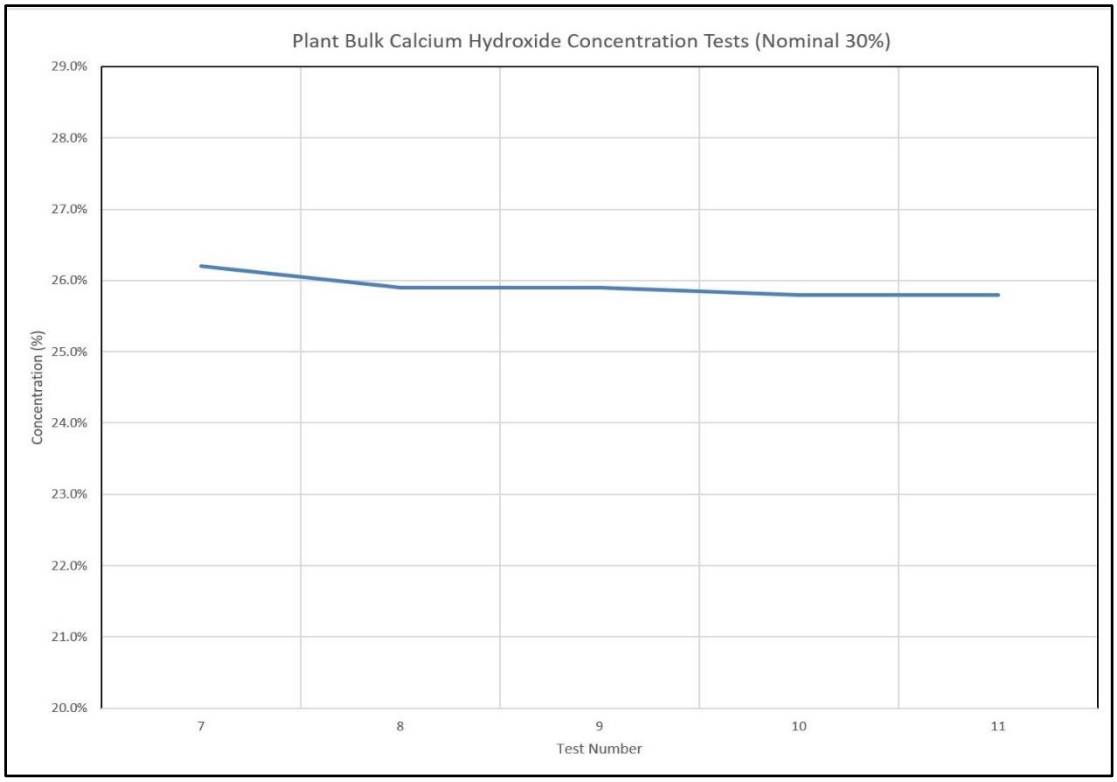

Figure 4.20: Plant Bulk Calcium Hydroxide (Nominal 30% concentration) Tests

After observing plant operations following the transition to 30% nominal calcium hydroxide, it was observed that the calcium hydroxide feed line blockages due to grit were reduced by over 75% (personal communication with the Mike Swint, DCPCMUD Maintenance Manager, on various dates). It was also observed, as discussed in Section 4.4 Series 3 and 4 Optimization Tests below, that using the nominal 30% calcium hydroxide provided much better correlation between the jar tests and the actual plant conditions.

As a part of the transition to the nominal 30% calcium hydroxide, it was also decided that due to the complexities and the number of variables involved, that rather than attempting to simultaneously optimize the calcium hydroxide dosage to pH, alkalinity, and turbidity, that the optimization for calcium hydroxide would be done for only pH and alkalinity as described in Part 3.3 of the Materials and Methods Section above.

4.4. Series 3 and Series 4 Optimization Tests

Following the transition to a 30% nominal calcium hydroxide solution, multiple ferric sulfate and calcium hydroxide dosages were tested at varying water temperatures using the methods described in Part 3.3 of the Materials and Methods Section above.

As in the Series 1 and 2 Optimization Test, a "Series 3" jar test, utilizing ferric sulfate only, would be run to determine the best ferric sulfate dosage based on both turbidity values and chemical costs. Immediately thereafter, a "Series 4" jar test with the ferric sulfate dosage fixed at the dosage determined from the "Series 3" test and then the calcium hydroxide dosage varied would be run to determine the best calcium hydroxide dosage in terms of turbidity, alkalinity, pH, and chemical costs.

Test Examples:

A. Depicted below are three representative sets of results from these "Series 3" and "Series 4" jar tests at high water temperatures, e.g. above 20°C (Tables 4.17 through 4.19 and Figures 4.21 through 4.23 below), and two representative sets of results from these "Series 3" and "Series 4" jar tests at low water temperatures, e.g. below 20°C (Tables 4.20 through 4.21 and Figures 4.24 through 4.26 below). As previously stated, many factors contribute to the optimum dosages, including the type and quantity of raw water turbidity, the raw water pH, the raw water temperature, and the actual raw water flow rates. Note also that additional factors not shown (such as the current state of nitrification in the distribution system) can influence the selection of the "best" results from the tests.

B. Table 4.17 and Figure 4.21 below show that for test set 73 with only the ferric sulfate, the best turbidity results were obtained at a ferric sulfate dosage of 35 mg/L as Fe^{3+}. Therefore, the 35 mg/L as Fe^{3+} dosage was selected for the corresponding test set 74. Test set 74, with the ferric sulfate dosage fixed while varying the calcium hydroxide dosage, showed that the best calcium hydroxide dosage was 92 mg/L as $Ca(OH)_2$ based primarily on the pH, and total alkalinity. The selected 'optimum' values are shown in red in Table 4.17 below.

C. Table 4.18 and Figure 4.22 below show that for test set 75 with only the ferric sulfate, the best turbidity results were obtained at a ferric sulfate dosage of 31 mg/L as Fe^{3+}., since the very minor turbidity decrease at 34 mg/L as Fe^{3+} does not justify the additional chemical cost. Therefore, the 31 mg/L as Fe^{3+} dosage was selected for the corresponding test set 76. Test set 76, with the ferric sulfate dosage fixed while varying the calcium hydroxide dosage, showed that the best calcium hydroxide dosage was 83 mg/L as $Ca(OH)_2$ based primarily on the pH, and total alkalinity. Note that the pH range is below optimum, but the small increase in pH for higher dosages does not justify the additional cost of the chemical. The selected 'optimum' values are shown in red in Table 4.18 below.

Jar #	Lime Dosage (mg/L as $Ca(OH)_2$)	Ferric Dosage (mg/L as Fe^{3+})	pH	Turbidity (ntu)	Total Alkalinity (mg/L as $CaCo_3$)	Total Alkalinity (cg/L as $CaCo_3$)	Water Temperature (°C)
1		29		3.9			22
2		31		3.4			22
3		33		2.8			22
4		35		1.3			22
5		37		1.4			22
6		39		1.7			22
1	76	35	9.10	4.9	65	6.5	22
2	80	35	9.30	4.8	61	6.1	22
3	84	35	9.45	4.6	49	4.9	22
4	88	35	9.49	4.0	45	4.5	22
5	92	35	9.58	3.7	33	3.3	22
6	96	35	9.61	4.5	31	3.1	21

Table 4.17: Optimization Series 3/4 Jar Sets 73 and 74

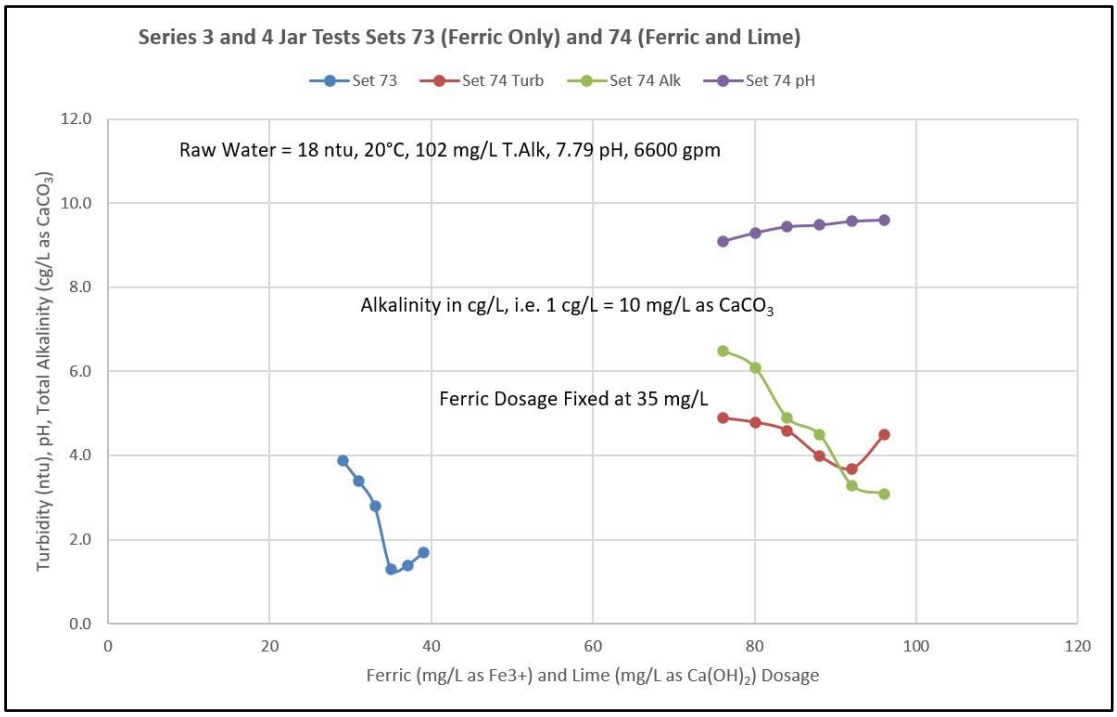

Figure 4.21: Optimization Series 3/4 Jar Sets 73 and 74 Results

Jar #	Lime Dosage (mg/L as $Ca(OH)_2$)	Ferric Dosage (mg/L as Fe^{3+})	pH	Turbidity (ntu)	Total Alkalinity (mg/L as $CaCo_3$)	Total Alkalinity (cg/L as $CaCo_3$)	Water Temperature (°C)
1		22		1.5			24
2		25		1.4			24
3		28		1.1			24
4		31		0.8			24
5		34		0.7			23
6		37		0.9			23
1	79	31	9.05	1.6	45	4.5	24
2	83	31	9.27	1.7	36	3.6	24
3	87	31	9.28	1.7	36	3.6	24
4	91	31	9.31	2.0	35	3.5	24
5	95	31	9.32	2.1	35	3.5	24
6	99	31	9.40	2.5	36	3.6	24

Table 4.18: Optimization Series 3/4 Jar Sets 75 and 76

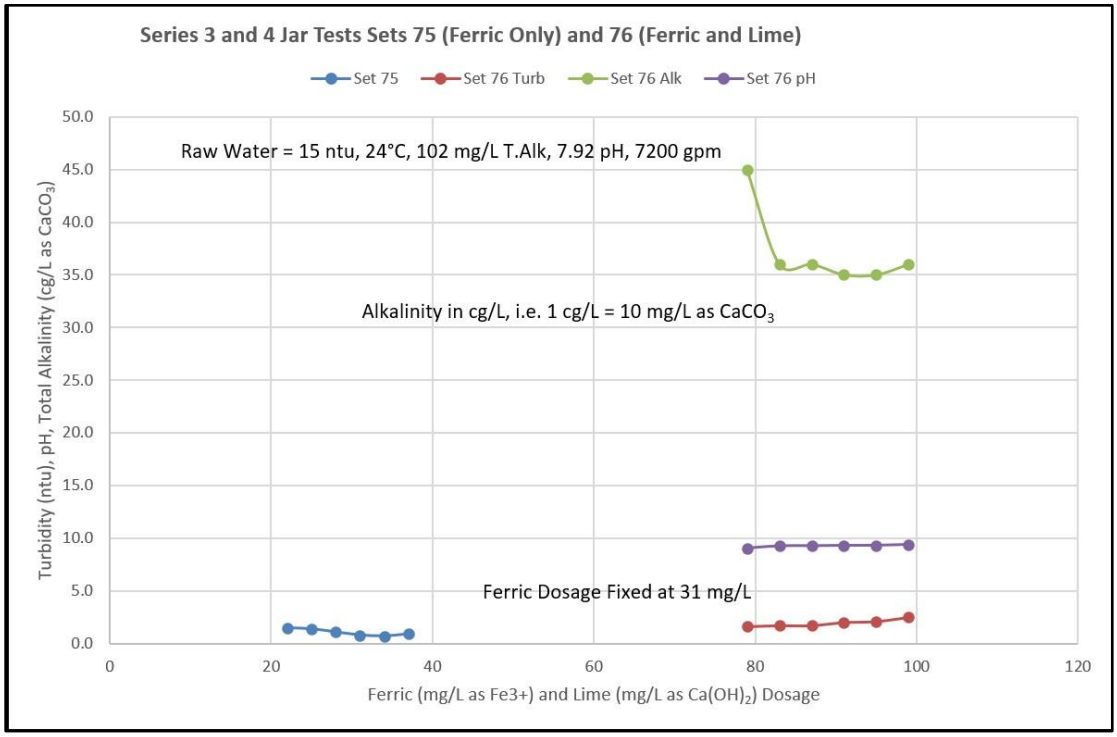

Figure 4.22: Optimization Series 3/4 Jar Sets 75 and 76 Results

D. Table 4.19 and Figure 4.23 below show that for test set 83 with only the ferric sulfate, the best turbidity results were obtained at a ferric sulfate dosage of 22 mg/L as Fe^{3+}., as the minor turbidity improvement at 24 mg/L as Fe^{3+} does not justify the additional chemical cost. Therefore, the 22 mg/L as Fe^{3+} dosage was selected for the corresponding test set 84. Test set 84, with the ferric sulfate dosage fixed while varying the calcium hydroxide dosage, showed that the best calcium hydroxide dosage was 59 mg/L as $Ca(OH)_2$ based primarily on the pH, and total alkalinity. Again, note that although the pH range is below optimum, the small increase in pH for higher dosages does not justify the additional cost of the chemical. The selected 'optimum' values are shown in red in Table 4.19 below.

E. Table 4.20 and Figure 4.24 below show that for test set 62 with only the ferric sulfate, the best turbidity results were obtained at a ferric sulfate dosage of 36 mg/L as Fe^{3+}, as the minor additional turbidity reduction at higher dosages does not justify the additional chemical cost. Therefore, the 36 mg/L dosage was selected for the corresponding test set 63. Test set 63, with the ferric sulfate dosage fixed while varying the calcium hydroxide dosage, showed that the best calcium hydroxide dosage was 60 mg/L as $Ca(OH)_2$ based primarily on the pH, and total alkalinity. Once again, although the pH and alkalinity ranges are slightly below optimum, the small increase in pH and decrease in alkalinity for higher dosages does not justify the additional cost of the chemical. Also, since this test was during low temperature and low flow conditions, distribution system nitrification was not an issue. The selected 'optimum' values are shown in red in Table 4.20 below.

F. Table 4.21 and Figure 4.25 below show that for test set 71 with only the ferric sulfate, the best turbidity results were obtained at a ferric sulfate dosage of 36 mg/L as Fe^{3+}. Therefore, the 36 mg/L as Fe^{3+} dosage was selected for the corresponding test set 72. Test set 72, with the ferric sulfate dosage fixed while varying the calcium hydroxide dosage, showed that the best calcium hydroxide dosage was 73 mg/L as $Ca(OH)_2$ based on a combination of turbidity, pH, and total alkalinity. Once again, even though the preferred pH and alkalinity ranges were not met, the pH actually rose slightly with a higher calcium hydroxide dosage, and the 1 mg/L as $CaCO_3$ alkalinity reduction does not justify the chemical cost. Also, since this test was during low temperature and low flow conditions, distribution system nitrification was not an issue. The selected 'optimum' values are shown in red in Table 4.21 below.

Jar #	Lime Dosage (mg/L as $Ca(OH)_2$)	Ferric Dosage (mg/L as Fe^{3+})	pH	Turbidity (ntu)	Total Alkalinity (mg/L as $CaCo_3$)	Total Alkalinity (cg/L as $CaCo_3$)	Water Temperature (°C)
1		14		8.1			28
2		16		6.9			28
3		18		5.6			28
4		20		4.0			28
5		22		3.5			28
6		24		3.4			28
1	53	22	8.60	8.7	65	6.5	28
2	56	22	8.82	6.8	60	6	28
3	59	22	8.85	6.4	54	5.4	28
4	62	22	8.91	6.3	51	5.1	28
5	65	22	8.93	6.1	52	5.2	28
6	68	22	8.91	6.0	45	4.5	28

Table 4.19: Optimization Series 3/4 Jar Sets 83 and 84

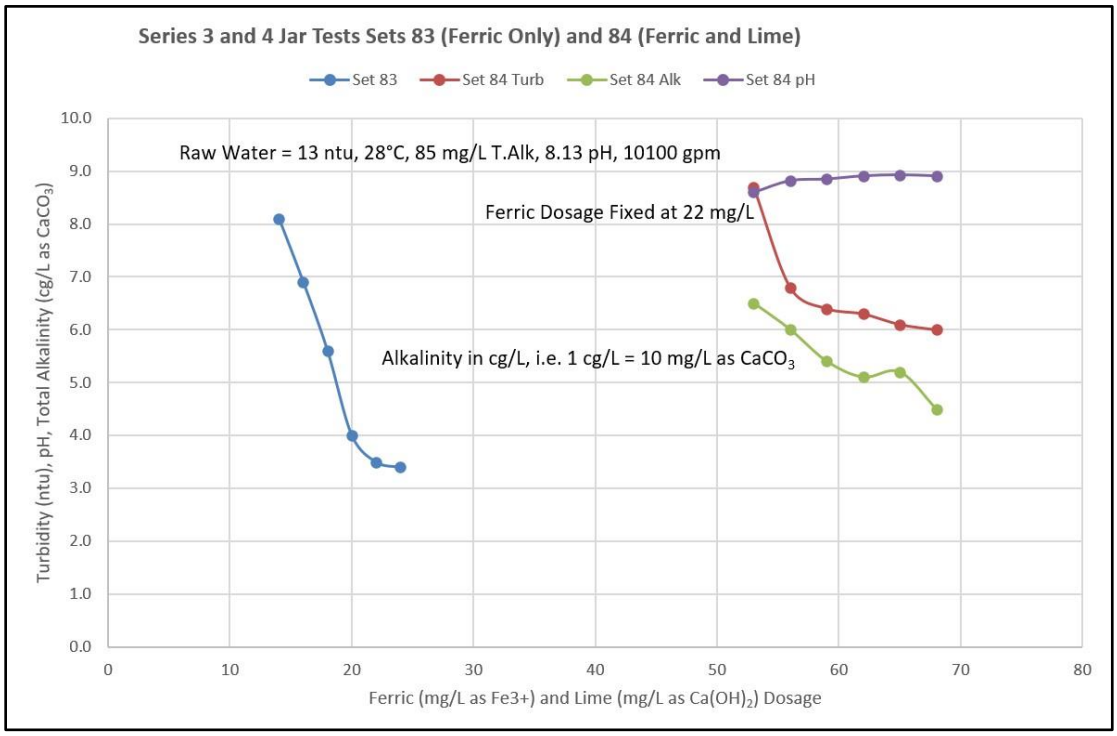

Figure 4.23: Optimization Series 3/4 Jar Sets 83 and 84 Results

Jar #	Lime Dosage (mg/L as $Ca(OH)_2$)	Ferric Dosage (mg/L as Fe^{3+})	pH	Turbidity (ntu)	Total Alkalinity (mg/L as $CaCo_3$)	Total Alkalinity (cg/L as $CaCo_3$)	Water Temperature (°C)
1		32		6.1			14
2		34		5.2			14
3		36		4.9			14
4		38		4.8			14
5		40		4.7			14
6		42		4.9			14
1	50	36	8.90	8.9	70	7	15
2	55	36	9.10	8.9	69	6.9	15
3	60	36	9.44	9.1	66	6.6	15
4	65	36	9.46	9.5	65	6.5	15
5	70	36	9.48	9.6	62	6.2	15
6	75	36	9.51	9.9	61	6.1	15

Table 4.20: Optimization Series 3/4 Jar Sets 62 and 63

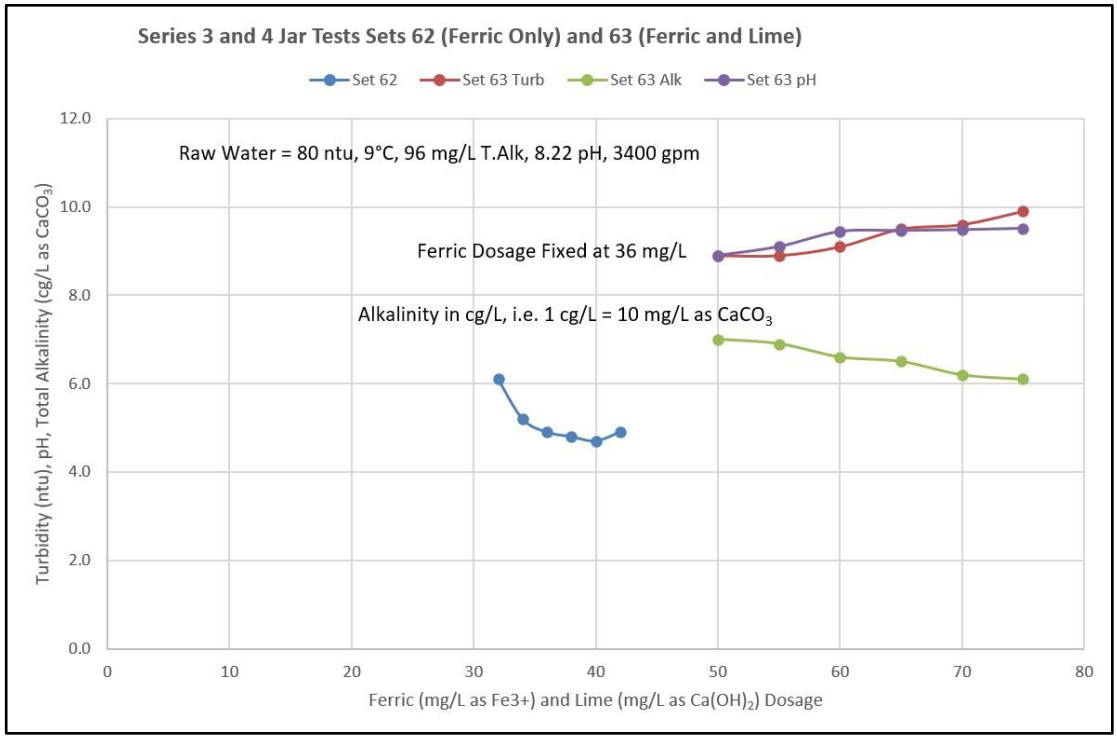

Figure 4.24: Optimization Series 3/4 Jar Sets 62 and 63 Results

Jar #	Lime Dosage (mg/L as $Ca(OH)_2$)	Ferric Dosage (mg/L as Fe^{3+})	pH	Turbidity (ntu)	Total Alkalinity (mg/L as $CaCo_3$)	Total Alkalinity (cg/L as $CaCo_3$)	Water Temperature (°C)
1							
2		27		6.1			15
3		30		5.0			15
4		33		4.3			15
5		36		3.9			15
6		39		3.9			15
1							
2	64	36	8.60	6.0	70	7	17
3	67	36	8.85	5.8	70	7	17
4	70	36	8.91	6.1	69	6.9	17
5	73	36	9.05	6.2	67	6.7	17
6	76	36	9.08	6.4	66	6.6	17

Table 4.21: Optimization Series 3/4 Jar Sets 71 and 72

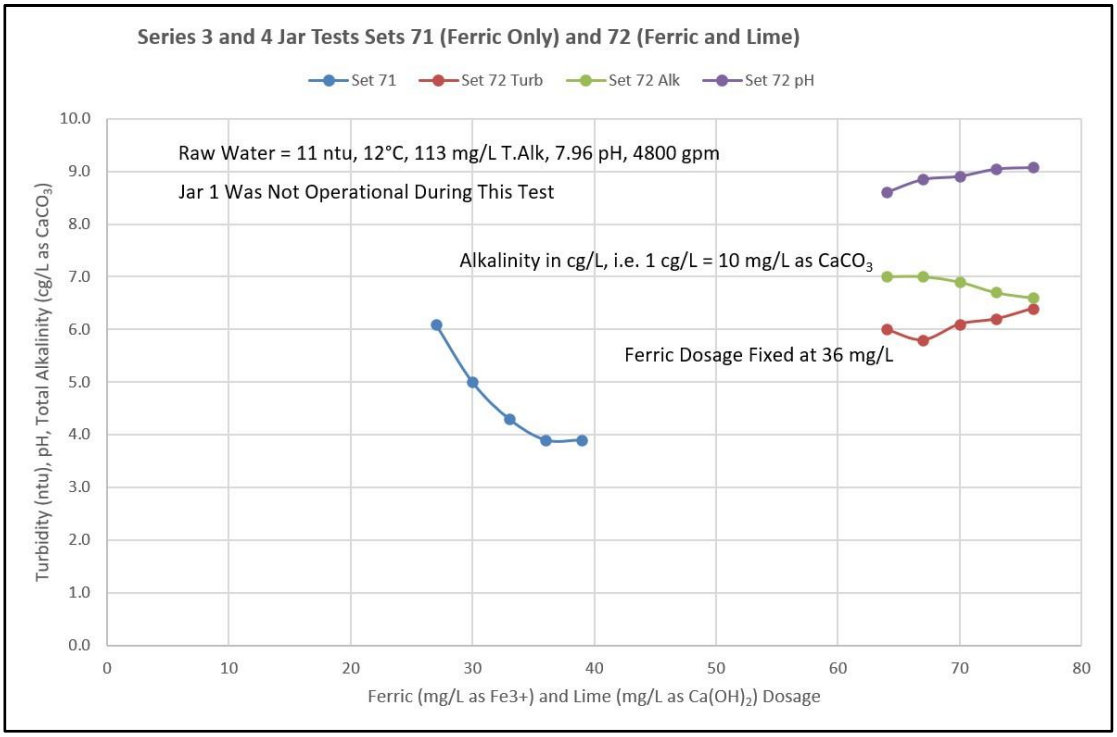

Figure 4.25: Optimization Series 3/4 Jar Sets 71 and 72 Results

Overall, the results of the combined "Series 3" and "Series 4" jar tests showed a marked improvement as compared to the "Series 1" and "Series 2" jar tests when compared to actual plant data. As shown in Figure 4.26 and 4.27 below, although the magnitudes of the jar turbidities, pH, and alkalinities still did not match the plant's data, the overall trends up and down stayed relatively consistent, in that as jar values increased, the corresponding plant value typically increased, and as jar values decreased, the corresponding plant values typically also decreased.

Mathematically defining the relationships between jar and plant turbidities, however, is problematic, as can be seen in Figure 4.28 below. Using a linear regression, the 0.3338 R^2 value for Turbidity is very low, and the variability between the jar and the plant results is high, indicating that defining a mathematical relationship for turbidity is likely problematic, especially when comparing the results to the 'perfect' 1:1 relationship as shown by the red line in Figure 4.28 below. However, at low turbidities, the jar turbidities were typically lower than the plant turbidities, while at high turbidities, the jar turbidities were typically higher than the plant turbidities. It is believed that this has to do with a combination of water temperatures and the difference between quiescent settling in the jars as opposed to the plant, where there is still movement in the water. Also, the higher turbidity values tend to be when the water temperatures are low, so the higher water density at lower temperatures could be slowing down the settling rates.`

Mathematically defining the relationships between jar and plant alkalinities appears to be slightly better using a linear regression, as shown in Figure 4.29 below. The 0.6342 R^2 value for Alkalinity is still low, and the variability of the jar versus plant results is still high (especially when comparing the results to the 'perfect' 1:1 relationship as shown by the red line in Figure 4.29 below), so there is not a large linear correlation between jar and plant alkalinity results. This could be better defined with a larger sample set. There also appears to be some correlation between water temperature and alkalinity, as shown in Figure 29. At lower water temperatures, the alkalinity tends to be higher, which is to be expected, since as the water temperature decreases, chemical reaction times tend to increase. The treatment plant also tends to outperform the jars at lower temperatures. It may be that since at low water temperatures, the plant's flow is typically low, and detention time in the plant clarifiers get very long (as much as 5-1/2 hours at 3,000 gpm), so there is more time for the chemical reactions to complete in the plant as opposed to the jars. Again, a larger sample set could help to make this case.

Also of note is that higher turbidities in both the plant and the jars tends correlate with higher alkalinities in both the plant and the jars (again, both turbidity and alkalinity tend to increase as water temperature decreases. It is likely that the higher turbidity is due primarily to un-settled calcium carbonate. If there is calcium carbonate still in suspension, then titrating for alkalinity with acid also

dissolves this suspended calcium carbonate, resulting in a higher alkalinity reading.

In terms of water temperature versus turbidity, the "Series 4" results showed a better correlation than the "Series 2" results, as shown in Figure 4.30 below. As expected, as water temperatures decreased, the plant's settled water turbidities typically increased (Hanson and Cleasby, 1990) (Morris and Knocke, 1984). This effect was typically mitigated by an increase in Ferric Sulfate Dosage as water temperature decreased, as shown in Figure 4.31 below. Using a mathematical linear regression for this data showed an R^2 value of only 0.7531. but without the 'dip' at the right end at a ferric sulfate dosage of 36 mg/L as Fe^{3+}, the R^2 value could be better. As with the alkalinities, a larger data set could mitigate this issue.

The expected turbidity removal percentages (based on jar test results) showed a much better correlation with the Series 4 tests than with the Series 2 tests, as shown in Figure 4.32 below. Again, the magnitudes had some significant variations, but they also tended to track with the increases and decreases between the expected and actual results.

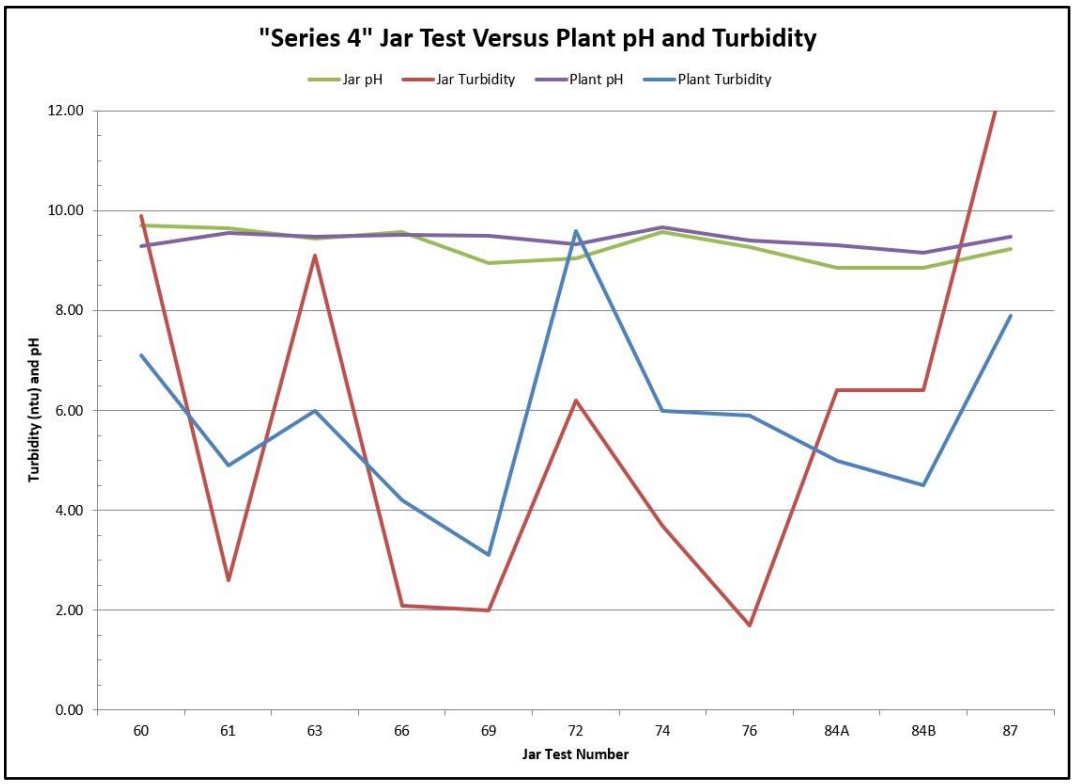

Figure 4.26: Series 4 Plant vs Jar Test pH and Turbidity

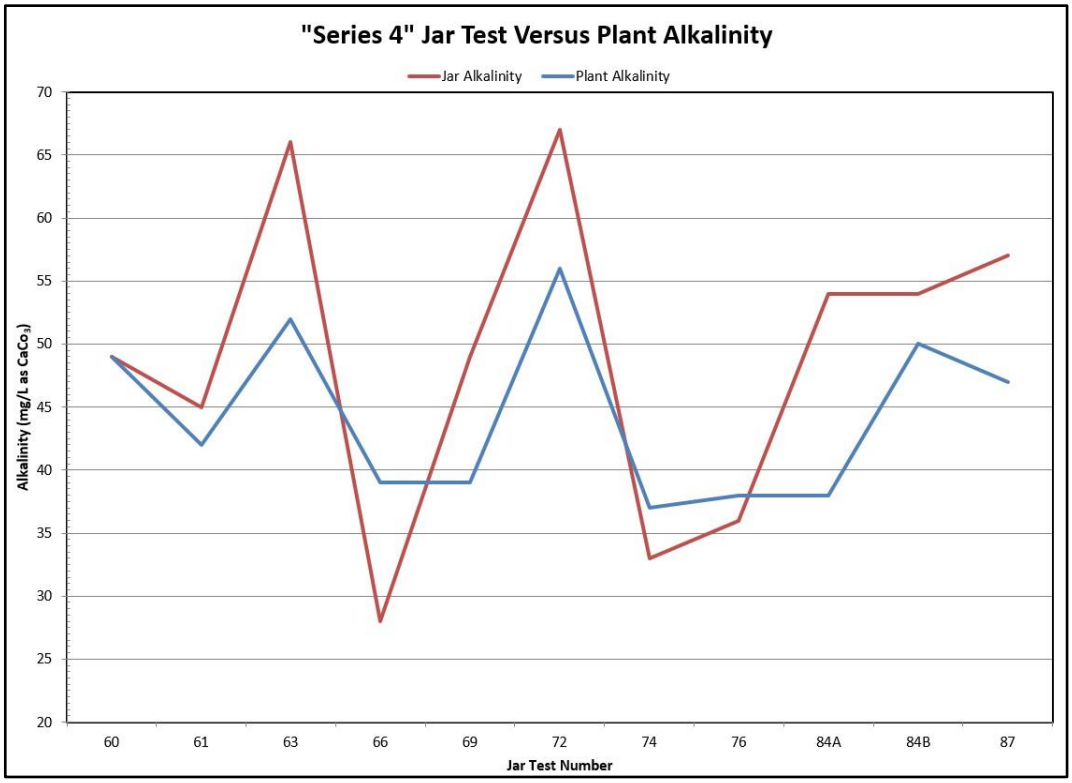

Figure 4.27: Series 4 Plant vs Jar Test Alkalinity

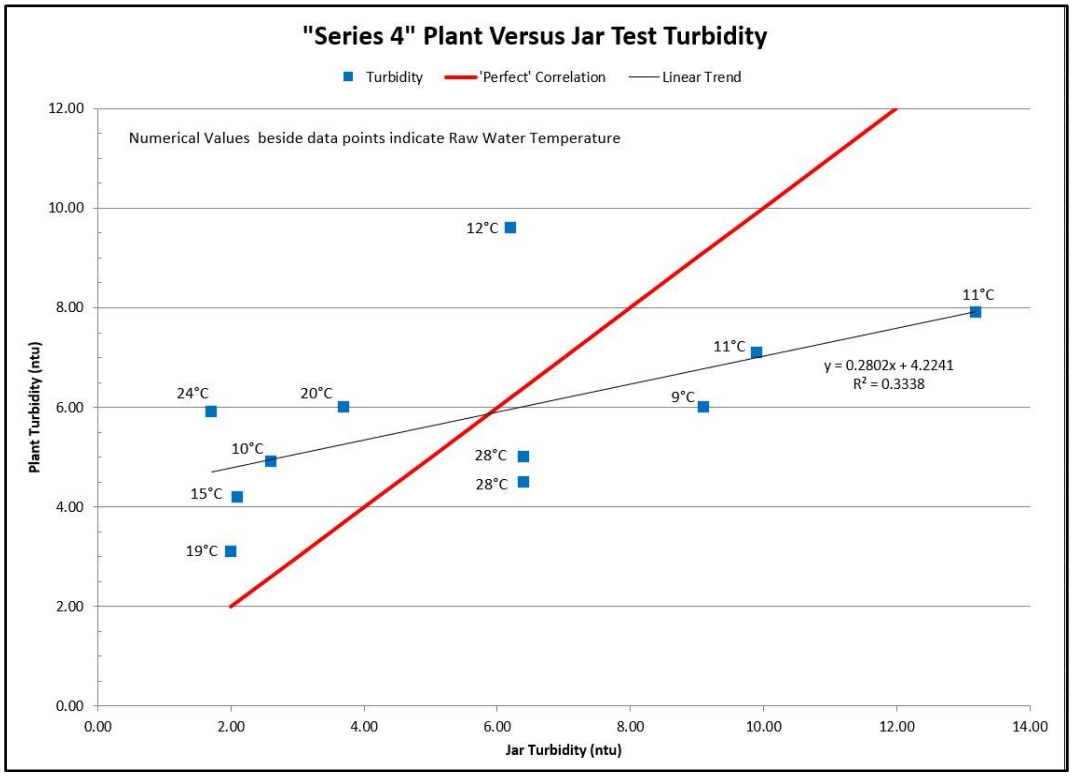

Figure 4.28: Series 4 Plant vs Jar Test Turbidity Regression

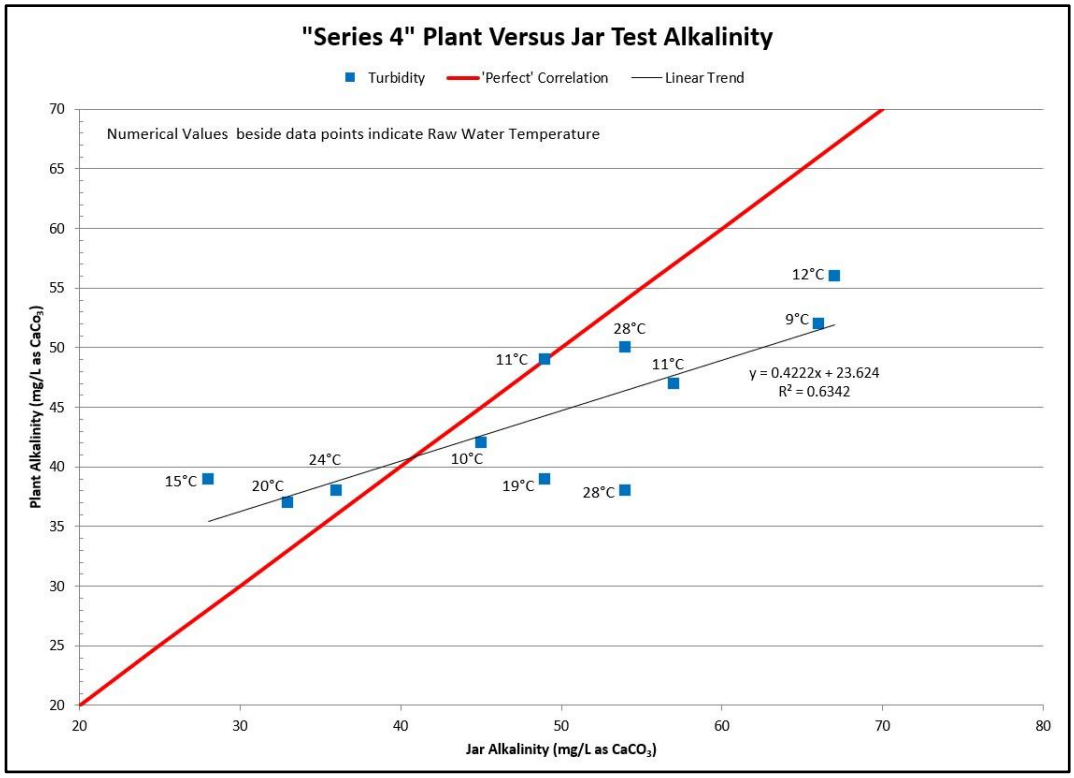

Figure 4.29: Series 4 Plant vs Jar Test Alkalinity Regression

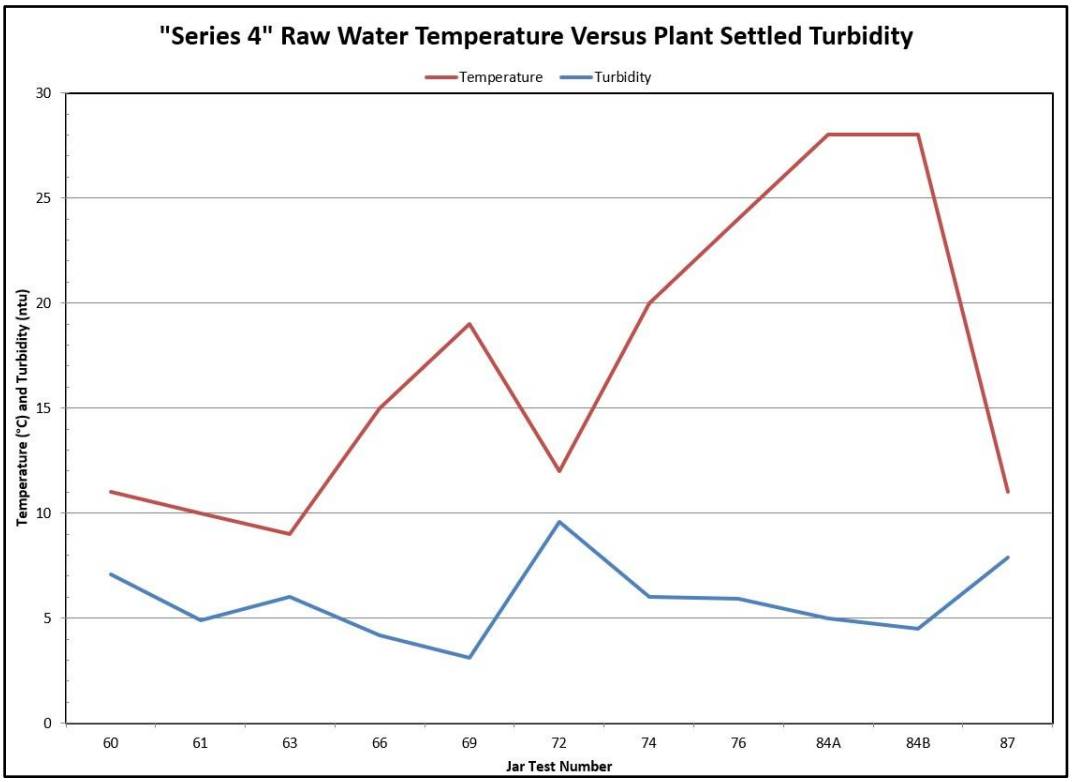

Figure 4.30: Series 4 Raw Water Temperature vs Plant Turbidity

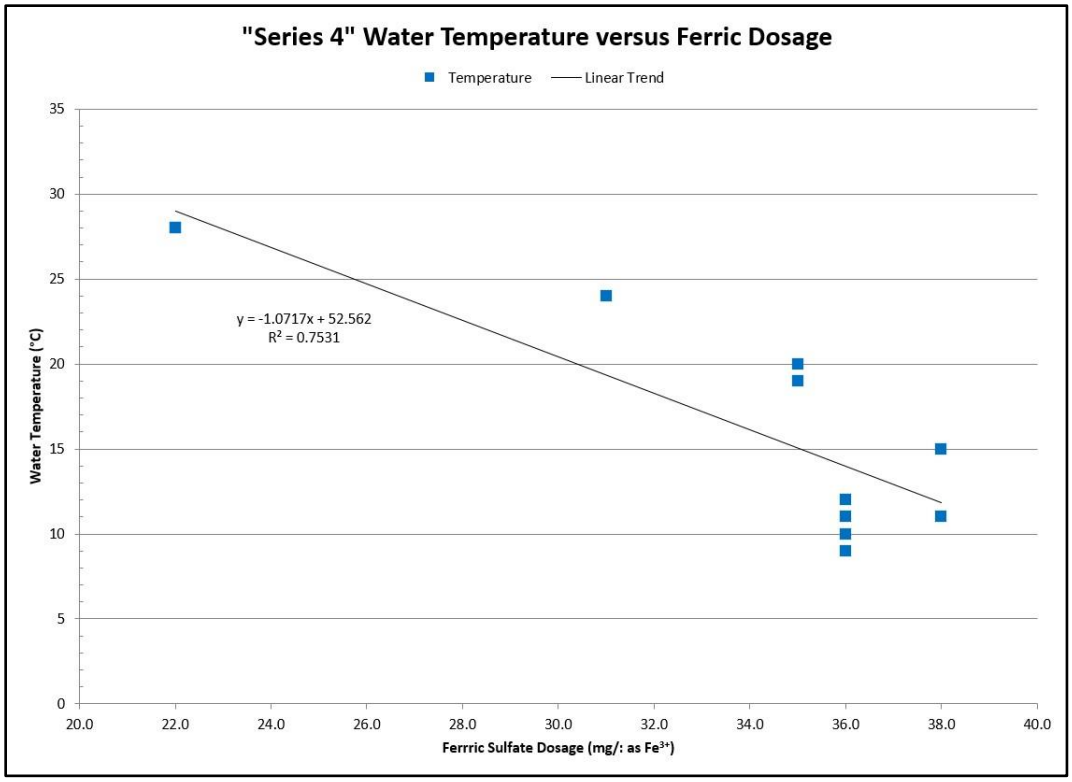

Figure 4.31: Series 4 Water Temperature vs Ferric Sulfate Dose Regression

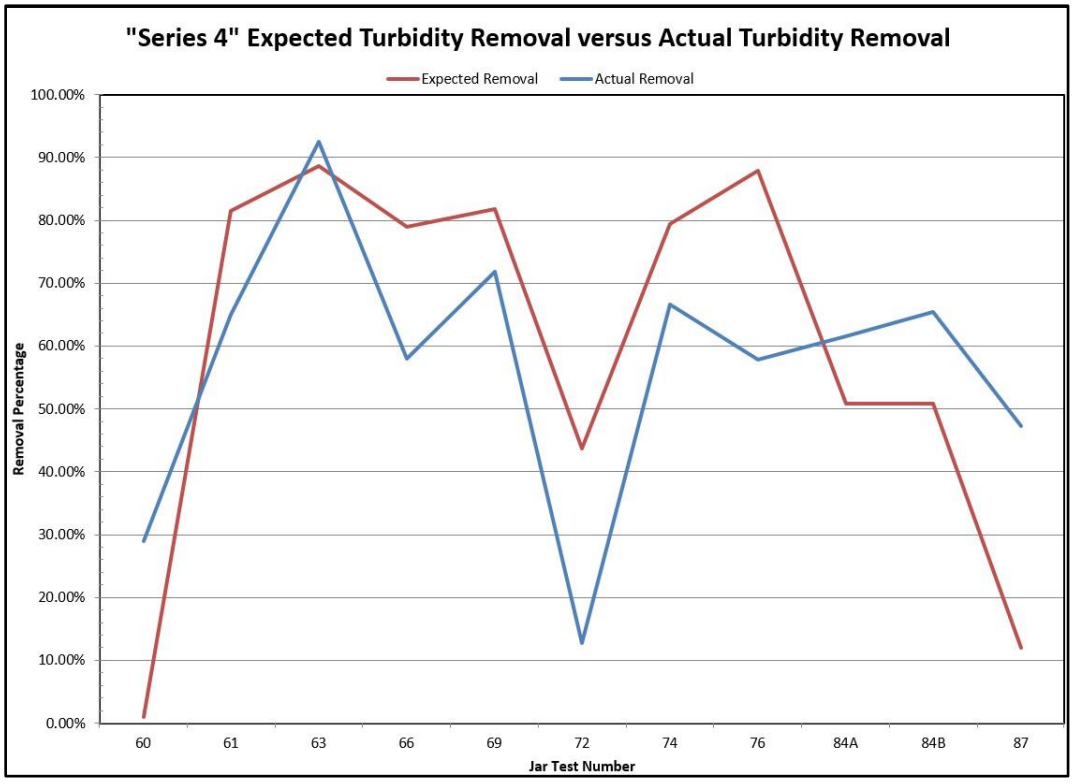

Figure 4.32: Series 4 Expected vs Actual Turbidity Removal Percentages

The magnitude mismatching discussed above is believed to be caused by many factors, some of which are beyond the scope of this study. Much additional research will be required to verify or discredit these theories. These factors include:

A. The volumes of the bulk chemical being used to make up stock solutions for the jar tests are small enough, and the dilution factors are large enough, that even a small error in either chemical or dilution water volume can create a discernable difference between jar and plant results.

B. During several of the jar tests (many of which were performed by the plant operators), it was observed that the jar velocity gradients were not always matched to the actual plant velocity gradients. However, this did not appear to make a large impact in the differences between actual plant and jar test results. This observation is backed up by other's research (Clark, 1985), (Cleasby, 1984), (Han and Lawler, 1992).

C. The actual chemical feed pumps used to dose ferric sulfate into the plant processes are small, low-cost peristaltic pumps with three pump heads each. These pump heads are not spring-loaded and as such can have some 'slip' due to a lack of full occlusion of the pump tubing after a few hundred hours of tubing operation, which then results in a slightly lower than nominal dosage being applied to the actual treatment process. The actual ferric sulfate feed lines are only ½" diameter stainless steel tubing, and as such it was decided not to attempt to use flow meters on the feed lines due to cost (modern magnetic flow meters can be obtained that in theory should accurately measure the flow in this tubing, but to date they have not been tested at the plant, primarily due to their cost).

D. Changes in raw water quality, e.g. alkalinity, pH, organics content, total solids content, rainfall (which results in changes both to the type and magnitude of raw water turbidity), and many other factors can drastically change the 'optimal' dosages of the primary treatment chemicals.

E. Changes in raw water temperature typically require dosage changes. These changes are typically gradual and traceable over time. As water temperature increases, the chemical dosages can typically be reduced.

F. Increasing temperature in the clarifier influent water temperature as compared to the overall clarifier water temperature as well as increasing wind speed can cause differential flow and result in short circuiting of the clarifiers (Goula, Kostoglou, Karapantsios, and Zouboulis, 2008). In fact, as temperatures rise at the treatment plant during the day, clarifier effluent turbidities at times tend to increase, and then tend to decrease once the sun sets (personal observation). In addition, it has been observed that

during high wind conditions at the treatment plant, some over-topping of the baffle wall in the clarifiers can occur, as the top of the baffle wall is only about an inch above the normal water surface.

G. Jar test results can be adversely affected during low temperature periods. Since the jar test mechanism is located in a climate-controlled room, given the low volume of water used (typically 2 L jars), and given the time it takes for rapid mixing, three stages of flocculation, and then settling, the water temperatures in the jars can increase by several degrees during the testing process (In higher temperature periods, the water temperature is typically much closer to the laboratory ambient temperature, so this temperature effect is not typically an issue).

H. After flocculation, the plant's water enters a 54" diameter pipe that runs from the train's flocculator exit to the clarifier entrance. For the 'A' train, this pipe is about 60 feet long, and for the 'B' train, this pipe is about 180 feet long. The typical velocity range through these pipes (when they are clean) is between 0.42 and 1.12 ft/sec (corresponding to a flow range of 3,000 gpm to 8,000 gpm). Historically, these pipes must be cleaned on an annual basis due to floc settling in the pipes, as they can accumulate enough sludge to fill up to 25% of the pipe volume in one year (when then increases the velocity through the pipes). It is difficult if not impossible to quantify when most of this settling occurs, although it is theorized that most of the settling occurs under low flow conditions (i.e., when water temperatures are low during the winter). These pipes can typically only be inspected once per year, as the train's clarifier and flocculation basins must be drained to inspect them. However, as shown in Figure 4.28 above, since the plant appears to perform better than the jars at lower temperatures, it is postulated that settling is occurring in the pipes during low flow conditions, and then during high flow (i.e. high temperature) conditions, the increased velocity could be scouring some sludge as it passes through the pipes. There is no known (economical) way to prove or disprove this theory.

I. It is extremely difficult to dose six jars with chemical simultaneously. It is possible using ceramic disks that hold very small amounts of chemical, but this requires the use of micro-pipettors that are delicate and expensive. These pipettors typically do not last long in a production environment when being used by multiple plant operators. So, exact timing of detention, especially in the "rapid mix" portion of the jar test, can result in mismatching between jars.

J. At times, the plant's water is not at CO_2 equilibrium, which causes issues during titration for alkalinity. This is mostly detectable as the titration approaches the end point, and can be observed by the indicated pH

beginning to rise rather than fall. This is due to the small (100 mL) sample size which is being stirred, resulting in a large air-water interface, which then allows rapid CO_2 transfer between the air and the water. When this occurs, actual plant alkalinity values can only be estimated.

K. Wall effects in jar testing (which is a well-known effect) can also contribute to mismatches between jar tests and plant results.

4.5. Alternative Chemicals

During the "Series 3" optimization trials, two alternative chemicals were trialed:

A. A proprietary poly ferric sulfate from Global Specialty Chemicals was trialed (the chemical supplier actually ran these jar tests at the District's treatment plant). The response from the chemical manufacturer following these trials was that the results were inconclusive, and that more testing was needed. The manufacturer did not supply the District with the actual jar test results. Unfortunately, the onset of the COVID-19 pandemic prevented them from coming to repeat the testing, and the company's Dallas area representative retired. The company has not returned for more testing since that time.

B. An alternative chemical for softening (as a substitute for calcium hydroxide) was also trialed in one set of jar tests. Sodium hydroxide was substituted, and was extremely unsuccessful. These results are shown in Table 4.3 below. As seen in the table, settled water turbidities looked very good for NaOH dosages of 40 mg/L as NaOH and above, and the pH ranges for NaOH dosages of 40 and 60 mg/L as NaOH were acceptable. However, the required alkalinity reduction to 60 mg/L as $CaCO_3$ or less did not happen. The lack of alkalinity reduction, the extreme cost difference between $Ca(OH)_2$ and NaOH, and the increased dangers of handling NaOH versus $Ca(OH)_2$ indicated that sodium hydroxide was not a good substitute for calcium hydroxide for the District.

Jar #	NaOH Dosage (mg/L as NaOH)	Ferric Dosage (mg/L as Fe^{3+})	pH	Turbidity (ntu)	Phenol Alkalinity (mg/L as $CaCO_3$)	Total Alkalinity (mg/L as $CaCO_3$)	Water Temperature (°C)
1	20.0	50.0	7.94	18.00	0	75	19.0
2	40.0	50.0	9.51	3.84	25	92	19.0
3	60.0	50.0	9.93	3.18	31	95	19.0
4	80.0	50.0	10.41	4.89	47	103	20.0
5	100.0	50.0	10.71	5.76	60	111	20.0
6	120.0	50.0	10.94	3.77	90	138	20.0

Table 4.22: Jar Tests using Sodium Hydroxide for pH and Alkalinity Control

4.6. Final Adjustments

During the last portion of the "Series 3" optimization trials, a minor adjustment was made to the calcium hydroxide application point. Originally, when the calcium hydroxide was moved to the rapid mix basins, it was placed at the entrance to the basins. This did result in a large buildup of calcium carbonate on both the mixer blades and the chamber walls, but as previously stated, the new rapid mixers were designed to be capable of continued operation without damage even with this buildup. However, on an annual basis, this buildup has to be removed, which is a time-consuming process that involves jackhammering the calcium carbonate off of the basin walls and the mixer blades.

In an attempt to minimize this buildup, the calcium hydroxide application point was moved to just before the exit of the rapid mix basin on one of the two treatment trains as a 'plant trial'. The water quality did not change, and after one year of operation, the two treatment trains had a drastic difference in the amount of calcium carbonate buildup on the mixer blades and basin walls. From both personal observations and personal communications with Mike Swint, the DCPCMUD Maintenance Manager, the train with the application point at the rapid mix basin exit had far less buildup than the train with the application point at the rapid mix basin entrance. As a result, the calcium hydroxide application point was moved to the exit of the rapid mix basin for both treatment trains, with no changes detected in water quality.

Based on the observed lack of change in water quality versus buildup of calcium carbonate in the rapid mix system after moving the calcium hydroxide application point, the rapid mixer itself was turned off for one treatment train while both trains were in operation (i.e., high-temperature and high flow summer operations). No change in water quality was observed. However, as water

temperature and flow rates decreased entering the end of summer, water quality began to degrade on the train with the mixer off. As this was the very end of the testing, more study and quantification of this phenomenon is required, but the preliminary results indicate that at higher flow rates and/or water temperatures, there is enough hydraulic mixing due to velocity in the rapid mix basins to eliminate the need for mechanical mixing, but when the water temperatures and/or flow rates drop sufficiently, some mechanical mixing is required to maintain consistent water quality.

5. Conclusions and Recommendations

The goal of this study was to find a way to optimize the primary treatment chemicals for the Dallas County Park Cities Municipal Utility District's 25 mgd potable water treatment plant in such a way as to allow plant operators to (relatively) easily optimize the chemical dosages of coagulation (i.e., ferric sulfate) and pH/alkalinity adjustment (i.e., calcium hydroxide) chemicals. This 'optimization', as shown in the analyses above, is not a single set of values, but is rather a moving target based on many raw water parameters such as pH, alkalinity, organics, turbidity magnitudes and types, and temperature.

The single biggest conclusion that can be made from this optimization effort is that the biggest contributor to acceptable water quality from flocculation and sedimentation, at least for the untreated water supply for the District, is the application point of the chemicals used rather than either the specific dosages of the chemicals used or the velocity gradients applied to the basins. Jar testing for optimization is also not a 'one-time' process, but rather must be periodically repeated to obtain starting point chemical dosages, which must then have adjustments applied based on the results of the actual treatment process. As previously stated, many factors can influence the 'optimal' dosages of the chemicals used. Other factors influencing the resultant water quality are the quality of the chemicals used and the accuracy of the chemical dosing process, both in the actual treatment process and in the jar test dosing process. Precise matching of jar velocity gradients to actual plant velocity gradient conditions does not appear to be critical to successful optimization, although this could warrant further study.

For the District's treatment plant, the final 'optimized' conditions show that feeding calcium hydroxide into the exit of the rapid mix basins while feeding ferric sulfate into the first flocculation chamber consistently produces the best water quality while simultaneously minimizing the cost of the treatment chemicals and the amount of annual plant maintenance required. The 'optimal' dosage of ferric sulfate and calcium hydroxide is a moving target, and must be periodically adjusted based on the raw water quality and temperature.

The recommendations resulting from this optimization study are:

A. The plant operators should perform a minimum of two jar tests per week, with the first test using only ferric sulfate to set the best 'base-line' ferric

sulfate dosage, and immediately thereafter the second test using both ferric sulfate (set to the fixed ferric sulfate dosage from the first test) and calcium hydroxide (at varying dosages) to determine the best 'base-line' dosage of calcium hydroxide. These dosages should then be applied to the actual plant process and then adjusted as necessary based on the actual plant results.

B. Any time a major shift occurs in the water quality of either the plant's raw water or settled water quality, jar tests should immediately be performed as described above to counteract such quality shifts.

C. The determination of the optimum ferric sulfate dosage as described above does not necessarily mean that it is the optimum dosage once calcium hydroxide is added; the two chemicals tend to work together as a symbiotic pair. Therefore, the District should investigate the potential that the optimum ferric sulfate dosage could possibly be lowered (at least slightly) by performing additional jar tests in a 'third' sequence after determining the 'optimum' calcium hydroxide dosage as described in the Materials and Methods Section above, in which the ferric sulfate dosage would be incrementally be lowered from its previously 'optimized' value to determine if the addition of calcium hydroxide has impacted this 'optimum' ferric sulfate dosage.

D. The plant's ferric sulfate feed pumps, although they are very inexpensive to purchase and maintain, have a noticeable 'slip' at high pump speeds (see Figure 5.1 below for a typical calibration curve for these pumps). The chemical feed formula used for automatically dosing the ferric sulfate is based in part on the calibrated theoretical flow rate at 100% speed (i.e., 60 Hz output from the VFD controlling the motor). However, these pumps are never operated (except for testing) at greater than 50 % (30 Hz) speeds. So, the actual feed rates of the plant's ferric sulfate feed pumps should be tested at 25% and 50% of the maximum pump speeds on a weekly basis. The 'maximum speed' flow rate setpoint of the pumps in the feed control systems should then be adjusted to twice the observed flow at 50% speed. If a large variation of flow or a non-linearity between 25% and 50% speed is observed, then the pump(s) should be checked for possible malfunctions (degradation of tubing, worn bearings, etc.).

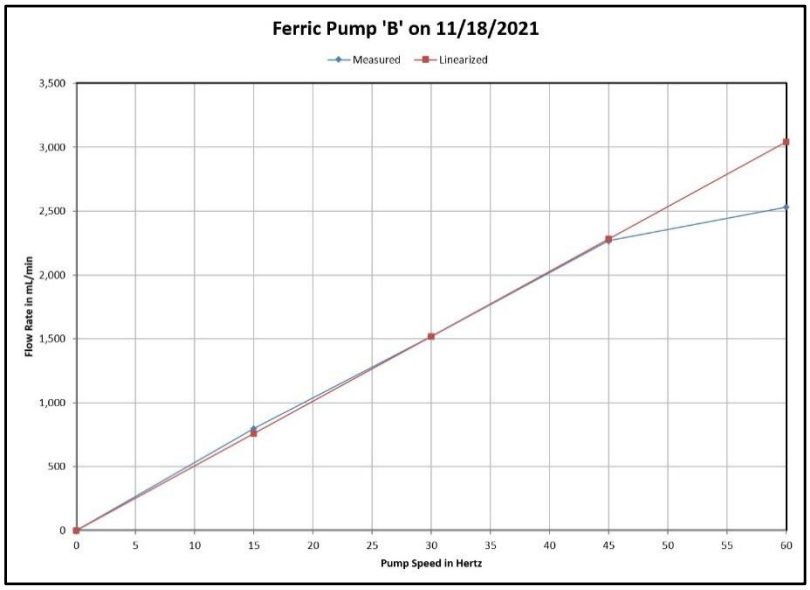

Figure 5.1: Ferric Sulfate Pump Typical Calibration Curve

E. The District should consider investment in magnetic flow meters for measuring the actual output of each ferric sulfate feed pump for even more precise dosage control.

F. The District should consider the installation of Stamford baffles below the sections of the clarifier effluent weirs where they float inside of the outer walls to reduce the effect of wall climb in the clarifiers.

G. The District should consider raising the height of the clarifier baffle walls to eliminate over-topping of the baffle walls (with should help mitigate short-circuiting) during high wind conditions.

H. Based on the observed lack of water quality change when turning off the rapid mixers at high flows, the District should conduct additional testing for further optimization by lowering and/or raising the velocity gradients in gradual steps (first in only jar tests) for each rapid mixer and flocculation basin. If the jar tests appear to indicate acceptable results, the same velocity gradient changes should be implemented on a plant scale. This must be done carefully, however, with the observation that the velocity gradients during flocculation must always be high enough be prevent settling in the flocculation chambers.

I. The District should investigate possible methods of simultaneously dosing chemicals into the six jars in the testing apparatus to allow for more consistent mimicking of the actual plant processes. The details of this recommendation are beyond the scope of this study.

6. Appendix 1: Treatment Plant Turbidity Data during the Plant Crisis

Table 6.1: Treatment Plant Turbidity Data During Plant Crisis

Date and Time	Clarifier Effluent (ntu)	Plant Effluent (ntu)
03/21/2012 00:00	7.6	0.17
03/21/2012 02:00	8.1	0.17
03/21/2012 04:00	7.9	0.17
03/21/2012 06:00	9.2	0.18
03/21/2012 08:00	5.4	0.18
03/21/2012 10:00	7.8	0.19
03/21/2012 12:00	6.7	0.19
03/21/2012 14:00	7.8	0.20
03/21/2012 16:00	11.8	0.22
03/21/2012 18:00	19.2	0.22
03/21/2012 20:00	17.1	0.22
03/21/2012 22:00	15.4	0.22
03/22/2012 00:00	15.6	0.23
03/22/2012 02:00	13.5	0.28
03/22/2012 04:00	11.5	0.33
03/22/2012 06:00	13.8	0.39
03/22/2012 08:00	13.5	0.41
03/22/2012 10:00	13.9	0.45
03/22/2012 12:00	12.9	0.35
03/22/2012 14:00	12.6	0.33
03/22/2012 16:00	13.8	0.33
03/22/2012 20:00	12.6	0.32
03/22/2012 22:00	9.6	0.30
03/23/2012 00:00	9.1	0.29
03/23/2012 02:00	9.1	0.30
03/23/2012 04:00	9.6	0.29
03/23/2012 06:00	9.3	0.30
03/23/2012 08:00	9.3	0.30
03/23/2012 10:00	8.6	0.33
03/23/2012 12:00	8.2	0.38
03/23/2012 14:00	9.5	0.41
03/23/2012 16:00	9.5	0.34
03/23/2012 18:00	10.3	0.32
03/23/2012 20:00	9.0	0.30
03/23/2012 22:00	7.5	0.30
03/24/2012 00:00	7.8	0.30
03/24/2012 02:00	8.1	0.30
03/24/2012 04:00	7.9	0.30
03/24/2012 06:00	8.0	0.30
03/24/2012 08:00	7.9	0.29
03/24/2012 10:00	8.0	0.29
03/24/2012 12:00	7.2	0.29
03/24/2012 14:00	7.8	0.28
03/24/2012 16:00	9.5	0.28
03/24/2012 18:00	8.7	0.28
03/24/2012 20:00	7.0	0.28

Date and Time	Clarifier Effluent (ntu)	Plant Effluent (ntu)
03/24/2012 22:00	7.9	0.28
03/25/2012 00:00	8.1	0.28
03/25/2012 02:00	7.8	0.29
03/25/2012 04:00	8.6	0.29
03/25/2012 06:00	8.5	0.29
03/25/2012 08:00	7.9	0.29
03/25/2012 10:00	8.3	0.29
03/25/2012 12:00	7.7	0.29
03/25/2012 14:00	8.4	0.29
03/25/2012 16:00	9.5	0.29
03/25/2012 18:00	10.0	0.29
03/25/2012 20:00	9.4	0.29
03/25/2012 22:00	9.0	0.29
03/26/2012 00:00	8.6	0.29
03/26/2012 02:00	9.1	0.29
03/26/2012 04:00	8.2	0.29
03/26/2012 06:00	8.9	0.29
03/26/2012 08:00	8.5	0.28
03/26/2012 10:00	9.4	0.28
03/26/2012 12:00	8.3	0.28
03/26/2012 14:00	9.3	0.28
03/26/2012 16:00	7.8	0.28
03/26/2012 18:00	5.9	0.28
03/26/2012 20:00	5.4	0.27
03/26/2012 22:00	5.2	0.26
03/27/2012 00:00	5.1	0.25
03/27/2012 02:00	4.6	0.25
03/27/2012 04:00	5.0	0.24
03/27/2012 06:00	4.8	0.23
03/27/2012 08:00	5.5	0.23
03/27/2012 10:00	5.3	0.23
03/27/2012 12:00	6.4	0.23
03/27/2012 14:00	5.7	0.22
03/27/2012 16:00	5.5	0.22
03/27/2012 18:00	4.6	0.21
03/27/2012 20:00	4.6	0.21
03/27/2012 22:00	4.8	0.20

7. Appendix 2: Jar Tester Velocity Gradient & Speed Formula Derivations

7.1. Jar Test Apparatus Velocity Gradient Formula Derivation

Figure 7.1 below shows the Phipps-Bird jar test velocity gradient chart as obtained from the manufacturer. Since the District's jar test apparatus does not include stators, this chart was magnified to aid in the determination of velocity gradients verse jar rpm at different water temperatures as shown in Figure 7.2 below.

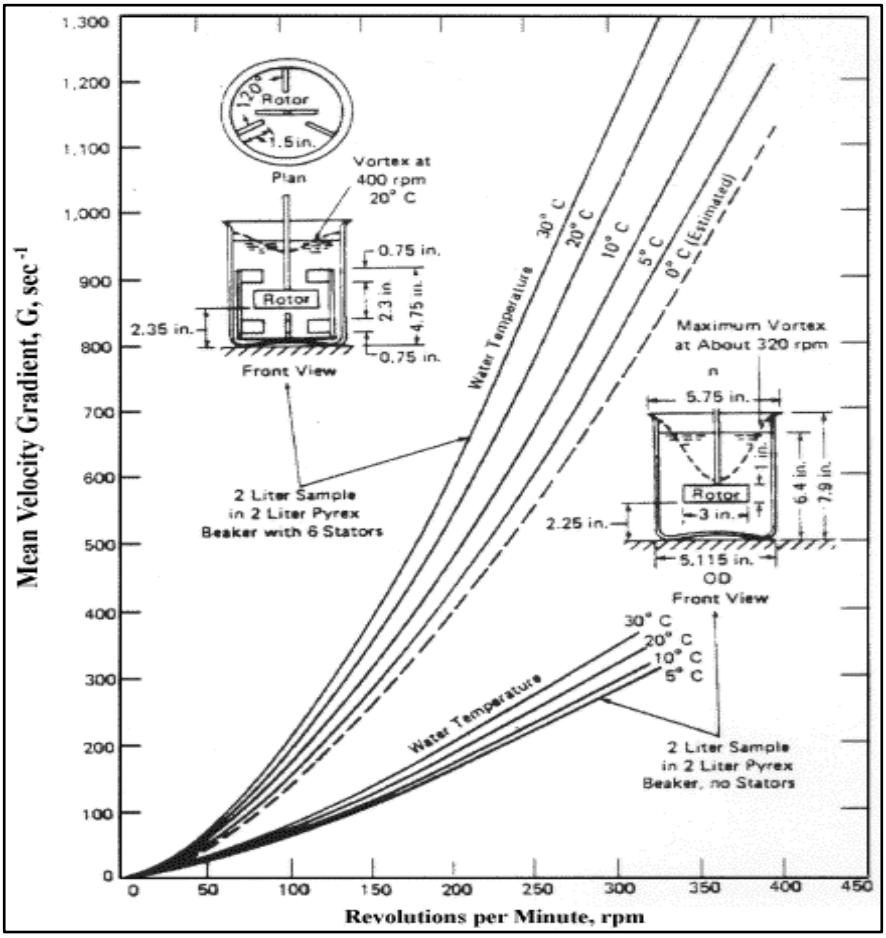

Figure 7.1: Phipps Bird Jar Test Apparatus Velocity Gradient Curves from Manufacturer

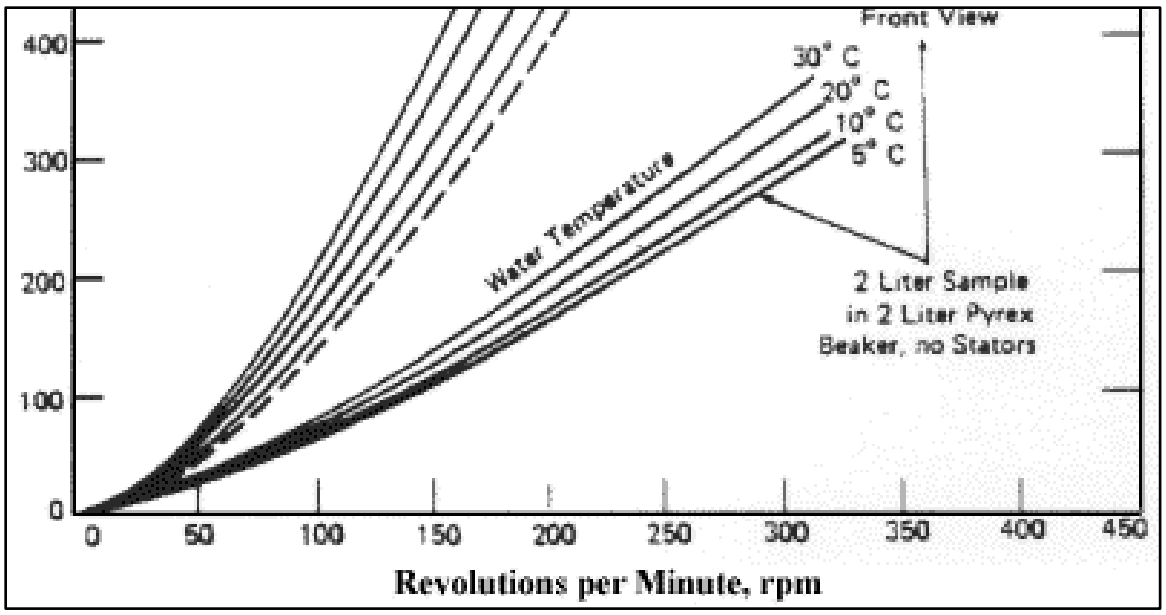

Figure 7.2: Phipps Bird Jar Test Apparatus Velocity Gradient Curves Magnified

The velocity gradients and jar speeds at the different water temperatures obtained from Figure 7.2 above were then manually entered into an Excel spreadsheet (note: the maximum available jar speed for the District's apparatus is 300 rpm). These values were then charted using an Excel chart, and then each curve was fitted to an equation using a 4^{th}-order polynomial trend line, as shown in Figure 7.3 below (Note that for each of the 6 equations shown in Figure 7.3, the R^2 value is extremely close to unity, indicating that the equation is a good fit for the curve). Therefore, it is deduced that a 4^{th}-order polynomial equation of the form $G = Ax^4 + Bx^3 + Cx^2 + Dx$, with the variable x based on paddle speed, is adequate for calculating a family of curves for velocity gradient based on paddle speed.

However, this still does not provide a single equation for velocity gradient based on a combination of paddle speed and temperature. So, the individual values for each A, B, C, and D coefficient were then plotted with respect to water temperature, as shown in Figures 7.4 to 7.7 below, and each of these plots was regressed using Excel's Trend Line functionality to produce an equation for each of the A, B, C, and D coefficients based on water temperature.

As shown in Figures 7.4 to 7.7 below, each coefficient's regression was exactly linear, with an R^2 value of 1.0. So, the coefficient equations obtained from Figures 7.4 to 4.7 were combined with the general $G = Ax^4 + Bx^3 + Cx^2 + Dx$ equation from Figure 7.3, with constants simplified, to obtain a final single equation for the velocity gradient of the jar tester apparatus based only on water temperature t in °C and jar speed S in rpm. The resulting formula is:

$$G = \left(\left((1.380e^{-10})(t) + 3.545e^{-9}\right)(S^4)\right) + \left(\left((-5.860e^{-8})(t) - 5.366e^{-6}\right)(S^3)\right) + \left(\left((1.364e^{-5})(t) + 3.215e^{-3}\right)(S^2)\right) + \left(\left((6.500e^{-3})(t) + 3.115e^{-1}\right)(S)\right)$$

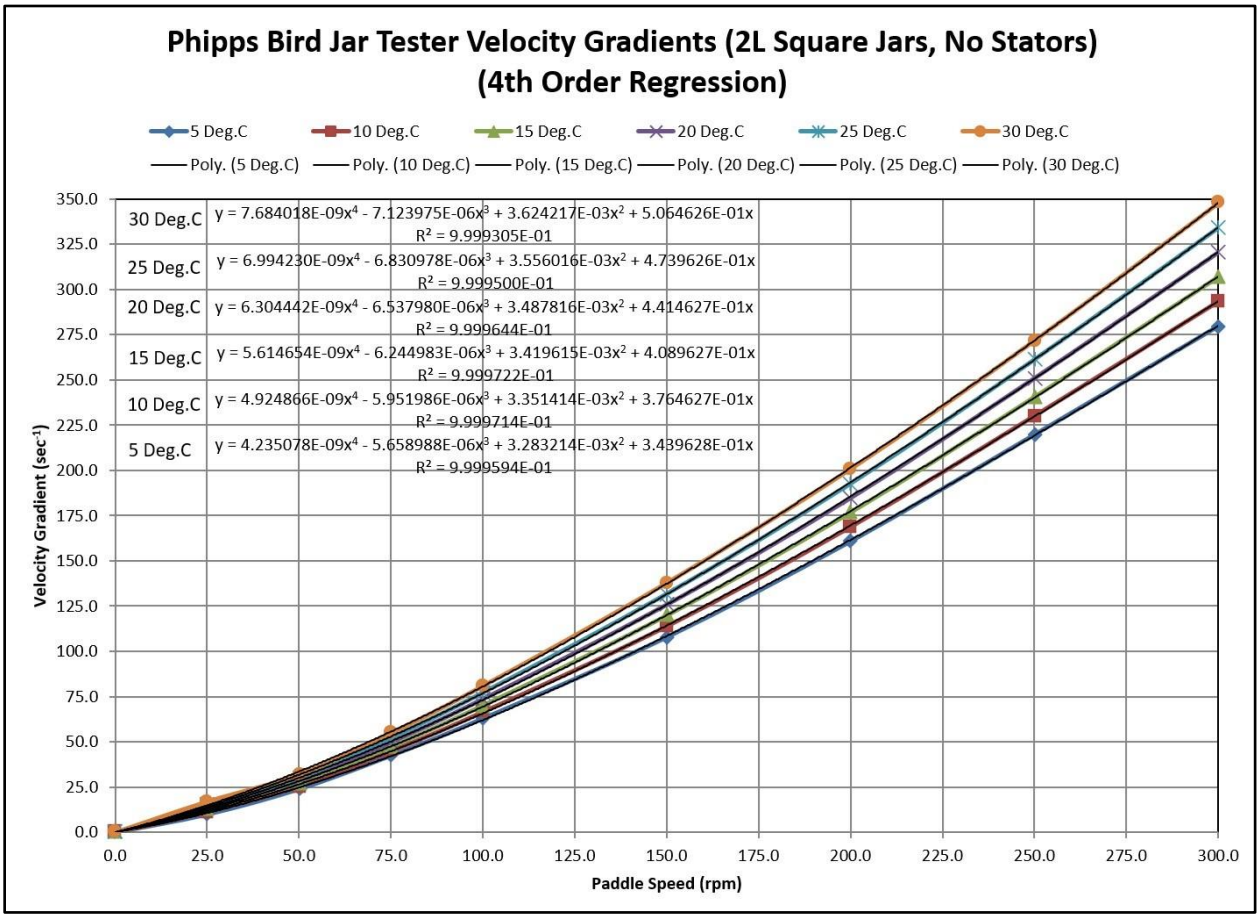

Figure 7.3: Jar Test Apparatus Velocity Gradient Curves Regressed

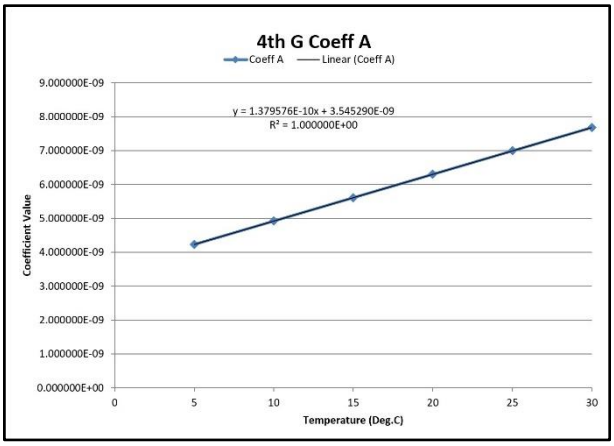

Figure 7.4: Jar Test Apparatus Velocity Gradient Formula Coefficient A Regression

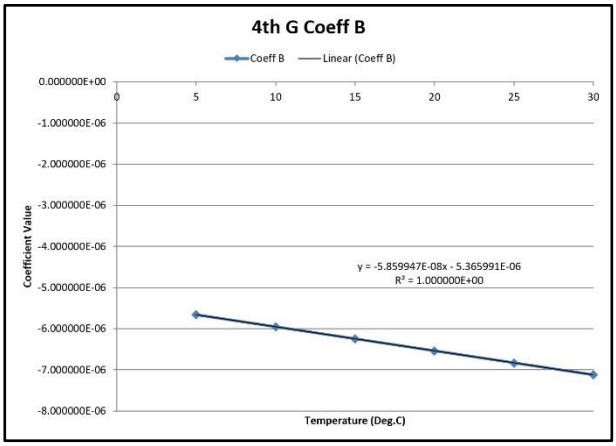

Figure 7.5: Jar Test Apparatus Velocity Gradient Formula Coefficient B Regression

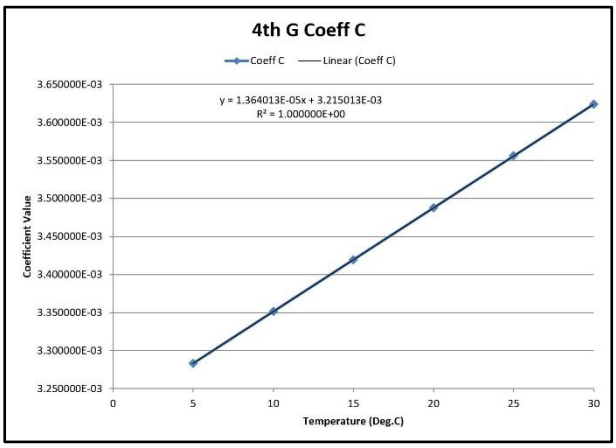

Figure 7.6: Jar Test Apparatus Velocity Gradient Formula Coefficient C Regression

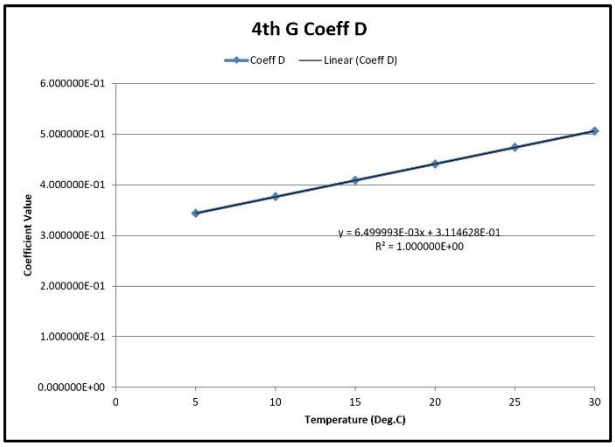

Figure 7.7: Jar Test Apparatus Velocity Gradient Formula Coefficient D Regression

7.2. Jar Test Apparatus Jar Speed Formula Derivation

To obtain a formula for Jar Speed based on a specified velocity gradient, the same method was employed. However, the axes from Figure 7.3 were reversed since the independent variable is now jar test apparatus speed rather than velocity gradient. The curves were then re-regressed, with Excel trend lines again based on a 4th -order polynomial. These results are shown in Figure 7.8 below.

As with the formula for the velocity gradient, the curves for the individual coefficients were then regressed to obtain formulas for the A, B, C, and D coefficients, as shown in Figures 7.9 to 7.12 below. Note that although these coefficient formulas are not 'perfect' (R^2 values in the 0.995 to 0.999 range), they are extremely close to unity, so are considered to be adequate.

So, the coefficient equations obtained from Figures 7.9 to 7.12 were combined with the general $S = Ax^4 + Bx^3 + Cx^2 + Dx$ equation from Figure 7.8, with constants simplified, to obtain a final single equation for jar speed based only on water temperature t in °C and desired velocity gradient in sec^{-1}. The resulting formula is:

$$\boldsymbol{S = \Big(\Big(\big((-4.410e^{-11})(t^2)\big) + (3.297e^{-9})(t) - 8.271e^{-8}\Big)(G^4)\Big) + \Big(\Big(\big((2.271e^{-8})(t^2)\big) - (1.871e^{-6})(t) + 5.562e^{-5}\Big)(G^3)\Big) + \Big(\Big(\big((-3.695e^{-6})(t^2)\big) + (3.516e^{-4})(t) - 1.359e^{-2}\Big)(G^2)\Big) + \Big(\Big(\big((2.401e^{-4})(t^2)\big) - (3.091e^{-2})(t) + 2.365\Big)(G)\Big)}$$

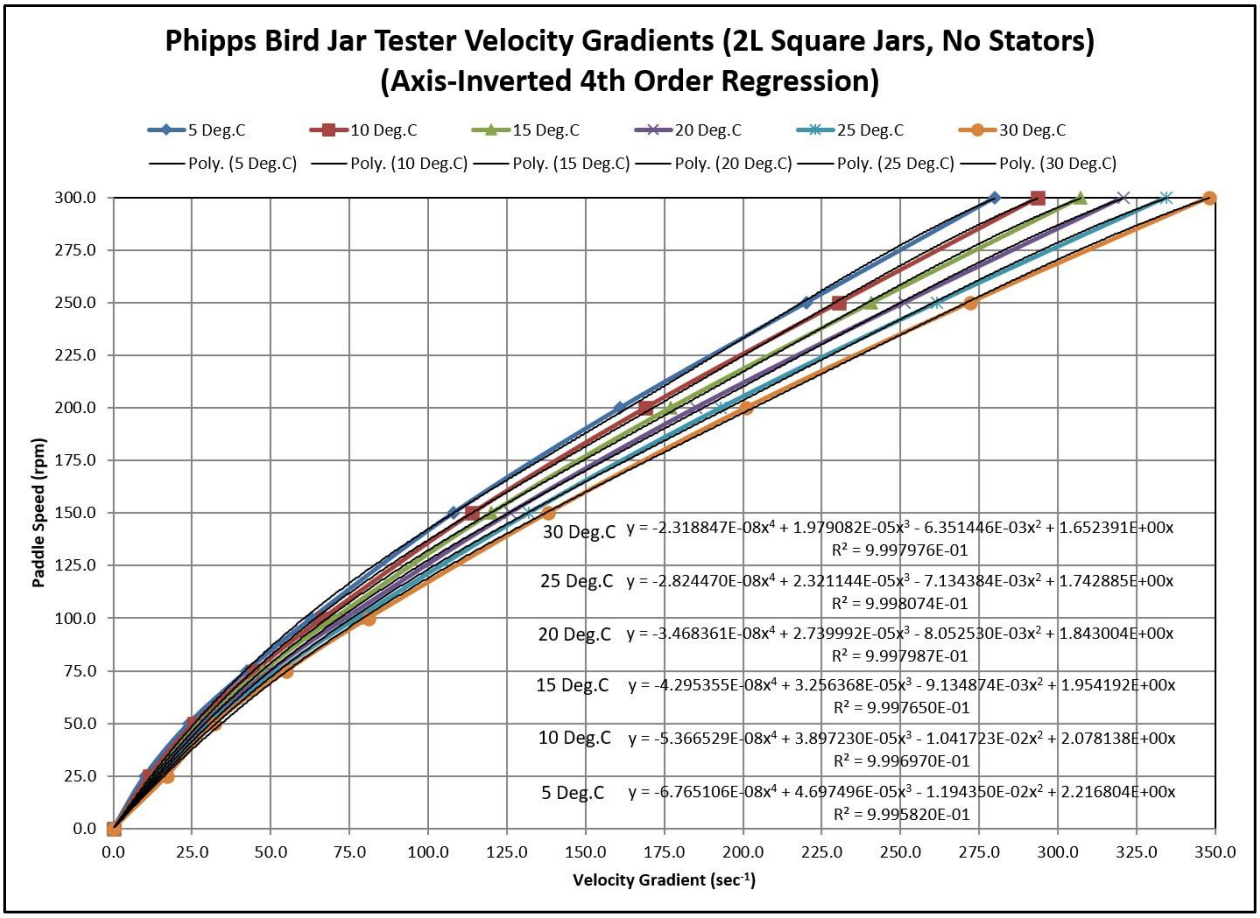

Figure 7.8: Jar Test Apparatus Paddle Speed Curves Regressed

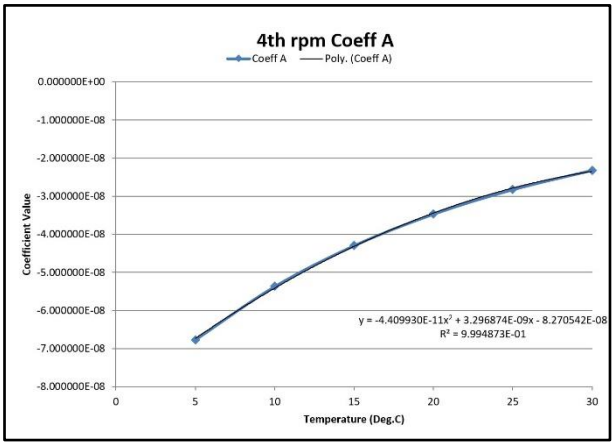

Figure 7.9: Jar Test Apparatus Speed (rpm) Formula Coefficient A Regression

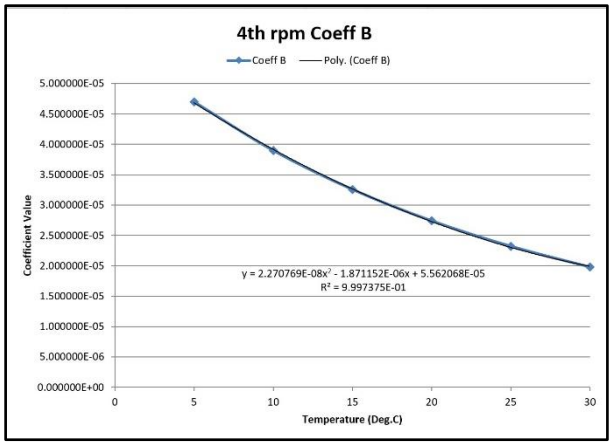

Figure 7.10: Jar Test Apparatus Speed (rpm) Formula Coefficient B Regression

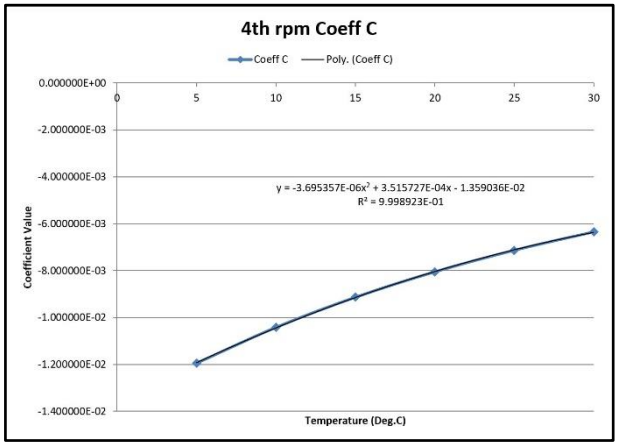

Figure 7.11: Jar Test Apparatus Speed (rpm) Formula Coefficient C Regression

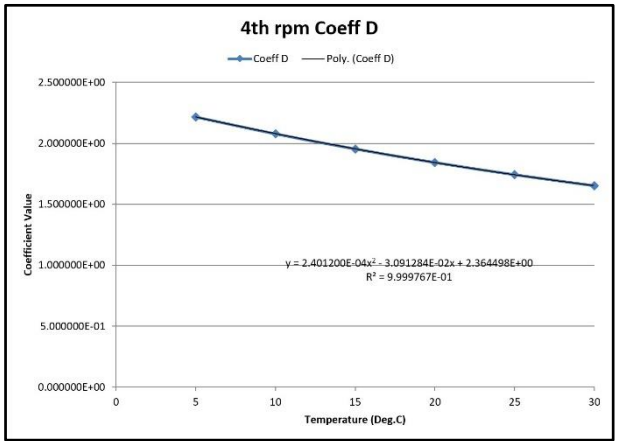

Figure 7.12: Jar Test Apparatus Speed (rpm) Formula Coefficient D Regression

8. Appendix 3: Rapid Mixer and Flocculator Velocity Gradient Derivations

8.1. Rapid Mixer Derivations

G = $(P / (\mu * V))^{0.5}$, where:

- G = Velocity Gradient, sec^{-1}
- μ = dynamic viscosity, $(lb \cdot sec/ft^2)$
- V = tank volume, ft^3
- P = $N_p*(0.5 * \rho * A * C * (v_d)^3)$, in lb·ft/sec *(equation provided by CDM Smith)*, where:
  - N_p = number of blades on mixer
  - ρ = fluid density, $slugs/ft^3$
  - A = Area of one mixer blade, ft^2
  - C = mixer blade drag coefficient, 1.8 *(value provided by CDM Smith)*
  - v_d = v_r, * v, where:
    - v_r = 0.76 *(units unknown, value provided by CDM Smith)*
    - v = $2 * \pi * r * (S / 60)$, in ft/sec, where:
      - r = Mixer Blade Radius, feet
      - S = Mixer Blade speed, rpm

Dynamic Viscosity of Water Formula:

(The formula input obtained from the source below is temperature t in °C, and provides an output of dynamic viscosity in Pa·s, assuming μ_{20} = 0.001002 Pa·s. The base formula was revised to provide a dynamic viscosity output in $lb \cdot s/ft^2$ using 1 Pa·s = 0.020886 $lb \cdot s/ft^2$). The base formula was obtained from www.nist.gov/data/PDFfiles/jpcrd121.pdf.

μ = $2.0886*10^{-2} * 1.002*10^{-3} * 10 ^ [((20-t) / (t+96) * (1.2378 - ((1.303*10^{-3}) * (20-t)) + ((3.06*10^{-6}) * ((20-t)^2)) + (((2.55*10^{-8}) * (20-t)^3)))))]$

Density of Water Formula:

(The formula input obtained from the source below is temperature t in °C, and provides an output of density in kg/m^3., assuming ρ_{20} = 999.972 kg/m^3. The formula was revised to provide a density output to $slugs/ft^3$ using 1 slug = 14.5939 kg and 1 m^3 = 35.315 ft^3). The base formula was obtained from http://metgen.pagesperso-orange.fr/metrologieen19.htm.

ρ = $999.972 * (1 - ((((t - 3.983035)^2) * (t + 301.797)) / (522528.9 * (t + 69.34881)))) / 14.5939 / 35.315$

Mixer Blade Speed Formula:

(The formula uses a VFD-driven motor with nameplate speed of 1760 rpm. The unit has a single gear reducer with a 17.42:1 reduction ratio. h = variable frequency drive output frequency. R = total gear reduction ratio.

S = $1760 * ((h) / 60) / R$

Final Generic Calculations:

The mixer is a vertical shaft unit with 6 vertical, straight blades mounted 60° apart. Each blade has an approximate area of 144 in^2. In CDM Smith's Design Calculations, the values for C and v_r were the same as in the flocculators. However, the manufacturer provided mixer performance data showing actual 'G' values at 10°C at various shaft speeds. By altering the Drag Coefficient value C in the formulas below to 0.9605, the G values calculated below almost precisely match the manufacturer's table (maximum error = 0.1 sec^{-1}).

So, G = $[(N_p * 0.5 * \rho * A * C * (2 * \pi * r * v_r * 1760 * h /60 / R / 60)^3) / (\mu * V)]^{0.5}$

Rapid Mixer Velocity Gradient Table

Water Parameters				Drag		Mixer	Total	Number	Area	Mixer	Mixer	
Temperature	Temperature	Density	Dynamic Viscosity	Coefficient		Motor Frequency	Gear Reduction	of Mixer Blades	Of One Blade	Blade Radius	Tank Volume	Velocity Gradient
t	t	ρ	μ	C	v_r	h	R	N_p	A	r	V	G
(°C)	(°F)	(slugs/ft^3)	(lb·s/ft^2)			(hz)			(ft^2)	(ft)	(ft^3)	(s^{-1})
5.0	41.0	1.940E+00	3.175E-05	0.9605	0.760	10.0	17.42	6	1.000	1.375	551	44.7
5.0	41.0	1.940E+00	3.175E-05	0.9605	0.760	20.0	17.42	6	1.000	1.375	551	126.5
5.0	41.0	1.940E+00	3.175E-05	0.9605	0.760	30.0	17.42	6	1.000	1.375	551	232.4
5.0	41.0	1.940E+00	3.175E-05	0.9605	0.760	40.0	17.42	6	1.000	1.375	551	357.7
5.0	41.0	1.940E+00	3.175E-05	0.9605	0.760	50.0	17.42	6	1.000	1.375	551	499.9
5.0	41.0	1.940E+00	3.175E-05	0.9605	0.760	60.0	17.42	6	1.000	1.375	551	657.2
10.0	50.0	1.940E+00	2.731E-05	0.9605	0.760	10.0	17.42	6	1.000	1.375	551	48.2
10.0	50.0	1.940E+00	2.731E-05	0.9605	0.760	20.0	17.42	6	1.000	1.375	551	136.4
10.0	50.0	1.940E+00	2.731E-05	0.9605	0.760	30.0	17.42	6	1.000	1.375	551	250.5
10.0	50.0	1.940E+00	2.731E-05	0.9605	0.760	40.0	17.42	6	1.000	1.375	551	385.7
10.0	50.0	1.940E+00	2.731E-05	0.9605	0.760	50.0	17.42	6	1.000	1.375	551	539.0
10.0	50.0	1.940E+00	2.731E-05	0.9605	0.760	60.0	17.42	6	1.000	1.375	551	708.5
20.0	68.0	1.937E+00	2.093E-05	0.9605	0.760	10.0	17.42	6	1.000	1.375	551	55.0
20.0	68.0	1.937E+00	2.093E-05	0.9605	0.760	20.0	17.42	6	1.000	1.375	551	155.6
20.0	68.0	1.937E+00	2.093E-05	0.9605	0.760	30.0	17.42	6	1.000	1.375	551	285.9
20.0	68.0	1.937E+00	2.093E-05	0.9605	0.760	40.0	17.42	6	1.000	1.375	551	440.2
20.0	68.0	1.937E+00	2.093E-05	0.9605	0.760	50.0	17.42	6	1.000	1.375	551	615.3
20.0	68.0	1.937E+00	2.093E-05	0.9605	0.760	60.0	17.42	6	1.000	1.375	551	808.8
30.0	86.0	1.932E+00	1.665E-05	0.9605	0.760	10.0	17.42	6	1.000	1.375	551	61.6
30.0	86.0	1.932E+00	1.665E-05	0.9605	0.760	20.0	17.42	6	1.000	1.375	551	174.3
30.0	86.0	1.932E+00	1.665E-05	0.9605	0.760	30.0	17.42	6	1.000	1.375	551	320.2
30.0	86.0	1.932E+00	1.665E-05	0.9605	0.760	40.0	17.42	6	1.000	1.375	551	492.9
30.0	86.0	1.932E+00	1.665E-05	0.9605	0.760	50.0	17.42	6	1.000	1.375	551	688.9
30.0	86.0	1.932E+00	1.665E-05	0.9605	0.760	60.0	17.42	6	1.000	1.375	551	905.6
40.0	104.0	1.925E+00	1.364E-05	0.9605	0.760	10.0	17.42	6	1.000	1.375	551	68.0
40.0	104.0	1.925E+00	1.364E-05	0.9605	0.760	20.0	17.42	6	1.000	1.375	551	192.2
40.0	104.0	1.925E+00	1.364E-05	0.9605	0.760	30.0	17.42	6	1.000	1.375	551	353.2
40.0	104.0	1.925E+00	1.364E-05	0.9605	0.760	40.0	17.42	6	1.000	1.375	551	543.7
40.0	104.0	1.925E+00	1.364E-05	0.9605	0.760	50.0	17.42	6	1.000	1.375	551	759.9
40.0	104.0	1.925E+00	1.364E-05	0.9605	0.760	60.0	17.42	6	1.000	1.375	551	998.9

Combination of all terms and simplification for final velocity gradient formula for this specific Unit. From Above,

G = $[(N_p * 0.5 * \rho * A * C * (2 * \pi * r * v_r * 1760 * h /60 / R / 60)^3) / (\mu * V)]^{0.5}$

Substitution of constants for this rapid mixer:

G = $[(6 * 0.5 * \rho * 1 * 0.9605 * (2 * \pi * 1.375 * 0.76 * 1760 * h /60 / 17.42 / 60)^3) / (\mu * 551)]^{0.5}$

Simplifying:

G = $5.720326e\text{-}03 * [\ \rho * h^3 / \mu\ ]^{0.5}$

Please note that this formula can be used directly if density and dynamic viscosity are calculated separately.

Substitution of density formula from above:

G = $5.720326e\text{-}03 * [\ (999.972 * (1 - ((((t - 3.983035)^2) * (t + 301.797)) / (522528.9 * (t + 69.34881)))) / 14.5939 / 35.315) * h^3 / \mu\ ]^{0.5}$

Simplifying:

G = $7.968002e\text{-}03 * [\ (1 - ((((t - 3.983035)^2) * (t + 301.797)) / (522528.9 * (t + 69.34881)))) * h^3 / \mu\ ]^{0.5}$

Substitution of viscosity formula from above:

G = $7.968002e\text{-}03 * [\ (1 - ((((t - 3.983035)^2) * (t + 301.797)) / (522528.9 * (t + 69.34881)))) * h^3 / (2.0886e\text{-}02 * 1.002e\text{-}03 * 10\ ^\ [((20\text{-}t) / (t+96) * (1.2378 - ((1.303e\text{-}03) * (20\text{-}t)) + ((3.06e\text{-}06) * ((20\text{-}t)^2)) + (((2.55e\text{-}08) * (20\text{-}t)^3)))))]\ ]^{0.5}$

Final simplification to a velocity gradient formula for this rapid mixer as a function only of motor speed and water temperature:

G = $1.741758 * [\ (1 - ((((t - 3.983035)^2) * (t + 301.797)) / (522528.9 * (t + 69.34881)))) * h^3 / (10^((20 - t) / (t + 96) * (1.2378 - (1.303e\text{-}03 * (20 - t)) + (3.06e\text{-}06 * ((20 - t)^2)) + ((2.55e\text{-}08 * (20 - t)^3))))))\ ]^{0.5}$

For direct use in most computer programs (substitution of actual variable names must be made for 'temp' and 'hertz'), the syntax would be:

G =

```
1.741758*((1-((((temp-3.983035)^2)*(temp+301.797))/(522528.9*(temp+69.34881))))*(hertz^3)/(10^((20-temp)/(temp+96)*(1.2378- (0.001303*(20-temp))+(0.00000306*((20-temp)^2))+((0.0000000255*(20-temp)^3))))))^0.5
```

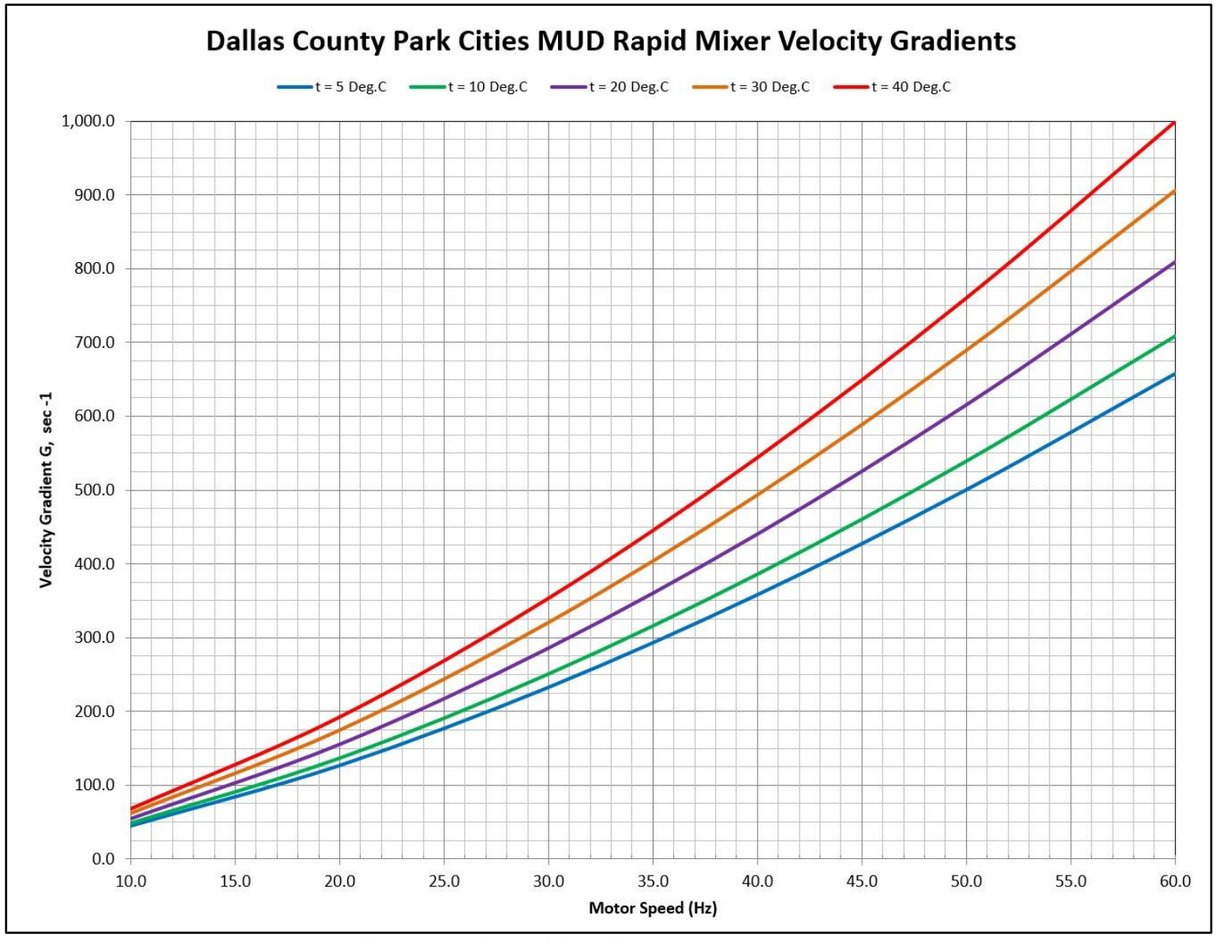

Figure 8.1: Rapid Mixer Velocity Gradient Chart

8.2. Flocculator Stage 1 Derivations

$G = (P / (\mu * V))^{0.5}$, where:

- G = Velocity Gradient, sec^{-1}
- μ = dynamic viscosity, $(lb \cdot sec/ft^2)$
- V = tank volume, ft^3
- P = $N_p*(0.5 * \rho * A * C * (v_d)^3)$, in lb·ft/sec *(equation provided by CDM Smith)*, where:
  - N_p = number of beams on flocculator at radius r
  - ρ = fluid density, $slugs/ft^3$
  - A = Area of one flocculator beam, ft^2
  - C = mixer blade drag coefficient, 1.8 (value provided by CDM Smith)
  - v_d = v_r, * v, where:
    - v_r = 0.76 *(units unknown, value provided by CDM Smith)*
    - v = $2 * \pi * r * (S / 60)$, in ft/sec, where:
      - r = Radius from Shaft to Flocculator Beam, feet
      - S = Flocculator speed, rpm

Dynamic Viscosity of Water Formula:

(The formula input obtained from the source below is temperature t in °C, and provides an output of dynamic viscosity in Pa·s, assuming μ_{20} = 0.001002 Pa·s. The formula was revised to provide a dynamic viscosity output in lb·s/ft² using 1 Pa·s = 0.020886 lb·s/ft²). The base formula was obtained from www.nist.gov/data/PDFfiles/jpcrd121.pdf.

$\mu = 2.0886*10^{-2} * 1.002*10^{-3} * 10 ^ [((20-t) / (t+96) * (1.2378 - ((1.303*10^{-3}) * (20-t)) + ((3.06*10^{-6}) * ((20-t)^2)) + (((2.55*10^{-8}) * (20-t)^3))))]$

Density of Water Formula:

(The formula input obtained from the source below is temperature t in °C, and provides an output of density in kg/m³., assuming ρ_{20} = 999.972 kg/m³. The formula was revised to provide a density output to slugs/ft³ using 1 slug = 14.5939 kg and 1 m³ = 35.315 ft³). The base formula was obtained from http://metgen.pagesperso-orange.fr/metrologieen19.htm.

$\rho = 999.972 * (1 - ((((t + (-3.983035))^2) * (t + 301.797)) / (522528.9 * (t + 69.34881)))) / 14.5939 / 35.315$

Flocculator Speed Formula:

(The formula uses a VFD-driven motor with nameplate speed of 1800 rpm. The unit has a primary gear reducer with a 125.78:1 reduction ratio, and a chain-sprocket drive reduction ratio of 3.09:1. h = variable frequency drive output frequency. R = total gear reduction ratio.

$S = 1800 * ((h) / 60) / R$

Final Generic Calculations:

The flocculator is a horizontal-shaft paddle wheel style mixer, with three sets of paddle assemblies driven by a single motor. Each paddle set has three paddle arms mounted 120° apart. Each arm has three "beams" with serve as the actual paddles. The centerlines of the inner, middle, and outer beams are 40.25", 57.25", and 74.25" from the shaft center respectively. So, there are a total of 9 beams at each radii (3 for each paddle). The first of the three paddle assemblies is longer than the other two in the longitudinal direction, so the calculations below were simplified by adding the length of one beam on each paddle to obtain a "total" beam length for each radii (each beam is 7.5" wide, and the 3 lengths are 11'-2", 10'-8", and 10'-8", providing a total beam length of 32'-6"). The power inputs calculated for the beams at each radii are summed to find the total power input, and this total power is then used to calculate the velocity gradient.

$G = ([\Sigma(N_p * 0.5 * \rho * A_k * C * (2 * \pi * r_k * v_r * 1800 * h / 60 / R / 60)^3)] / (\mu * V))^{0.5}$ for k = 1 to the number of different beam radii.

Flocculator Stage 1 Velocity Gradients

Water Parameters								Radius 1			Radius 2			Radius 3				
Temp t (°C)	Temp t (°F)	Density ρ (slugs/ft³)	Dynamic Viscosity μ (lb·s/ft²)	C	v_r	Floc Motor Freq. h (hz)	Total Gear Red. R	# of Beams N_p	Area Of 1 Beam A (ft²)	Beam Radius r_1 (ft)	# of Beams N_p	Area Of 1 Beam A (ft²)	Beam Radius r_2 (ft)	# of Beams N_p	Area Of 1 Beam A (ft²)	Beam Radius r_3 (ft)	Floc Tank Volume V (ft³)	Velocity Gradient G (s^{-1})
5.0	41.0	1.940E+00	3.175E-05	1.800	0.760	10.0	388.66	3	20.313	6.188	3	20.313	4.771	3	20.313	3.354	9,995	5.5
5.0	41.0	1.940E+00	3.175E-05	1.800	0.760	20.0	388.66	3	20.313	6.188	3	20.313	4.771	3	20.313	3.354	9,995	15.4
5.0	41.0	1.940E+00	3.175E-05	1.800	0.760	30.0	388.66	3	20.313	6.188	3	20.313	4.771	3	20.313	3.354	9,995	28.4
5.0	41.0	1.940E+00	3.175E-05	1.800	0.760	40.0	388.66	3	20.313	6.188	3	20.313	4.771	3	20.313	3.354	9,995	43.7
5.0	41.0	1.940E+00	3.175E-05	1.800	0.760	50.0	388.66	3	20.313	6.188	3	20.313	4.771	3	20.313	3.354	9,995	61.0
5.0	41.0	1.940E+00	3.175E-05	1.800	0.760	60.0	388.66	3	20.313	6.188	3	20.313	4.771	3	20.313	3.354	9,995	80.2
10.0	50.0	1.940E+00	2.731E-05	1.800	0.760	10.0	388.66	3	20.313	6.188	3	20.313	4.771	3	20.313	3.354	9,995	5.9
10.0	50.0	1.940E+00	2.731E-05	1.800	0.760	20.0	388.66	3	20.313	6.188	3	20.313	4.771	3	20.313	3.354	9,995	16.6
10.0	50.0	1.940E+00	2.731E-05	1.800	0.760	30.0	388.66	3	20.313	6.188	3	20.313	4.771	3	20.313	3.354	9,995	30.6
10.0	50.0	1.940E+00	2.731E-05	1.800	0.760	40.0	388.66	3	20.313	6.188	3	20.313	4.771	3	20.313	3.354	9,995	47.1
10.0	50.0	1.940E+00	2.731E-05	1.800	0.760	50.0	388.66	3	20.313	6.188	3	20.313	4.771	3	20.313	3.354	9,995	65.8
10.0	50.0	1.940E+00	2.731E-05	1.800	0.760	60.0	388.66	3	20.313	6.188	3	20.313	4.771	3	20.313	3.354	9,995	86.5
20.0	68.0	1.937E+00	2.093E-05	1.800	0.760	10.0	388.66	3	20.313	6.188	3	20.313	4.771	3	20.313	3.354	9,995	6.7
20.0	68.0	1.937E+00	2.093E-05	1.800	0.760	20.0	388.66	3	20.313	6.188	3	20.313	4.771	3	20.313	3.354	9,995	19.0
20.0	68.0	1.937E+00	2.093E-05	1.800	0.760	30.0	388.66	3	20.313	6.188	3	20.313	4.771	3	20.313	3.354	9,995	34.9
20.0	68.0	1.937E+00	2.093E-05	1.800	0.760	40.0	388.66	3	20.313	6.188	3	20.313	4.771	3	20.313	3.354	9,995	53.7
20.0	68.0	1.937E+00	2.093E-05	1.800	0.760	50.0	388.66	3	20.313	6.188	3	20.313	4.771	3	20.313	3.354	9,995	75.1
20.0	68.0	1.937E+00	2.093E-05	1.800	0.760	60.0	388.66	3	20.313	6.188	3	20.313	4.771	3	20.313	3.354	9,995	98.7
30.0	86.0	1.932E+00	1.665E-05	1.800	0.760	10.0	388.66	3	20.313	6.188	3	20.313	4.771	3	20.313	3.354	9,995	7.5
30.0	86.0	1.932E+00	1.665E-05	1.800	0.760	20.0	388.66	3	20.313	6.188	3	20.313	4.771	3	20.313	3.354	9,995	21.3
30.0	86.0	1.932E+00	1.665E-05	1.800	0.760	30.0	388.66	3	20.313	6.188	3	20.313	4.771	3	20.313	3.354	9,995	39.1
30.0	86.0	1.932E+00	1.665E-05	1.800	0.760	40.0	388.66	3	20.313	6.188	3	20.313	4.771	3	20.313	3.354	9,995	60.2
30.0	86.0	1.932E+00	1.665E-05	1.800	0.760	50.0	388.66	3	20.313	6.188	3	20.313	4.771	3	20.313	3.354	9,995	84.1
30.0	86.0	1.932E+00	1.665E-05	1.800	0.760	60.0	388.66	3	20.313	6.188	3	20.313	4.771	3	20.313	3.354	9,995	110.5
40.0	104.0	1.925E+00	1.364E-05	1.800	0.760	10.0	388.66	3	20.313	6.188	3	20.313	4.771	3	20.313	3.354	9,995	8.3
40.0	104.0	1.925E+00	1.364E-05	1.800	0.760	20.0	388.66	3	20.313	6.188	3	20.313	4.771	3	20.313	3.354	9,995	23.5
40.0	104.0	1.925E+00	1.364E-05	1.800	0.760	30.0	388.66	3	20.313	6.188	3	20.313	4.771	3	20.313	3.354	9,995	43.1
40.0	104.0	1.925E+00	1.364E-05	1.800	0.760	40.0	388.66	3	20.313	6.188	3	20.313	4.771	3	20.313	3.354	9,995	66.4
40.0	104.0	1.925E+00	1.364E-05	1.800	0.760	50.0	388.66	3	20.313	6.188	3	20.313	4.771	3	20.313	3.354	9,995	92.8
40.0	104.0	1.925E+00	1.364E-05	1.800	0.760	60.0	388.66	3	20.313	6.188	3	20.313	4.771	3	20.313	3.354	9,995	121.9

Combination of all terms and simplification for final velocity gradient formula specific to this Unit. From Above,

$G = ([\Sigma(N_p * 0.5 * \rho * A_k * C * (2 * \pi * r_k * v_r * 1800 * h / 60 / R / 60)^3)] / (\mu * V))^{0.5}$ for k = 1 to the number of different beam radii.

Substitution of constants for this flocculator:

$G = ([\Sigma(3 * 0.5 * \rho * A_k * 1.8 * (2 * \pi * r_k * 0.76 * 1800 * h / 60 / 388.66 / 60)^3)] / (\mu * 9994.6))^{0.5}$ for k = 1 to the number of different beam radii.

Simplifying:

G = $([\Sigma(2.7 * \rho * A_k * (6.143185e\text{-}03 * r_k * h)^3)] / (\mu * 9994.6))^{0.5}$ for k = 1 to the number of different beam radii.

Summation Expansion for 3 beam radii:

G = $((2.7 * \rho * A_1 * (6.143185e\text{-}03 * r_1 * h)^3) + (2.7 * \rho * A_2 * (6.143185e\text{-}03 * r_2 * h)^3) + (2.7 * \rho * A_3 * (6.143185e\text{-}03 * r_3 * h)^3) / (\mu * 9994.6))^{0.5}$

Substitution of constants for this flocculator:

G = $((2.7 * \rho * 20.3125 * (6.143185e\text{-}03 * 6.1875 * h)^3) + (2.7 * \rho * 20.3125 * (6.143185e\text{-}03 * 4.77083 * h)^3) + (2.7 * \rho * 20.3125 * (6.143185e\text{-}03 * 3.35417 * h)^3) / (\mu * 9994.6))^{0.5}$

Simplifying:

G = $6.982188e\text{-}04 * (\rho * h^3 / \mu)^{0.5}$

Please note that this formula can be used directly if density and dynamic viscosity are calculated separately.

Substitution of density formula from above:

G = $6.982188e\text{-}04 * ((999.972 * (1 - ((((t - 3.983035)^2) * (t + 301.797)) / (522528.9 * (t + 69.34881)))) / 14.5939 / 35.315) * h^3 / \mu)^{0.5}$

Simplifying:

G = $9.725685e\text{-}04 * ((1 - ((t - 3.983035)^2 * (t + 301.797) / (522528.9 * (t + 69.34881)))) * h^3 / \mu)^{0.5}$

Substitution of viscosity formula from above:

G = $9.725685e\text{-}04 * ((1 - ((t - 3.983035)^2 * (t + 301.797) / (522528.9 * (t + 69.34881)))) * h^3 / (2.0886e\text{-}02 * 1.002e\text{-}03 * 10 ^ [((20 - t) / (t + 96) * (1.2378 - (1.303e\text{-}03 * (20 - t)) + (3.06e\text{-}06 * ((20 - t)^2)) + ((2.55e\text{-}08 * (20 - t)^3)))))])^{0.5}$

Final simplification to a velocity gradient formula for this flocculator as a function only of motor speed and water temperature:

G = $2.125978e\text{-}01 * ((1 - ((t - 3.983035)^2 * (t + 301.797) / (522528.9 * (t + 69.34881)))) * h^3 / (10 ^ [((20 - t) / (t + 96) * (1.2378 - (1.303e\text{-}03 * (20 - t)) + (3.06e\text{-}06 * ((20 - t)^2)) + ((2.55e\text{-}08 * (20 - t)^3)))))])^{0.5}$

For direct use in most computer programs (substitution of actual variable names must be made for 'temp' and 'hertz'), the syntax would be:

G =

```
0.2125978*((1-(((temp-3.983035)^2)*(temp+301.797)/(522528.9*(temp+69.34881))))*(hertz^3)/(10^(((20-temp)/(temp+96)*(1.2378-(0.001303*(20-temp))+(0.00000306*((20-temp)^2))+((0.0000000255*(20-temp)^3)))))))^0.5
```

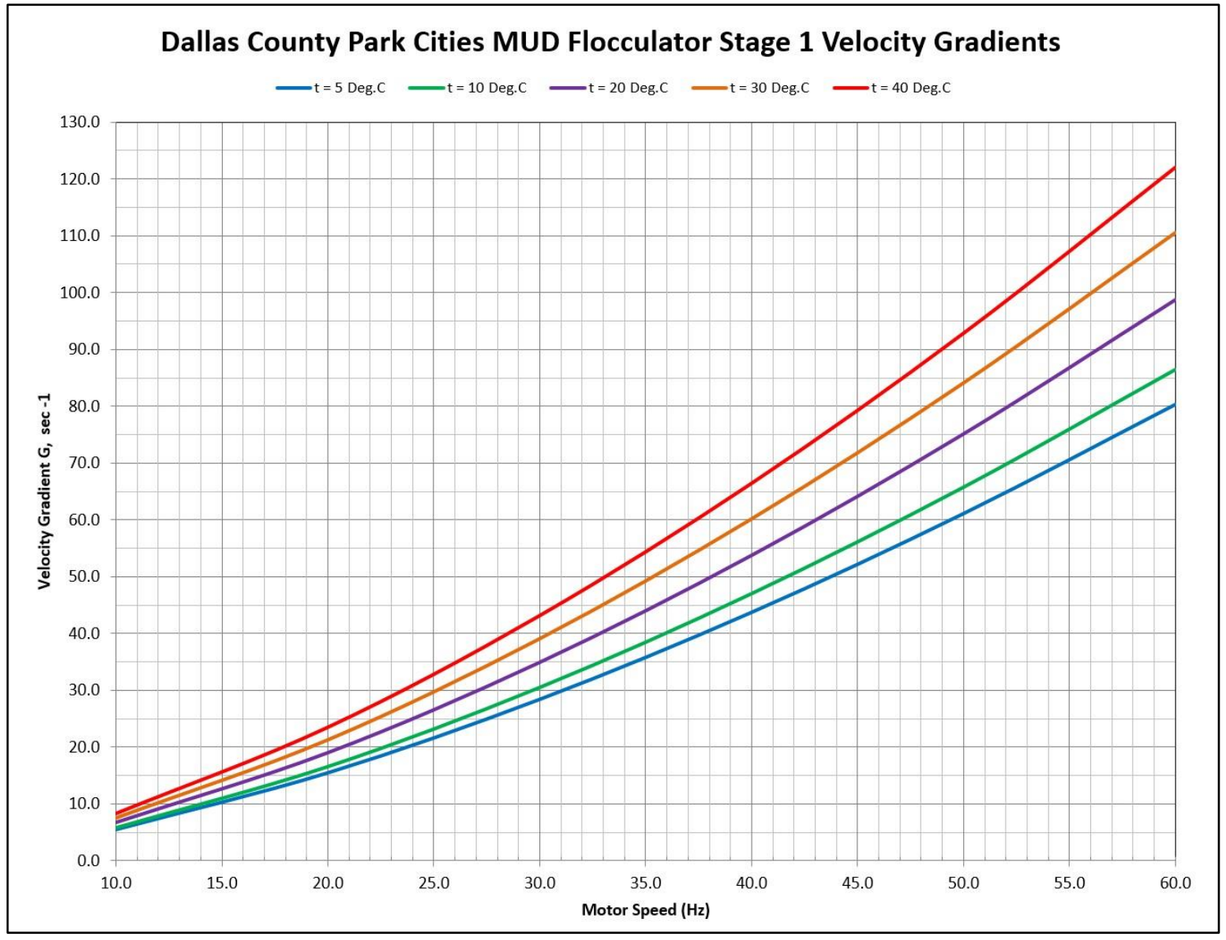

Figure 8.2: Flocculator Stage 1 Velocity Gradient Chart

8.3. Flocculator Stage 2 Derivations

G = $(P / (\mu * V))^{0.5}$, where:

G = Velocity Gradient, sec^{-1}

μ = dynamic viscosity, $(lb \cdot sec/ft^2)$

V = tank volume, ft^3

P = $N_p*(0.5 * \rho * A * C * (v_d)^3)$, in lb·ft/sec *(equation provided by CDM Smith)*, where:

N_p = number of beams on flocculator at radius r

ρ = fluid density, $slugs/ft^3$

A = Area of one flocculator beam, ft^2

C = mixer blade drag coefficient, 1.8 (value provided by CDM Smith)

v_d = v_r, * v, where:

v_r = 0.76 *(units unknown, value provided by CDM Smith)*

v = $2 * \pi * r * (S / 60)$, in ft/sec, where:

r = Radius from Shaft to Flocculator Beam, feet

S = Flocculator speed, rpm

Dynamic Viscosity of Water Formula:

(The formula input obtained from the source below is temperature t in °C, and provides an output of dynamic viscosity in Pa·s, assuming μ_{20} = 0.001002 Pa·s. The formula was revised to provide a dynamic viscosity output in $lb \cdot s/ft^2$ using 1 Pa·s = 0.020886 $lb \cdot s/ft^2$). The base formula was obtained from www.nist.gov/data/PDFfiles/jpcrd121.pdf.

μ = $2.0886*10^{-2} * 1.002*10^{-3} * 10 ^ [((20-t) / (t+96) * (1.2378 - ((1.303*10^{-3}) * (20-t)) + ((3.06*10^{-6}) * ((20-t)^2)) + (((2.55*10^{-8}) * (20-t)^3))))]$

Density of Water Formula:

(The formula input obtained from the source below is temperature t in °C, and provides an output of density in kg/m^3., assuming ρ_{20} = 999.972 kg/m^3. The formula was revised to provide a density output to $slugs/ft^3$ using 1 slug = 14.5939 kg and 1 m^3 = 35.315 ft^3). The base formula was obtained from http://metgen.pagesperso-orange.fr/metrologieen19.htm.

ρ = $999.972 * (1 - ((((t + (-3.983035))^2) * (t + 301.797)) / (522528.9 * (t + 69.34881)))) / 14.5939/35.315$

Flocculator Speed Formula:

(The formula uses a VFD-driven motor with nameplate speed of 1800 rpm. The unit has a primary gear reducer with a 136.70:1 reduction ratio, and a chain-sprocket drive reduction ratio of 3.09:1. h = variable frequency drive output frequency. R = total gear reduction ratio.

S = 1800 * ((h) / 60) / R

Final Generic Calculations:

The flocculator is a horizontal-shaft paddle wheel style mixer, with two sets of paddle assemblies driven by a single motor. Each paddle set has two paddle arms mounted 180° apart. Each arm has three "beams" with serve as the actual paddles. The centerlines of the inner, middle, and outer beams are 45.25", 60.25", and 75.25" from the shaft center respectively. So, there are a total of 4 beams at each radii (2 for each paddle). Each beam is 5.5" wide and 10'-6" long. The power inputs calculated for the beams at each radii are summed to find the total power input, and this total power is then used to calculate the velocity gradient.

G = $([\Sigma(N_p * 0.5 * \rho * A * C * (2 * \pi * r_k * v_r * 1800 * h /60 / R / 60)^3)] / (\mu * V))^{0.5}$ for k = 1 to the number of different beam radii.

Flocculator Stage 2 Velocity Gradients, Base Water Temperatures in Degrees C

Water Parameters						Floc Motor Freq.	Total Gear Red.	Radius 1			Radius 2			Radius 3			Floc Tank Volume	Velocity Gradient
								# of Beams	Area Of 1 Beam	Beam Radius	# of Beams	Area Of 1 Beam	Beam Radius	# of Beams	Area Of 1 Beam	Beam Radius		
Temp t (°C)	Temp t (°F)	Density ρ (slugs/ft³)	Dynamic Viscosity μ (lb·s/ft²)	C	v_r	h (hz)	R	N_p	A (ft²)	r_1 (ft)	N_p	A (ft²)	r_2 (ft)	N_p	A (ft²)	r_3 (ft)	V (ft³)	G (s⁻¹)
5.0	41.0	1.940E+00	3.175E-05	1.800	0.760	10.0	422.40	4	4.813	6.271	4	4.813	5.021	4	4.813	3.771	6,490	3.5
5.0	41.0	1.940E+00	3.175E-05	1.800	0.760	20.0	422.40	4	4.813	6.271	4	4.813	5.021	4	4.813	3.771	6,490	10.0
5.0	41.0	1.940E+00	3.175E-05	1.800	0.760	30.0	422.40	4	4.813	6.271	4	4.813	5.021	4	4.813	3.771	6,490	18.4
5.0	41.0	1.940E+00	3.175E-05	1.800	0.760	40.0	422.40	4	4.813	6.271	4	4.813	5.021	4	4.813	3.771	6,490	28.4
5.0	41.0	1.940E+00	3.175E-05	1.800	0.760	50.0	422.40	4	4.813	6.271	4	4.813	5.021	4	4.813	3.771	6,490	39.6
5.0	41.0	1.940E+00	3.175E-05	1.800	0.760	60.0	422.40	4	4.813	6.271	4	4.813	5.021	4	4.813	3.771	6,490	52.1
10.0	50.0	1.940E+00	2.731E-05	1.800	0.760	10.0	422.40	4	4.813	6.271	4	4.813	5.021	4	4.813	3.771	6,490	3.8
10.0	50.0	1.940E+00	2.731E-05	1.800	0.760	20.0	422.40	4	4.813	6.271	4	4.813	5.021	4	4.813	3.771	6,490	10.8
10.0	50.0	1.940E+00	2.731E-05	1.800	0.760	30.0	422.40	4	4.813	6.271	4	4.813	5.021	4	4.813	3.771	6,490	19.9
10.0	50.0	1.940E+00	2.731E-05	1.800	0.760	40.0	422.40	4	4.813	6.271	4	4.813	5.021	4	4.813	3.771	6,490	30.6
10.0	50.0	1.940E+00	2.731E-05	1.800	0.760	50.0	422.40	4	4.813	6.271	4	4.813	5.021	4	4.813	3.771	6,490	42.7
10.0	50.0	1.940E+00	2.731E-05	1.800	0.760	60.0	422.40	4	4.813	6.271	4	4.813	5.021	4	4.813	3.771	6,490	56.2
20.0	68.0	1.937E+00	2.093E-05	1.800	0.760	10.0	422.40	4	4.813	6.271	4	4.813	5.021	4	4.813	3.771	6,490	4.4
20.0	68.0	1.937E+00	2.093E-05	1.800	0.760	20.0	422.40	4	4.813	6.271	4	4.813	5.021	4	4.813	3.771	6,490	12.3
20.0	68.0	1.937E+00	2.093E-05	1.800	0.760	30.0	422.40	4	4.813	6.271	4	4.813	5.021	4	4.813	3.771	6,490	22.7
20.0	68.0	1.937E+00	2.093E-05	1.800	0.760	40.0	422.40	4	4.813	6.271	4	4.813	5.021	4	4.813	3.771	6,490	34.9
20.0	68.0	1.937E+00	2.093E-05	1.800	0.760	50.0	422.40	4	4.813	6.271	4	4.813	5.021	4	4.813	3.771	6,490	48.8
20.0	68.0	1.937E+00	2.093E-05	1.800	0.760	60.0	422.40	4	4.813	6.271	4	4.813	5.021	4	4.813	3.771	6,490	64.1
30.0	86.0	1.932E+00	1.665E-05	1.800	0.760	10.0	422.40	4	4.813	6.271	4	4.813	5.021	4	4.813	3.771	6,490	4.9
30.0	86.0	1.932E+00	1.665E-05	1.800	0.760	20.0	422.40	4	4.813	6.271	4	4.813	5.021	4	4.813	3.771	6,490	13.8
30.0	86.0	1.932E+00	1.665E-05	1.800	0.760	30.0	422.40	4	4.813	6.271	4	4.813	5.021	4	4.813	3.771	6,490	25.4
30.0	86.0	1.932E+00	1.665E-05	1.800	0.760	40.0	422.40	4	4.813	6.271	4	4.813	5.021	4	4.813	3.771	6,490	39.1
30.0	86.0	1.932E+00	1.665E-05	1.800	0.760	50.0	422.40	4	4.813	6.271	4	4.813	5.021	4	4.813	3.771	6,490	54.6
30.0	86.0	1.932E+00	1.665E-05	1.800	0.760	60.0	422.40	4	4.813	6.271	4	4.813	5.021	4	4.813	3.771	6,490	71.8
40.0	104.0	1.925E+00	1.364E-05	1.800	0.760	10.0	422.40	4	4.813	6.271	4	4.813	5.021	4	4.813	3.771	6,490	5.4
40.0	104.0	1.925E+00	1.364E-05	1.800	0.760	20.0	422.40	4	4.813	6.271	4	4.813	5.021	4	4.813	3.771	6,490	15.2
40.0	104.0	1.925E+00	1.364E-05	1.800	0.760	30.0	422.40	4	4.813	6.271	4	4.813	5.021	4	4.813	3.771	6,490	28.0
40.0	104.0	1.925E+00	1.364E-05	1.800	0.760	40.0	422.40	4	4.813	6.271	4	4.813	5.021	4	4.813	3.771	6,490	43.1
40.0	104.0	1.925E+00	1.364E-05	1.800	0.760	50.0	422.40	4	4.813	6.271	4	4.813	5.021	4	4.813	3.771	6,490	60.3
40.0	104.0	1.925E+00	1.364E-05	1.800	0.760	60.0	422.40	4	4.813	6.271	4	4.813	5.021	4	4.813	3.771	6,490	79.2

Combination of all terms and simplification for final velocity gradient formula specific to this Unit. From Above,

G = $([\Sigma(N_p * 0.5 * \rho * A_k * C * (2 * \pi * r_k * v_r * 1800 * h / 60 / R / 60)^3)] / (\mu * V))^{0.5}$ for k = 1 to the number of different beam radii.

Substitution of constants:

G = $([\Sigma(4 * 0.5 * \rho * A_k * 1.8 * (2 * \pi * r_k * 0.76 * 1800 * h / 60 / 422.403 / 60)^3)] / (\mu * 6490))^{0.5}$ for k = 1 to the number of different beam radii.

Simplifying:

G = $([\Sigma(3.6 * \rho * A_k * (5.652447e\text{-}03 * r_k * h)^3)] / (\mu * 6490))^{0.5}$ for k = 1 to the number of different beam radii.

Summation Expansion:

$$G = \left((3.6 * \rho * A_1 * (5.652447e\text{-}03 * r_1 * h)^3) + (3.6 * \rho * A_2 * (5.652447e\text{-}03 * r_2 * h)^3) + (3.6 * \rho * A_3 * (5.652447e\text{-}03 * r_3 * h)^3) / (\mu * 6490) \right)^{0.5}$$

Substitution of constants:

$$G = \left((3.6 * \rho * 4.8125 * (5.652447e\text{-}03 * 6.270833 * h)^3) + (3.6 * \rho * 4.8125 * (5.652447e\text{-}03 * 5.020833 * h)^3) + (3.6 * \rho * 4.8125 * (5.652447e\text{-}03 * 3.770833 * h)^3) / (\mu * 6490) \right)^{0.5}$$

Simplifying:

$$G = 4.535965e\text{-}04 * (\rho * h^3 / \mu)^{0.5}$$

Please note that this formula can be used directly if density and dynamic viscosity are calculated separately.

Substitution of density formula from above:

$$G = 4.535965e\text{-}04 * ((999.972 * (1 - ((((t - 3.983035)^2) * (t + 301.797)) / (522528.9 * (t + 69.34881)))) / 14.5939 / 35.315) * h^3 / \mu)^{0.5}$$

Simplifying:

$$G = 6.318272e\text{-}04 * ((1 - ((t - 3.983035)^2 * (t + 301.797) / (522528.9 * (t + 69.34881)))) * h^3 / \mu)^{0.5}$$

Substitution of viscosity formula:

$$G = 6.318272e\text{-}04 * ((1 - ((t - 3.983035)^2 * (t + 301.797) / (522528.9 * (t + 69.34881)))) * h^3 / (2.0886e\text{-}02 * 1.002e\text{-}03 * 10 \wedge [((20 - t) / (t + 96) * (1.2378 - (1.303e\text{-}03 * (20 - t)) + (3.06e\text{-}06 * ((20 - t)^2)) + ((2.55e\text{-}08 * (20 - t)^3)))))]))^{0.5}$$

Final simplification to a velocity gradient formula for this flocculator as a function only of motor speed and water temperature:

$$G = 1.381137e\text{-}01 * ((1 - ((t - 3.983035)^2 * (t + 301.797) / (522528.9 * (t + 69.34881)))) * h^3 / (10 \wedge [((20 - t) / (t + 96) * (1.2378 - (1.303e\text{-}03 * (20 - t)) + (3.06e\text{-}06 * ((20 - t)^2)) + ((2.55e\text{-}08 * (20 - t)^3)))))]))^{0.5}$$

For direct use in most computer programs (substitution of actual variable names must be made for 'temp' and 'hertz'), the syntax would be:

```
G = 0.1381137*((1-(((temp-3.983035)^2)*(temp+301.797)/(522528.9*(temp+69.34881))))*(hertz^3)/(10^(((20-temp)/(temp+96)*(1.2378-(0.001303*(20-temp))+(0.00000306*((20-temp)^2))+((0.0000000255*(20-temp)^3)))))))^0.5
```

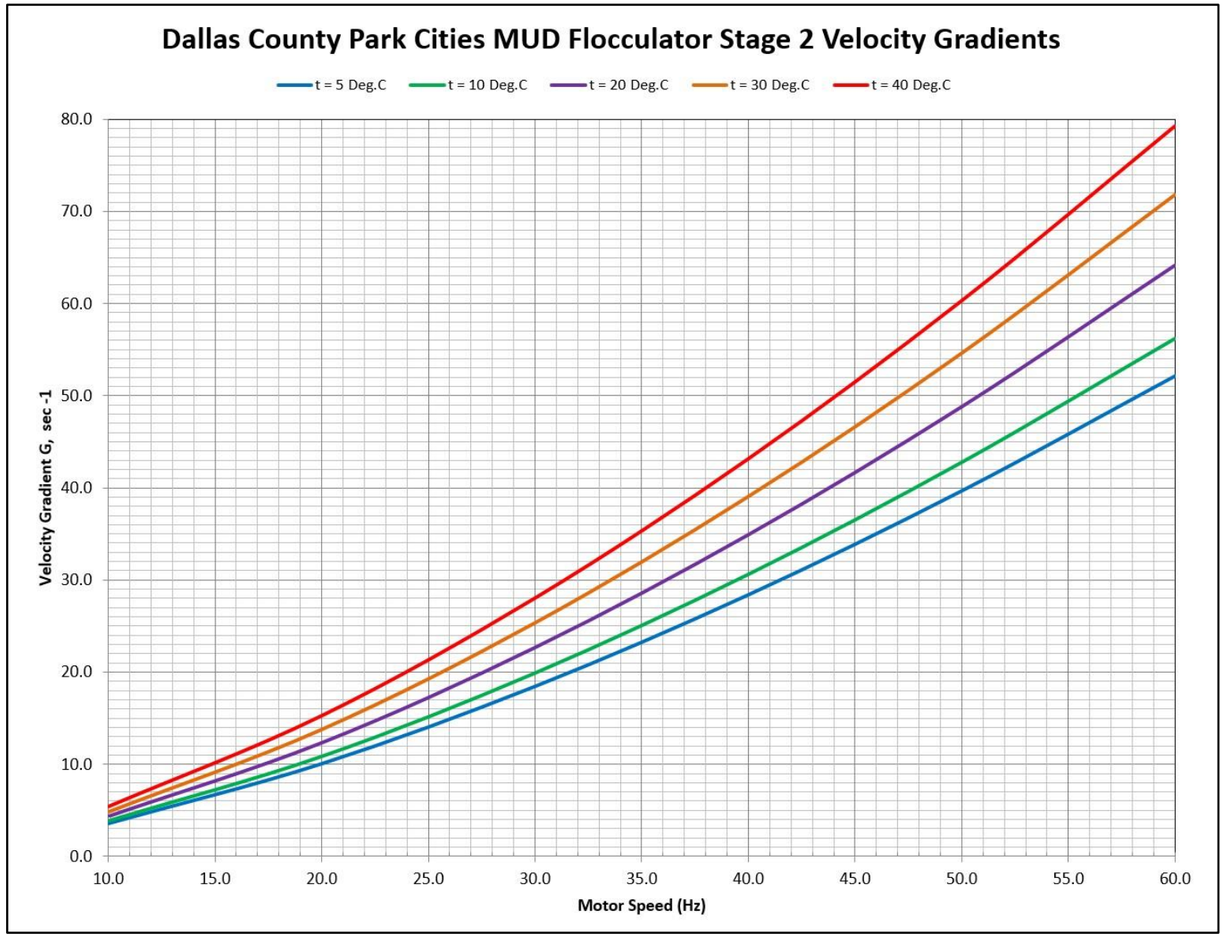

Figure 8.3: Flocculator Stage 2 Velocity Gradient Chart

8.4. Flocculator Stage 3 Derivations

G = $(P / (\mu * V))^{0.5}$, where:

G = Velocity Gradient, sec^{-1}

μ = dynamic viscosity, $(lb \cdot sec/ft^2)$

V = tank volume, ft^3

P = $N_p*(0.5 * \rho * A * C * (v_d)^3)$, in lb·ft/sec *(equation provided by CDM Smith)*, where:

N_p = number of beams on flocculator at radius r

ρ = fluid density, $slugs/ft^3$

A = Area of one flocculator beam, ft^2

C = mixer blade drag coefficient, 1.8 (value provided by CDM Smith)

v_d = v_r, * v, where:

v_r = 0.76 *(units unknown, value provided by CDM Smith)*

v = 2 * π * r * (S / 60), in ft/sec, where:

r = Radius from Shaft to Flocculator Beam, feet

S = Flocculator speed, rpm

Dynamic Viscosity of Water Formula:

(The formula input obtained from the source below is temperature t in °C, and provides an output of dynamic viscosity in Pa·s, assuming μ_{20} = 0.001002 Pa·s. The formula was revised to provide a dynamic viscosity output in lb·s/ft² using 1 Pa·s = 0.020886 lb·s/ft²). The base formula was obtained from www.nist.gov/data/PDFfiles/jpcrd121.pdf.

μ = $2.0886*10^{-2} * 1.002*10^{-3} * 10 ^ [((20-t) / (t+96) * (1.2378 - ((1.303*10^{-3}) * (20-t)) + ((3.06*10^{-6}) * ((20-t)^2)) + (((2.55*10^{-8}) * (20-t)^3)))))]$

Density of Water Formula:

(The formula input obtained from the source below is temperature t in °C, and provides an output of density in kg/m³., assuming ρ_{20} = 999.972 kg/m³. The formula was revised to provide a density output to slugs/ft³ using 1 slug = 14.5939 kg and 1 m³ = 35.315 ft³). The base formula was obtained from http://metgen.pagesperso-orange.fr/metrologieen19.htm.

ρ = $999.972 * (1 - ((((t + (-3.983035))^2) * (t + 301.797)) / (522528.9 * (t + 69.34881)))) / 14.5939/35.315$

Flocculator Speed Formula:

(The formula uses a VFD-driven motor with nameplate speed of 1800 rpm. The unit has a primary gear reducer with a 152.45:1 reduction ratio, and a chain-sprocket drive reduction ratio of 3.09:1. h = variable frequency drive output frequency. R = total gear reduction ratio.

S = 1800 * ((h) / 60) / R

Final Generic Calculations:

The flocculator is a horizontal-shaft paddle wheel style mixer, with two sets of paddle assemblies driven by a single motor. Each paddle set has two paddle arms mounted 180° apart. Each arm has three "beams" with serve as the actual paddles. The centerlines of the inner, middle, and outer beams are 45.25", 60.25", and 75.25" from the shaft center respectively. So, there are a total of 4 beams at each radii (2 for each paddle). Each beam is 5.5" wide and 10'-6" long.. The power inputs calculated for the beams at each radii are summed to find the total power input, and this total power is then used to calculate the velocity gradient..

G = $([\Sigma(N_p * 0.5 * \rho * A * C * (2 * \pi * r_k * v_r * 1800 * h /60 / R / 60)^3)] / (\mu * V))^{0.5}$ for k = 1 to the number of different beam radii.

Flocculator Stage 3 Velocity Gradients, Base Water Temperatures in Degrees C

Water Parameters						Floc	Total	Radius 1			Radius 2			Radius 3			Floc	Velocity
								# of	Area Of 1	Beam	# of	Area Of 1	Beam	# of	Area Of 1	Beam	Tank	Gradient
Temp	Temp	Density	Dynamic Viscosity	C	v_r	Motor Freq.	Gear Red.	Beams	Beam	Radius	Beams	Beam	Radius	Beams	Beam	Radius	Volume	G
t	t	ρ	μ			h	R	N_p	A	r_1	N_p	A	r_2	N_p	A	r_3	V	
(°C)	(°F)	(slugs/ft³)	(lb·s/ft²)			(hz)			(ft²)	(ft)		(ft²)	(ft)		(ft²)	(ft)	(ft³)	(s^{-1})
5.0	41.0	1.940E+00	3.175E-05	1.800	0.760	10.0	471.07	4	4.813	6.271	4	4.813	5.021	4	4.813	3.771	6,490	3.0
5.0	41.0	1.940E+00	3.175E-05	1.800	0.760	20.0	471.07	4	4.813	6.271	4	4.813	5.021	4	4.813	3.771	6,490	8.5
5.0	41.0	1.940E+00	3.175E-05	1.800	0.760	30.0	471.07	4	4.813	6.271	4	4.813	5.021	4	4.813	3.771	6,490	15.6
5.0	41.0	1.940E+00	3.175E-05	1.800	0.760	40.0	471.07	4	4.813	6.271	4	4.813	5.021	4	4.813	3.771	6,490	24.1
5.0	41.0	1.940E+00	3.175E-05	1.800	0.760	50.0	471.07	4	4.813	6.271	4	4.813	5.021	4	4.813	3.771	6,490	33.7
5.0	41.0	1.940E+00	3.175E-05	1.800	0.760	60.0	471.07	4	4.813	6.271	4	4.813	5.021	4	4.813	3.771	6,490	44.2
10.0	50.0	1.940E+00	2.731E-05	1.800	0.760	10.0	471.07	4	4.813	6.271	4	4.813	5.021	4	4.813	3.771	6,490	3.2
10.0	50.0	1.940E+00	2.731E-05	1.800	0.760	20.0	471.07	4	4.813	6.271	4	4.813	5.021	4	4.813	3.771	6,490	9.2
10.0	50.0	1.940E+00	2.731E-05	1.800	0.760	30.0	471.07	4	4.813	6.271	4	4.813	5.021	4	4.813	3.771	6,490	16.9
10.0	50.0	1.940E+00	2.731E-05	1.800	0.760	40.0	471.07	4	4.813	6.271	4	4.813	5.021	4	4.813	3.771	6,490	26.0
10.0	50.0	1.940E+00	2.731E-05	1.800	0.760	50.0	471.07	4	4.813	6.271	4	4.813	5.021	4	4.813	3.771	6,490	36.3
10.0	50.0	1.940E+00	2.731E-05	1.800	0.760	60.0	471.07	4	4.813	6.271	4	4.813	5.021	4	4.813	3.771	6,490	47.7
20.0	68.0	1.937E+00	2.093E-05	1.800	0.760	10.0	471.07	4	4.813	6.271	4	4.813	5.021	4	4.813	3.771	6,490	3.7
20.0	68.0	1.937E+00	2.093E-05	1.800	0.760	20.0	471.07	4	4.813	6.271	4	4.813	5.021	4	4.813	3.771	6,490	10.5
20.0	68.0	1.937E+00	2.093E-05	1.800	0.760	30.0	471.07	4	4.813	6.271	4	4.813	5.021	4	4.813	3.771	6,490	19.3
20.0	68.0	1.937E+00	2.093E-05	1.800	0.760	40.0	471.07	4	4.813	6.271	4	4.813	5.021	4	4.813	3.771	6,490	29.6
20.0	68.0	1.937E+00	2.093E-05	1.800	0.760	50.0	471.07	4	4.813	6.271	4	4.813	5.021	4	4.813	3.771	6,490	41.4
20.0	68.0	1.937E+00	2.093E-05	1.800	0.760	60.0	471.07	4	4.813	6.271	4	4.813	5.021	4	4.813	3.771	6,490	54.5
30.0	86.0	1.932E+00	1.665E-05	1.800	0.760	10.0	471.07	4	4.813	6.271	4	4.813	5.021	4	4.813	3.771	6,490	4.1
30.0	86.0	1.932E+00	1.665E-05	1.800	0.760	20.0	471.07	4	4.813	6.271	4	4.813	5.021	4	4.813	3.771	6,490	11.7
30.0	86.0	1.932E+00	1.665E-05	1.800	0.760	30.0	471.07	4	4.813	6.271	4	4.813	5.021	4	4.813	3.771	6,490	21.6
30.0	86.0	1.932E+00	1.665E-05	1.800	0.760	40.0	471.07	4	4.813	6.271	4	4.813	5.021	4	4.813	3.771	6,490	33.2
30.0	86.0	1.932E+00	1.665E-05	1.800	0.760	50.0	471.07	4	4.813	6.271	4	4.813	5.021	4	4.813	3.771	6,490	46.4
30.0	86.0	1.932E+00	1.665E-05	1.800	0.760	60.0	471.07	4	4.813	6.271	4	4.813	5.021	4	4.813	3.771	6,490	61.0
40.0	104.0	1.925E+00	1.364E-05	1.800	0.760	10.0	471.07	4	4.813	6.271	4	4.813	5.021	4	4.813	3.771	6,490	4.6
40.0	104.0	1.925E+00	1.364E-05	1.800	0.760	20.0	471.07	4	4.813	6.271	4	4.813	5.021	4	4.813	3.771	6,490	12.9
40.0	104.0	1.925E+00	1.364E-05	1.800	0.760	30.0	471.07	4	4.813	6.271	4	4.813	5.021	4	4.813	3.771	6,490	23.8
40.0	104.0	1.925E+00	1.364E-05	1.800	0.760	40.0	471.07	4	4.813	6.271	4	4.813	5.021	4	4.813	3.771	6,490	36.6
40.0	104.0	1.925E+00	1.364E-05	1.800	0.760	50.0	471.07	4	4.813	6.271	4	4.813	5.021	4	4.813	3.771	6,490	51.2
40.0	104.0	1.925E+00	1.364E-05	1.800	0.760	60.0	471.07	4	4.813	6.271	4	4.813	5.021	4	4.813	3.771	6,490	67.3

Combination of all terms and simplification for final velocity gradient formula specific to this Unit. From Above,

G = $([\Sigma(N_p * 0.5 * \rho * A_k * C * (2 * \pi * r_k * v_r * 1800 * h / 60 / R / 60)^3)] / (\mu * V))^{0.5}$ for k = 1 to the number of different beam radii.

Substitution of constants for this flocculator:

G = $([\Sigma(4 * 0.5 * \rho * A_k * 1.8 * (2 * \pi * r_k * 0.76 * 1800 * h / 60 / 471.0705 / 60)^3)] / (\mu * 6490))^{0.5}$ for k = 1 to the number of different beam radii.

Simplification:

G = $([\Sigma(3.6 * \rho * A_k * (5.068478e\text{-}03 * r_k * h)^3)] / (\mu * 6490))^{0.5}$ **for k = 1 to the number of different beam radii.**

Summation Expansion for 3 beam radii:

G = $((3.6 * \rho * A_1 * (5.068478e\text{-}03 * r_1 * h)^3) + (3.6 * \rho * A_2 * (5.068478e\text{-}03 * r_2 * h)^3) + (3.6 * \rho * A_3 * (5.068478e\text{-}03 * r_3 * h)^3) / (\mu * 6490))^{0.5}$

Substitution of constants for this flocculator:

G = $((3.6 * \rho * 4.8125 * (5.068478e\text{-}03 * 6.270833 * h)^3) + (3.6 * \rho * 4.8125 * (5.068478e\text{-}03 * 5.020833 * h)^3) + (3.6 * \rho * 4.8125 * (5.068478e\text{-}03 * 3.770833 * h)^3) / (\mu * 6490))^{0.5}$

Simplification:

G = $3.851512e\text{-}04 * (\rho * h^3 / \mu)^{0.5}$

Note that this formula can be used directly if density and dynamic viscosity are calculated separately.

Substitution of density formula from above:

G = $3.851512e\text{-}04 * ((999.972 * (1 - ((((t - 3.983035)^2) * (t + 301.797)) / (522528.9 * (t + 69.34881)))) / 14.5939 / 35.315) * h^3 / \mu)^{0.5}$

Simplification:

G = $5.364879e\text{-}04 * ((1 - ((t - 3.983035)^2 * (t + 301.797) / (522528.9 * (t + 69.34881)))) * h^3 / \mu)^{0.5}$

Substitution of viscosity formula from above:

G = $5.364879e\text{-}04 * ((1 - ((t - 3.983035)^2 * (t + 301.797) / (522528.9 * (t + 69.34881)))) * h^3 / (2.0886e\text{-}02 * 1.002e\text{-}03 * 10 ^ [((20 - t) / (t + 96) * (1.2378 - (1.303e\text{-}03 * (20 - t)) + (3.06e\text{-}06 * ((20 - t)^2)) + ((2.55e\text{-}08 * (20 - t)^3)))))])^{0.5}$

Final simplification to a velocity gradient formula for this flocculator as a function only of motor speed and water temperature:

G = $1.172731e\text{-}01 * ((1 - ((t - 3.983035)^2 * (t + 301.797) / (522528.9 * (t + 69.34881)))) * h^3 / (10 ^ [((20 - t) / (t + 96) * (1.2378 - (1.303e\text{-}03 * (20 - t)) + (3.06e\text{-}06 * ((20 - t)^2)) + ((2.55e\text{-}08 * (20 - t)^3)))))])^{0.5}$

For direct use in most computer programs (substitution of actual variable names must be made for 'temp' and 'hertz'), the syntax would be:

G =

```
0.1172731*((1-(((temp-3.983035)^2)*(temp+301.797)/(522528.9*(temp+69.34881))))*(hertz^3)/(10^(((20-temp)/(temp+96)*(1.2378-(0.001303*(20-temp))+(0.00000306*((20-temp)^2))+((0.0000000255*(20-temp)^3)))))))^0.5
```

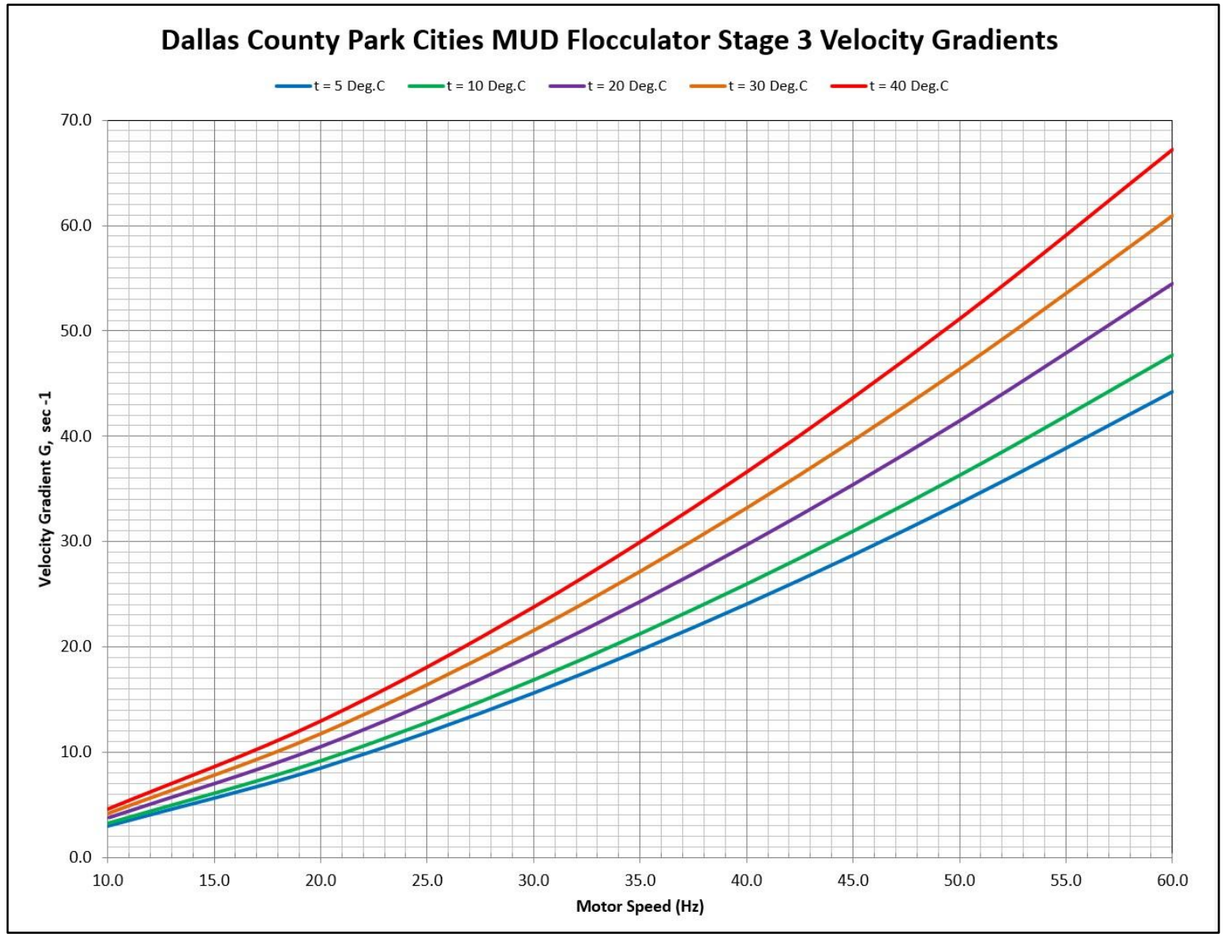

Figure 8.4: Flocculator Stage 3 Velocity Gradient Chart

9. Appendix 4: Stock Solution Makeup Derivations

Dilution of Ferric Sulfate

Dallas County Park Cities MUD

Dilution of ferric sulfate solution such that 1 mL of new solution equals a true dosage of 10 mg/L as Fe^{3+} when added to 2 L of sample:

Chemical Formula: $Fe^{3+}_2(SO_4^{2-})_3$

Atom	Atomic Weight	Number of Atoms		Unit
Fe	55.850	2	111.7	g/mol
S	32.060	3	96.18	g/mol
O	16.000	12	192	g/mol
Total			**399.88**	**g/mol**
Water Density, 20°C			998	g/L
Stock Ferric Sulfate Sp. Gravity			1.55	
Stock Ferric Sulfate Solution			60.0%	
Stock Ferric Sulfate Density			928.140	g/L
Stock Ferric Sulfate Molarity			2.321	mol/L
Desired Ferric Solution Density			10	g/L
Desired Ferric Solution Molarity			0.025	mol/L
now $M_1V_1 = M_2V_2$ so $V_1 = M_2V_2 / M_1$ so:				
		V_1 =	0.011	L
		so V_1 =	**10.774**	**mL**

Put 10.77 mL of ferric sulfate into a 1000 mL beaker and fill with distilled water to the 500 mL line.

Table 9.1: Ferric Sulfate Dilution Method

Dilution of Calcium Hydroxide (Nominal 40% Solution)
Dallas County Park Cities MUD

Dilution of calcium hydroxide solution such that 1 mL of new solution equals a true dosage of 10 mg/L as $Ca(OH)_2$ when added to 2 L of sample:

Chemical Formula: $Ca(OH)_2$

Atom	Atomic Weight	Number of Atoms		Unit
Ca	40.080	1	40.080	g/mol
H	1.008	2	2.016	g/mol
O	16.000	2	32.000	g/mol
Total			**74.096**	**g/mol**
Water Density, 20°C			998	g/L
Stock $Ca(OH)_2$ Sp. Gravity			1.248	
Stock $Ca(OH)_2$ Solution Percentage			40.0%	
Stock $Ca(OH)_2$ Density			498.089	g/L
Stock $Ca(OH)_2$ Molarity			6.722	mol/L
Desired $Ca(OH)_2$ Solution Density			10	g/L
Desired $Ca(OH)_2$ Solution Molarity			0.135	mol/L
now $M_1V_1 = M_2V_2$ so $V_1 = M_2V_2 / M_1$ so:				
V_1 =			0.020	L
so V_1 =			**20.077**	**mL**

Put 20.08 mL of $Ca(OH)_2$ into a 1000 mL beaker and fill with distilled water to the 500 mL line.

Table 9.2: Calcium Hydroxide (40%) Dilution Method

Dilution of Calcium Hydroxide (Nominal 30% Solution)
Dallas County Park Cities MUD

Dilution of calcium hydroxide solution such that 1 mL of New Solution equals a true dosage of 10 mg/L as $Ca(OH)_2$ when added to 2L of sample:

Chemical Formula: $Ca(OH)_2$

Atom	Atomic Weight	Number of Atoms		Unit
Ca	40.080	1	40.080	g/mol
H	1.008	2	2.016	g/mol
O	16.000	2	32.000	g/mol
Total			**74.096**	**g/mol**
Water Density, 20°C			998	g/L
Stock Lime Sp. Gravity			1.181	
Stock Lime Solution			25.9%	
Stock Lime Density			305.267	g/L
Stock Lime Molarity			4.120	mol/L
Desired Lime Density			10	g/L
Desired Lime Molarity			0.135	mol/L
now $M_1V_1 = M_2V_2$ so $V_1 = M_2V_2 / M_1$ so:				
		V_1 =	0.033	L
		so V_1 =	**32.758**	**mL**

Put 32.76 mL of $Ca(OH)_2$ into a 1000 mL beaker and fill with Distilled Water to the 500 mL line.

Table 9.3: Calcium Hydroxide (30%) Dilution Method

10. References

Camp, T.R., and Stein, P.C., (1943). *Velocity Gradients and Internal Work in Fluid Motion*, Journal of the Society of Civil Engineering, Vol. 30.

CDM Smith, Inc (2012). [Velocity Gradient Calcs for Rapid Mix and Flocs.xlsx] [Unpublished raw data].

Clark, M.M., (1985). *Critique of Camp and Stein's RMS Velocity Gradient*, Journal of Environmental Engineering, Vol. 111:741-754.

Cleasby, J.L., (1984). *Is Velocity Gradient a Valid Turbulent Flocculation Parameter?*, Journal of Environmental Engineering, Vol. 110:875-897.

Edzwald, James K. (Ed.), (2011). *Water Quality and Treatment – A Handbook on Drinking Water*, 6th Edition, McGraw-Hill, New York.

Metcalf and Eddy, Inc, (2003). *Wastewater Engineering – Treament and Reuse*, 4th Edition, McGraw-Hill, New York.

Goula, A.M., Kostoglou, M., Karapantsios, T.D. and Zouboulis, A.I., (2008). *The Effect of Influent Temperature Variations in a Sedimentation Tank for Potable Water Treatment – A Computational Fluid Dynamics Study*, Water Research Vol. 42, 3405-3414.

Han, M. and Lawler, D., (1992). *The (Relative) Insignificance of G in Flocculation,* Journal (American Water Works Association), Vol. 94. No. 10.

Hanson, A.T., and Cleasby, J.L., (1990). *The Effects of Temperature on Turbulent Flocculation: Fluid Dynamics and Chemistry*, Journal American Water Works Association, Vol. 82, No. 11.

Kestin, J., Sokolov, M., and Wakeham, W., (1978). *Viscosity of Liquid Water in the Range -8°C to 150°C*, Journal of Physical and Chemical Reference Data Vol. 7, No. 941; https://doi.org/10.1063/1.555581 Published Online: 15 October 2009.

Metgen (2012). *Metrology Article N°18: Calculation of the Density of Water*. http://metgen.pagesperso-orange.fr/metrologieen19.htm.

Morris, J.K., and Knocke, W.R., (1984). *Temperature Effect on the Use of Metal-Ion Coagulants for Water Treatment*, Journal American Water Works Association, Vol 76, No. 3.

National Institute of Standards and Technology (2012). *Dynamic Viscosity of Water*. www.nist.gov/data/PDFfiles/jpcrd121.pdf.

Pedocchi, F., and Piedra-Cueva, I., (2005). *Camp and Stein's Velocity Gradient Formalization*, Journal of Environmental Engineering, Vol. 131, No. 10.

Phipps & Bird, (2012). G-Curves. Source: Water and Air Research, Inc. http://www.phippsbird.com/gcurve.html

Reed, G.D., and Robinson, R.B., (1984). *Similitude Interpretation of Jar Test Data*, Journal of Environmental Engineering, Vol. 110, No. 3.

Stanley, S.J., and Smith, D.W., (1995). *Measurement of Turbulent Flow in Standard Jar Test Apparatus*, Journal of Environmental Engineering, Vol. 121, No. 12.